NASA-CR-199363

Final Report to

NASA Lewis Research Center

for the project entitled

Durability and Life Prediction Modeling in Polyimide Composites

NCC 3-188

by

Wieslaw K. Binienda
The University of Akron
Akron, OH 44325-3905
Tel: (216) 972-6693
Fax: (216) 972-6020

September 19, 1995

Introduction

Polyimide Composites have received considerable attention due to their present and potential future application, owing to their small structural weight and higher glass transition temperature, Tg. In this work the formation of cracks from smooth surfaces of brittle materials was studied.

It is known from the previously published research that polyimide composite plates are sensitive to thermal aging that manifest itself by the degradation of the effective mechanical properties and weight loss due to oxidation processes. Microscopical examination revealed generation of the microcracks perpendicular to fiber direction and voids in polymer matrix material.

The microcracking generation mechanisms depend on the environmental conditions such as time and temperature but also on the load history for a given material. Microstructure of the material itself, fiber volume ratio, type of reinforcement, fiber distribution and fiber alignment definitely influence the aging and microcracking processes.

As the first approximation of the aging process the crack formation in isotropic material can be studied due to non uniform strain distribution caused by aging phenomenon. Cracking is the main failure mode for brittle materials when the stress is tension dominant. The starting point of cracking can be determined by various strength criteria. However, the strength criteria does not contain any information that dictates the behavior of the following cracking in the material.

In the following section a copy the Ph.D dissertation of the student Anping Hong supported by this NASA project is included as a report of the research efforts. This work can be expanded in the future to address the cracking in the orthotropic materials. The theoretical results should be first examined using aging of the resin plate that can be modeled by the work done in the presented studies.

THEORY OF CRACK INITIATION
FROM SMOOTH SURFACES AND ITS APPLICATION

A Dissertation

Presented to

The Graduate Faculty of The University of Akron

In Partial Fulfillment for the Degree

Doctor of Philosophy

Anping Hong

ABSTRACT

Sudden appearance of cracks on a macroscopically smooth surface of brittle materials due to cooling or drying shrinkage is a phenomenon related to many engineering problems. Although conventional strength theories can be used to predict the necessary condition for crack appearance, they are unable to predict crack spacing and depth. On the other hand, fracture mechanics theory can only study the behavior of existing cracks. The theory of crack initiation can be summarized into three conditions, which is a combination of a strength criterion and laws of energy conservation, the average crack spacing and depth can thus be determined. The problem of crack initiation from the surface of an elastic half plane is solved and compares quite well with available experimental evidence.

The theory of crack initiation is also applied to concrete pavements. The influence of cracking is modeled by the additional compliance according to Okamura's method. The theoretical prediction by this structural mechanics type of model correlates very well with the field observation. The model may serve as a theoretical foundation for future pavement joint design.

The initiation of interactive cracks of quasi-brittle material is studied based on a theory of cohesive crack model. These cracks may grow simultaneously, or some of them may close during certain stages. The concept of crack unloading of cohesive crack model is proposed. The critical behavior (crack bifurcation, maximum loads) of the cohesive crack model are characterized by rate equations. The post-critical behavior of crack initiation is also studied.

TABLE OF CONTENTS

LIST OF FIGURES vi

CHAPTER

I. INTRODUCTION. 1

II. LITERATURE REVIEW 6

2.1 A System of Parallel Cracks from a Smooth Surface 6

2.2 Classical Cohesive Crack Models .11

2.3 Fracture Mechanics of Concrete .14

2.4 Crack Spacing in Concrete Pavement Due to Temperature Effects 21

III. INITIATION THEORY — FOR BRITTLE MATERIALS 27

3.1 Statement of Problem 28

3.2 Conditions Governing Crack Initiation from Smooth Surfaces 30

3.3 Mathematical Formulation 33

3.4 Numerical Method 35

3.5 Analysis of Numerical Results 39

3.6 Experimental Evidence 44

3.7 Additional Comments and Brief Summary 46

3.8 Outline of a Proposed Experiment 48

IV. CRACK INITIATION IN CONCRETE PAVEMENTS 54

4.1 Mechanical Modeling of Pavement 56

4.2 Structural Analysis 58

4.3 Stress Intensity Factors and Additional Compliance Functions 63

4.4 Crack Initiation Theory 65

4.5 Numerical Method 70

4.6 General Behavior of the Model 73

4.7 The Effect of Nonlinear Temperature Distribution 76

4.8 Discussion and Conclusions. 78

V. INITIATION THEORY — FOR QUASI-BRITTLE MATERIALS 91

5.1 Basic Conditions and Definition 93

5.2 Cohesive Model with Interactive Cracks 96

5.3 Mathematical Formulation and Numerical Method 99

5.4 Computational Procedure and Observation 105

5.5 Rate Equation of CCM 107

5.6 Maximum Load and Bifurcation 111

5.7 Maximum Load with One Crack Unloading 112

5.8 Post-critical Behavior and Lower Crack Spacing Limit 114

5.9 Concluding Remarks 116

VI. CONCLUSIONS AND FUTURE RESEARCH 123

BIBLIOGRAPHY 129

APPENDIX 1 THE STRESS INTENSITY FACTOR. 142

APPENDIX 2 ADDITIONAL COMPLIANCE FUNCTIONS 144

LIST OF FIGURES

3-1 (a) Geometry definition of parallel crack system 51

(b) Initial strain profile 51

(c) Unit cell of width *b* 51

3-2 (a) Crack spacing versus load depth. 52

(b) Initial crack length versus load depth. 52

3-3 Energy release rate and average energy release rate as a function of a/d in the limit case. 53

4-1 Geometry definitions for (a) pavement on an elastic foundation 81

(b) a unit cell with an edge crack in the center 81

4-2 The length-dependent bending compliance of a beam on Winkler foundation . 82

4-3 Schematic of crack initiation theory 83

4-4 Definitions of effective energy and total fracture energy. 83

4-5 Total stress intensity factor as a function of crack length and loading configuration 84

4-6 Crack spacing as a function of l_0 without axial constraint 85

4-7 Crack spacing as a function of l_0 with axial constraint 86

4-8 Crack spacing with tangential bonding 87

4-9 The effect of nonlinearity coefficient β on crack spacing. 88

4-10 The effect of axial thermal stress 89

4-11 Schematic of nonlinear distribution of thermal stress. 90

5-1 (a) Cracking of quasi-brittle Materials. 118

(b) The cohesive crack model. 118

5-2 (a) Geometry definition of parallel crack system with alternative lengths . . . 119

(b) Unit cell of width 2b. 119

5-3 Possible crack initiation paths. 120

5-4 Bifurcation and critical curves 121

5-5 (a) Loading parameter γ versus crack length a^*_1 for two paths 122

(b) Crack mouth opening versus crack length a^*_1 for unloading path. 122

CHAPTER I

INTRODUCTION

Formation of initial macroscopic cracks from smooth surfaces of brittle materials can be frequently observed. For instance, in large blocks of concrete, nearly periodic cracks can appear suddenly due to drying shrinkage or hydration heat. In the case of reinforced concrete beams, cracks of a certain spacing form at the tensile face when the applied load becomes large enough. In drying lake beds and mud flats, cracks with a honeycomb pattern emerge after some period of drying. When a floating sea ice plate is subjected to a vertical load, star-shaped cracks of finite length radiate suddenly from the loaded area when the applied load reaches a certain level. Highway pavement develops cracks each year due to various environmental changes such as temperature and moisture. In all these situations, cracks of macroscopic sizes form suddenly from a smooth surface.

Cracking is the main failure mode for brittle materials when the stress state is tension dominant. The starting point of cracking can be marked by various strength criteria depending on the specific material under specific environment. In the simplest case, one can use the condition that the maximum tensile stress should not exceed the tensile strength of the material. However, the strength criteria does not contain any information that dictates the behavior of following cracking in the material. Engineers used to avoid the cracking by reducing the maximum stress in their designs. However, cracking in some cases is either inevitable or uneconomical. For instance, the asphalt concrete pavement in northern America and Canada develops crack each and every winter, it cannot be avoided. It would not be cost effective to design a reinforced concrete beam prohibiting cracking on its tension side. Sometimes, it may become crucial to know what will happen after cracking occurs. For instance, due to safety concern, it is very important to know the behavior of nuclear reactor structure after cracking has occurred. Obviously, the conventional strength criteria are not sufficient to answer these questions.

Cracking has been studied by the theory of fracture mechanics. During the recent half century since the practical applications pioneered by Irwin, fracture mechanics has been significantly developed and enriched in terms of practical applicability and theoretical understanding. Although the original intention of the fracture mechanics, initiated by Griffith (1924), was to understand the strength of brittle materials and its relation with the inevitable defects in the material, the later development was more focused on the problems of crack growth. As a result, a new type of material strength, called the toughness of the material (or fracture energy), was brought into the light and became the subject of intensive research. Fracture toughness of the material determines whether a crack of a given size will propagate under a given load. Fracture mechanics works where the conventional strength criteria fail, because at crack tip the stress is infinite so the conventional strength is inapplicable. However, fracture mechanics does not encompass the territory of the conventional strength criteria, either. If there are no pre-existing cracks in material (or the pre-existing cracks are very small in sizes), fracture mechanics would predict unreasonably high failure load. Mathematically this is because the energy release rate for a very short crack approaches zero like a linear function of crack length (so the stress intensity factor due to a unit load approaches zero like the square root of the crack length).

It is, therefore, seen that the theory of fracture mechanics and the strength criteria have their own domains of applicability that do not overlap. The phenomenon of crack initiation lies partially in both of these two domains, but not entirely in either one. This is because the strength theory alone cannot describe the cracking behavior, but fracture mechanics cannot be adequately employed either where there is no pre-existing cracks. A new theory that combines these two different aspects of material strengths must be found to study the crack initiation theory. This kind of theory does not seem to have been systematically studied before.

From the practical point of view, the pattern of initial cracking can be important for many engineering problems. Sometimes sparse cracking patterns are preferred, sometimes dense but small cracking patterns are more desirable. For the former case one can mention pavement cracking. The longer crack spacing is preferred because one can use less joints to control cracking at less cost. For the later case, one can mention cracking in the reinforced concrete. To prevent corrosion of reinforcement, the cracks must remain hairline thin, and so we need the crack spacing to remain sufficiently small.

In all these cases, it is important to understand the mechanism of crack initiation so that we can know what can be done to control cracking. The main focus of this dissertation is to establish the formulation of the crack initiation theory, solve the crack initiation problems of different geometric structures as well as different material properties. It is hoped that these new knowledge can shed new light on many engineering problems in which cracking is inevitable.

Some basic idea of crack initiation theory for the case of vertical penetration of a floating sea ice plate was contained in the study by Li and Bazant (1994). Since the penetration load depends on the number of radial cracks, it is essential to understand how the number of cracks can be determined. In this dissertation, the crack initiation theory is stated in a form that facilitates further development.

The structure of the dissertation is organized as follows. Chapter II. related literature review. The basic concept and definition of crack initiation theory is introduced in chapter III, the problem of periodic parallel cracks initiated from the surface of a perfect brittle and elastic half plane under the action of initial strains will be discussed. The initial strains can be caused by a drop of temperature or by drying shrinkage of the material. The elastic stress distribution is solved by a integral equation. The solution of this problem can be related to the behavior of crack initiation that happens sufficiently far away from material boundaries.

For the pavement problem, the cracking is normally confined in the top layer of the pavement, and the structure can be more appropriately modeled as an elastic beam. A new type of elastic analysis is introduced in chapter IV. Since the pavement layer is usually about 10 inches thick, the nonlinear process zone of the crack is significantly large, and the consequence of the nonlinearity of the pavement material must be taken into consideration, which results in a further refinement of the crack initiation theory. However, the treatment should be considered as an empirical simplification.

To fully consider the effect of nonlinear process zone, the cohesive crack model must be employed. In the cohesive crack model (CCM), the material does not fail immediately. Instead, there is gradual decreasing of bridging stress for increasing crack opening displacement, a phenomenon called strain softening, or simply softening. When the cohesive crack model is used, the concept of crack initiation needs to be generalized further. In addition, the theory of the cohesive crack model also needs to be expanded to consider the interaction between the cohesive cracks and the description of a unloading cohesive crack. Applying the cohesive crack model to study the problem of parallel cracks initiated from the surface of a half-plane is discussed in chapter V.

Many problems of crack initiation theory still remain open. The main existing problems and possible solutions will be discussed. Future research direction will be described as a closure to this dissertation.

CHAPTER II

LITERATURE REVIEW

In this chapter, some of the literature that are related to this study will be briefly reviewed. In addition, some nonlinear fracture models for quasibrittle material are also discussed because some of the analysis is based on these theories. To apply the crack initiation theory to concrete pavements, the literature of the concrete pavements design and research regarding temperature response are outlined.

2.1 A System of Parallel Cracks from a Smooth Surface

Consider the two-dimensional problem of a homogeneous isotropic elastic half-plane in which a system of parallel equidistant cracks normal to the surface is produced by cooling or drying shrinkage. This problem arises in many applications. In the later 70's and early 80's an interest to extract heat from the hot-dry-rock by circulating the water through the cracks attracted a lot of researches. Also, there are applications of shrinkage cracking of concrete. Base and Murray (1982) called that "shrinkage cracking" is the most troublesome and frustrating quirk of structural concrete.

Bazant and Ohtsubo (1977) first carried out stability analysis in which the conditions of stability of a system of Mode I cracks propagating along given paths were determined by analyzing the second variation of the work needed to create the cracks as well as by formulating the conditions of adjacent equilibrium. The crack system that is in equilibrium state is stable if the second variation of the strain energy $\delta^2 W$ is always positive, and unstable if it is negative, i.e.

$$\delta^2 W = \frac{1}{2}\sum_{i=1}^{n}\sum_{j=1}^{n} W_{ij}\,\delta a_i \delta a_j \begin{cases} >0 & \text{stable} \\ =0 & \text{critical} \\ <0 & \text{unstable} \end{cases} \qquad \textbf{(2-1)}$$

Bazant, Ohtsubo, and Aoh (1979) continued their work to determine the critical states, bifurcation of equilibrium path and postcritical behavior. When a system of parallel equidistant cooling cracks propagates, it reaches a critical points, and the equilibrium path of the system bifurcates. The stable post-critical path consists of extension of every other cracks upon further cooling, initially with a crack jump at constant temperature, while the intermediate cracks stop growing and gradually diminish their stress intensity factor. Subsequently the leading cracks grow at equal length until they again reach a critical state, at which every other crack stops growing, and the process in which the crack spacing double is repeated. In both papers the finite element approach was adopted for completing numerical analysis. Bazant and Wahab (1979) also discussed the effect for different temperature profiles.

Nemat-Nasser, Keer, and Parihar (1978) formulated the problem in terms of a singular integral equation of Cauchy type with continuous dislocation functions as basic unknowns for alternative cracks. They analyzed the crack growth regimes based on stability analysis of crack growth by checking the derivatives of the stress intensity factors with regard to crack lengths. It is equivalent to the Bazant's stability analysis.

They pointed out that the equal crack growth regime is stable as long as the following condition holds

$$\frac{\partial K_1}{\partial a_1} = \frac{\partial K_2}{\partial a_2} < 0 \tag{2-2}$$

Where K_1 and K_2 are stress intensity factors, a_1 and a_2 are crack lengths for the corresponding crack. An unstable critical state is reached when

$$\frac{\partial K_1}{\partial a_1} = \frac{\partial K_2}{\partial a_2} = 0 \tag{2-3}$$

After this state, one crack, say crack 2, stops as the other crack, i.e. crack 1, grows spontaneously.

Keer, Nemat-Nasser and Oranratnachai (1978) extended their work to the array whose unit cell contains three interacting cracks. The model can exam the crack growth regime at and after the second critical state, at which every other of those cracks which had continued growing stop growing, while the remaining one continue to grow at a faster rate. It is shown that when the temperature profile is in the form of an error function, the inclusion of the third interacting crack changes the previous obtained results qualitatively (i.e. no crack closure is attained in this case). The lack of symmetry in this model implies that crack extension involves in both Modes I and II, and the calculation requires the correspondingly great number of simultaneous integral equations, which causes the computational complexity.

The above stability analysis requires accurate estimates of the values of the stress intensity factors at various crack tips, and their derivatives with respect to the crack lengths. Actually K_{I} is obtained by extrapolation of the solution of system equations, and the calculation of $\frac{\partial K_i}{\partial a_j}$ is more difficult and less accurate. Sumi, Nemat-Nasser and Keer (1980) proposed a combined analytical and finite-element solution method which leads to a rather effective solution procedure. Nemat-Nasser, Sumi and Keer (1980) also used this method to study stable and unstable bifurcation points and critical points. In particular, they pointed out the stability of this kind is highly imperfection-sensitive.

To verify the previous theoretical results Geyer and Nemat-Nasser (1982) conducted experimental investigation on thermal induced parallel edge cracks in half-plane of brittle material. Glass plates were heated to a uniform temperature and then brought in contact with dry ice. The thermal contraction of boundary layer produced interactive tension cracks. They observed that the cracking occurred in a dynamic fashion seconds after initial contact with the dry ice bath. However, dynamic crack growth is related more to the problem of "crack initiation" than "crack growth", as was recognized by the authors.

Bazant and Wahab (1980) used previous formulation of stability condition to investigate the reinforced concrete (one layer of steel reinforcement) by finite element approach. The bond slip (between concrete and steel) length was assumed and taken into account.

In Chapter 12 of his book (Bazant and Cedolin,1991), Bazant summarized the stability analysis of a system of parallel cracks. In all these works it was found that instability of a system of parallel shrinkage or cooling cracks may cause some cracks to close and the remaining ones to extend and widen.

However, most attention is focused on the problem of how cracks develop in structures that already have them. Since cracks propagation happens after crack initiation, thus the problem of crack initiation becomes an issue.

Although there were some crude estimates. Keer, Nemat-Nasser (1978, 1979) estimated crack spacing with several approaches. One is by energy consideration, its idea is that the portion of the total strain energy before cracking is used to generate new surfaces as the thermal crack initially form ($\theta W = 2a\gamma$). Then the minimum crack spacing b is obtained in this way as

$$b = k_0 \frac{1}{\theta}\frac{a}{d} \tag{2-4}$$

where a is crack length, d is penetration depth of drying or cooling, and $0 < \theta < 1$, denotes the fraction of the total strain energy that will be released. The coefficient k_0 depends on the temperature profile and material properties. However, neither ratio a/d nor fraction θ can be determined in their analysis, as was admitted by Nemat-Nasser (1979). Also Bazant and Wahab (1979) and Bazant and Cedolin (1991) gave a similar estimate of the minimum cracking spacing for the parabolic temperature profile as:

$$b = \frac{20(1-\nu)\gamma}{\theta(1+\nu)\alpha^2 \Delta T^2 E}\frac{a}{d} \tag{2-5}$$

where γ is the surface energy density, α the coefficient of thermal expansion, ΔT the surface temperature drop.

2.2 Classical Cohesive Crack Models

Barenblatt (1959a, 1959b, 1962) was the first one to challenge the concept of stress singularity in fracture mechanics. His basic argument is that stress should always be finite. His mathematical model of crack differs from that of Griffith's model in that the cohesive interatomic and/or intermolecular forces are explicitly included in the equilibrium of the crack. It is noted that in Griffith's approach the cohesive forces are only accounted for in surface energy computation but ignored totally in the equilibrium consideration. Barenblatt pointed out an interesting fact that the smoothness of crack opening profile is equivalent to the finiteness of stress at crack tip, which can be seen from the solution of the infinite plane with a semi-infinite cut on the negative x-axis. Besides the external loads that make the crack open, there are distributed forces p(x) defined symmetrically on the both sides of the crack that tend to close the crack. The normal stress and displacement in y-direction near the crack tip can be expressed as

$$\sigma_y = \frac{K}{\sqrt{s_1}} + p(0) + O(\sqrt{s_1}); \quad v = \mp\frac{4(1-\nu^2)K\sqrt{s_2}}{E} + O(s_2^{3/2}) \qquad \textbf{(2-6)}$$

where s_1 is in the positive x-direction while s_2 in the negative x-direction, the sign in front of displacement indicates that each crack face goes to opposite directions. ν is the Poisson's ratio. When K is zero in these expression, then crack opening is smooth at the crack tip. Besides, it is noted that when stress singularity is nullified, the normal stress component in y-direction is continuous at crack tip. The connection between the smoothness of crack opening and the finiteness of stress was perhaps first demonstrated by Westergaard (1933) in a paper on the stress distribution in a RC beam with crack.

The cohesive force generally depends on the crack opening displacement, therefore the cohesive crack models are generally nonlinear. However, Barenblatt argued that if the process zone is small when compared with the crack length, then the cohesive force can be considered to be independent of crack opening displacement. Furthermore, the cohesive force can be used to determine the modulus of cohesion K_c:

$$K_c = \frac{1}{\pi}\int_0^{l_p} \frac{p(s_2)ds_2}{\sqrt{s_2}} \qquad \textbf{(2-7)}$$

where l_p is the length of process zone. It is to be remembered that now p(x) depends only on its position rather than crack separation. The distinction between the classical cohesive crack model and the cohesive crack model discussed herein lies in whether cohesive forces are considered dependent on the evolution of crack opening displacement. By adopting the above assumptions, the process of crack formation is no longer considered.

It should be noted that in the original definition, the factor $(1/\pi)$ is not included. Furthermore Barenblatt argued that the modulus of cohesion has the same relation with the strain energy rate G as the stress intensity factor K when crack is about to propagate. It is therefore fair to say that Barenblatt's theory did not yield any operational difference from linear elastic fracture except for a more realistic picture of what is happened near crack tip.

The postulation of equivalence between Barenblatt's criterion and Griffith's criterion was examined mathematically by Willis (1967). Willis found that in order for the two theories to be compatible, it is necessary to require that the cohesion zone be small compared to the crack length, and the load level must be very low with respect to the Young's modulus of the material. The problem of the profile of crack separation within cohesion zone was addressed by Smith (1974). Instead of solving for crack separation for given cohesion law, which is a nonlinear problem, an inverse approach is employed, that is, stress-separation law is deduced from given separation which is usually of very simple form. At this point, one should keep in mind that Smith's results rely completely on the assumption of smallness of cohesion zone, any extension to nonlinear fracture mechanics (e.g. Karihaloo et. al. 1989) is, therefore, unlikely to be justifiable.

Dugdale (1960) was credited for demonstrating the usefulness of cohesive crack model in nonlinear problem. Actually his objective was to find the extent of yielding in front of crack tip as a function of loading over yielding stress. Assuming that the plastic region is a thin strip extending from the crack tip, the cohesive force is considered to be constant at the magnitude of yielding stress. Since no stress should exceed yielding stress, the stress intensity factor should be zero which in turn becomes a condition for determination of cohesive zone length. According to Dugdale's experiment, the theory provided excellent prediction. Eight years later Cotterell (1968) affirmed that Dugdale's model is equally applicable to organic glass.

The drawback of Dugdale's work is that no crack propagation criterion was provided, which was not the intention of his paper, the cohesion zone can be stretched to arbitrary length for sufficient load level. To remedy the situation, the crack opening displacement (COD) was proposed to serve as the cracking criterion for Dugdale model. When COD exceeds some critical value, which is assumed as a material constant, the crack will propagate. Later it will be seen that COD is not a constant in the cohesive crack model.

2.3 Fracture Mechanics of Concrete

Quasibrittle materials such as concrete, rock, ceramic, paper, lumber etc., are very different from metals, because they exhibit significant softening behavior while plastic hardening deformation is negligible. On the other hand, these materials are not as totally brittle as materials such as glass and mica. Quasibrittle materials also can include advanced cementitious composite, fiber reinforced composite, etc. (Shah 1991). In quasibrittle materials fracture is preceded by a fracture process zone, which may be caused by microcracking or other material defeats that the major source of nonlinearity come from. Some experiment observations of concrete indicate that within this zone, fracture is manifested in the form of aggregate debonding and overlapping microcracking, mainly parallel to each other, with some intact grain bridges between them (Mier, Rots and Bakker, 1991). Concrete has an added complication in that the scale of its mesostructure is relative large compared to other materials. Kaplan (1961) applied linear fracture mechanics to concrete for the first time. Since then most efforts have been directed towards better understanding of the pronounced nonlinearity in concrete and how to deal with such nonlinearity as has been summarized in the excellent review articles by Mindess (1983, 1984).

Kaplan (1961) was the first one to acknowledge the slow crack growth in concrete, which is a stable crack extension under increasing load before final rupture occurs. Kaplan was able to relate the length of slow crack growth with the size of the specimen. As a matter of fact, the phenomenon of slow crack extension is not unique to concrete. Irwin (1958) was probably the first one to undertake this problem by identifying it with plastic deformation. Slow crack led its way to the so-called R-curve approach by Broek (1968) in his study of an aluminum-copper alloy. Since then the R-curve approach became a very popular practice also in concrete fracture mechanics research (e.g. Bazant, 1984b; Wecharatana and Shah; 1983a, 1983b; Mai, 1984; Foote, 1986, etc.). Although Broek (1986) realized that R-curve is not likely to be a material property, as has been indicated by numerous researches that R-curve is dependent on the loading configurations (Wecharatana, 1983b, e.g.) as well as specimen size (Foote, et.al, 1986). However, due to the fact that there has been no better approach available, R-curve method still enjoys wide applications among some of more pragmatic researchers (e.g. Mobasher,1989; Shah, 1990).

Another difficulty with linear fracture mechanics of concrete is the so called notch sensitivity problem. Griffith (1924) is the first one to consider the smallest size of crack which can cause the observable decrease in the strength of materials. For glass, Griffith found that this size is about $1.5*10^{-3}$ (mm). When this size is relatively large, the material may be called notch insensitive. While many researchers agree that hardened cement paste is a notch sensitive material, the opinions about concrete and fiber reinforced concrete are divided, both sides claimed having experimental evidence backups. When it comes to the experimental measurement of K_c and G_c, the results are again highly contradictory, especially in the study of the dependency of K_c and G_c on the geometry of specimens. Although obviously the highly heterogeneous nature of concrete is responsible at least in part for this apparent inconsistency, nevertheless by the end of seventies the linear fracture mechanics was not considered directly applicable to concrete material by most researchers.

Hillerborg's fictitious crack model (FCM) was advanced during the late seventies and early eighties (1976,1985) as the first nonlinear fracture mechanics model in concrete. Apparently encouraged by the success of Dugdale's model, Hillerborg proposed to use a declining cohesion law (i.e. stress-separation relation) to describe the strain softening behavior of cementitious materials. The total area below the stress-separation curve defines a quantity called fracture energy G_f, which is experimentally found to be less dependent on specimen size than any other fracture parameters (Hilsdorf and Brameshuber, 1984). An important difference from that of Dugdale's model is that the cohesive stress now is displacement (crack separation) dependent, therefore the model became truly nonlinear because the cohesive stress is neither constant nor proportional to the crack separation. It is so difficult that no analytical solution even for the simplest geometry has been found. Convenience in finite element application is one of the objective in the original paper (Hillerborg, 1976), since the removal of stress singularity made it possible to use regular coarse mesh.

When Bazant proposed his crack band theory, his major objective seemed to aim at the formulation of a nonlinear fracture model for concrete (and its similar material, of course) such that the distributed microcracking as well as coalesced (that is, localized) cracking can be treated in a unified way (e.g. 1984a, 1984c, 1986a, 1990a, 1990b). The starting point is a numerical technique called smeared crack simulation proposed by Rashid (1968) where crack is represented by elements with tensile Young's modulus equals to zero. Bazant employed the method to include strain softening in the formulation. No sooner than the scheme was implemented, the result was found mesh dependent, i.e., the energy dissipated by strain softening diminishes as the mesh shrinks. The strategy used in his crack band model is to take softening modulus E_T as a function of Young's modulus E, tensile strength f_t, the fracture energy G_f and the cracking front width w_c such that the fracture energy G_f is constant:

$$G_f = \frac{(f_t)^2}{2}\left(\frac{1}{E}+\frac{1}{-E_T}\right) w_c = \text{constant} \tag{2-8}$$

where the factor that multiplied by w_c can be recognized as the specific strain energy, that is, the area under stress-strain diagram. But if E_T is determined independently, then w_c can be determined from the above equation. Bazant considered w_c as a material property and refused to take elements smaller than w_c.

A comparison between FCM and crack band model was made by Bazant (1986a) in which Bazant recognized certain similarity after microcracks are localized into one macroscopic crack. It is fair to say that Bazant's goal is more ambitious, it is a serious strive towards a unified theory of distributed cracking as well as localized cracking. On the other hand, Hillerborg's objective is modest, he chose to deal only with those cases where localization is known *a priori*. Consequently FCM is simple both mathematically and physically. The introduction of stress-separation relations in place of stress-strain relation circumvented the predicament of unobjective softening modulus E_T, leading to a much simpler numerical scheme. The attractiveness of this approach was enhanced by Ottosen (1986). Using stability and uniqueness arguments, he demonstrated the ominous incongruity accompanied with strain softening concept.

One of the interesting feature of FCM is the unified treatment of notched fracture and unnotched fracture. As it was mentioned in the beginning of this section, notch is not necessary for concrete to rupture by cracking as most metals do, since it is its only way of rupture under tension. Extensive calculations of FCM on 3-point beams was made by Carpinteri (e.g. 1989) for different sizes and different notch ratios including zero notch ratio. A boundary element simulation was made by Liang and Li (1991a). The size effect of FCM is examined (Liang and Li, 1991b). It is fascinating to see how size effect curves gradually shift towards a curve of bending strengthening. Li, et.al. (1986) used the Green's function method to solve FCM for a centrally cracked infinite plane using different stress-separation curves with the same G_f and the same tensile strength. Among many conclusions, they found that the shape of the stress-separation curve has a significant effect on the load versus crack opening diagram, and that the length of process zone is not a material property, but rather a variable depending on the loading configuration and structural geometry. Liaw et.al. (1990) recently demonstrated that better results can be obtained by adopting a more refined stress-separation curve in FCM computation. Li and Liang (1993) developed a theory of CCM in which the peak load of the Griffith problem (a Central tensile crack in an infinite plane) was solved through the condition of stability limit. The critical condition can be transformed into a linear eigenvalue problem under the assumption of linear softening law. Using the same technique, Li and Hong (1992) solved cohesive crack problems of double-notched or center notched infinite strip under remote tensile loading.

There is another nonlinear fracture mechanics model of concrete material called two-parameter model by Jenq and Shah (1985a,1985b). As is well known that the critical stress intensity factor K_c and critical energy release rate G_c calculated from the peak load depend on the dimensions of specimens, Jenq and Shah proposed to use crack mouth opening displacement (CMOD) as a second crack parameter to complement linear fracture mechanics parameter such as K_c. In computation, CMOD is used to determine the length of process zone in which a stress-separation relation is assumed. After the adjustment caused by the bridging effect in the process zone, the calculated net stress intensity factor at peak load is found to be constant by their experiments. Actually the idea of using cohesive force as a modifying factor in linear fracture mechanics exits in Shah's research before 1985, as can be seen in their earlier papers by Wecharatana and Shah (1983a, 1983b), and a discussion by Hillerborg (1984) in which some ambiguity in definition as well as in concept was commented. The two-parameter model published later is just a manifestation that Shah hardened his position in defending his notion that the stress singularity still exists in spite of the presence of pronounced cohesive force in process zone. Recently Shah in a keynote lecture (1989) vindicated his model by categorizing the dissipation mechanism in concrete into three sources, one that corresponding to surface energy, one due to microcracking and the one that dissipated in the wake of crack path. According to this classification Shah claimed that the two-parameter model is the best in terms of energy balance consideration.

It is a generally accepted idea that when concrete specimen is small, the strength criterion will dictate the rupture load, and when the dimension becomes sufficiently large, the well-known inverse-square-root scaling law of linear fracture mechanics will govern. Now the question is what happens in between these two extremes. Walsh (1972) tried for the first time to establish the size effect. It is very interesting to note that he used $(f_t/\sigma_n)^2$ as ordinate and d/d_a as abscissa to plot his result which is a straight line, and this is basically the same form as the one proposed by Bazant (1984a) for his size effect law. According to Bazant (1984a), for a family of geometrically similar specimens with size characterized by d, the peak load when represented in terms of nominal stress σ_n can be expressed as

$$\frac{\sigma_n}{f_t} = \frac{B}{\sqrt{1+\lambda d}} \tag{2-9}$$

where B and λ are fitting parameters. For some reason Bazant preferred to define $\lambda=1/\lambda_0 d_a$, where λ_0 is a nondimensional parameter and d_a is the size of the aggregate of concrete. This form of size effect law describes quite well for many failure modes of concrete material. However, if the notch length is very small or zero, then the above equation must be modified.

2.4 Crack Spacing in Concrete Pavement Due to Temperature Effects

The first Portland cement concrete pavement in the United States consisted of a 10-ft wide by 220-ft long slab constructed in Bellefontaine, Ohio in 1891. During the following 100 years tremendous increased pavements were build at various locations in the Unite States. In 1991, the Federal-aid highway system comprised more than 850,000 miles of pavements of various design. (FHWA, NCHRP Synthesis 189, 1993).

It is necessary to briefly review the basic consideration regarding temperature effect in concrete pavement design from "AASHTO Guide for Design of Pavement Structures 1993". The rigid pavement (Portland cement concrete pavements) includes plain jointed (JCP), jointed reinforced (JRCP), and continuously reinforced (CRCP). Joints are placed in concrete pavements to permit expansion and contraction of the pavement, thereby relieving stresses due to environmental changes (i.e., temperature and moisture) and friction. There are three types of joints for JCP: contraction, expansion and construction and their functions are as follows:

(1) Contraction or weakened-plane joints are provided to relieve the tensile stresses due to temperature, moisture, and friction, thereby controlling cracking. If contraction joints were not installed, random cracking would occur on the surface of pavement.

(2) The primary function of an expansion joint is to provide space for the expansion of the pavement, thereby preventing the development of compressive stresses, which can cause the pavement to buckle.

(3). Construction joints are required to facilitate construction.

For contraction joints, according to the AASHTO (1993), the spacing decreases as the thermal coefficient, temperature change, or subbase frictional resistance increases; and the spacing increases as the concrete tensile strength increases. The spacing also is related to the slab thickness and the joint sealant capabilities. It is suggested, as a rule of thumb, the joint spacing (in feet) for plain concrete pavements should not greatly exceed twice the slab thickness (in inches). For example, the maximum joint spacing for an 8-inch slab is 16 feet. In 'Rigid Pavement analysis and Design"(FHWA-RD-88-068, 1989) joint spacing for plain concrete pavement ranges between 12 and 20 feet, with maximum 20 feet. California instituted the practice of specifying joints at 12, 15, 13, and 14 feet. The use of a random spacing pattern was instituted in the early 1960's to minimize excessive vibration problems (FHWA-RD-86-040, 1986).

The width of the joint is controlled by the joint sealant extension. The depth of contraction joints should be adequate enough to ensure that cracking occurs at the desired location rather than in a random pattern. Normally, the depth of transverse contraction joints should be 1/4 of the slab thickness. These joints may be developed by sawing, inserts, or forming. Time of sawing is critical to prevent uncontrolled cracking.

The use of expansion joints is generally minimized on a project due to cost, complexity, and performance problems. They are used at structures where pavement types change (e.g., CRCP to jointed), with prestressed pavements and at intersections. In 'Pavement Structural Design Practices" (1993) it is stated that the use of expansion joints was virtually standard practice by the mid 1930s, but has since been found to be unnecessary except where the pavement abuts a structure.

Major distress problems of concrete pavements generally start with crack formation caused by the combined effects of traffic load and service temperature. Water and salt can easily infiltrate into the pavement at the location of cracks and create durability and structural problems.

The structural response of concrete pavements under traffic loads is highly dependent on temperature and its variation. Temperature effects on concrete pavement behavior have been recognized since the mid-1920s. Westergaard (1926) identified temperature curling as an important parameter affecting the structural behavior of concrete pavements. Westergaard's method (1925) for computing stresses in concrete pavement was based on an assumption that the subgrade acts as a Winkler foundation: the pressure between slab and subgrade is proportional to deflection. Teller and Sutherland (1935) reported the results of tests conducted on concrete pavements to study the effects of variations in temperature and moisture. Lang (1940) studied the movement of concrete pavement slabs resulting from changes in temperature and moisture. Friberg (1954) presented a mathematical evaluation of horizontal slab movements, and effect of the subgrade frictional resistance, on stress development in long pavement slab. Harr and Leonards (1959) conducted laboratory tests to measure temperature curling and compute subsequent stresses. They correlated the results from the laboratory tests with predicted response with an analytical model that they developed.

Armaghani, Larsen and Smith (1987) try to more precisely describe the displacements (vertical and horizontal) of a concrete pavement slab associated with temperature variation and weather. Temperature data, accumulated by Bergen from 1983 to June 1986 from a test road (in Florida), are analyzed. Slab displacements were monitored and evaluated. It is found that maximum daily displacements were concurrent with maximum temperature differentials in the slab. They pointed out "in many analysis of thermal stresses, temperature gradients have been assumed to be linear. This assumption has simplified the modeling of pavements without significantly affecting the accuracy of the computations. Therefore for all practical purposes the temperature gradient can be approximated by a linear curve." Richardson and Armaghani employed a parabolic function to model the nonlinear temperature parallel to the pavement thickness. In their particular case the nonlinear temperature stress is only 17 percent of the flexural strength. Although the importance of nonlinear temperature may not be important for deformation due to normal daily temperature fluctuation, they did not rule out the importance of the nonlinear temperature distribution during dramatic temperature changes. Because cracks are most likely to initiate during dramatic temperature changes, the nonlinear distribution can be important for our purposes.

In 1970's, continuously reinforced concrete pavement (CRCP) increase dramatically in use, for instance, from 1961 to 1971, increase is 20 time. In design of CRCP, allows the effects of shrinkage and temperature change to produce random cracks but keep the cracks tightly closed together. Comparing with plain concrete pavements, it has much shorter crack spacing and width. The average mature crack spacing is around 5 feet. The average percentage of steel is 0.6 (the more steel, the shorter the crack spacing.)

Most studies on the crack formation mechanisms in concrete pavements are still limited to the conventional models developed on the basis of stress-based or strain-based elasticity analysis. Jenq, Liaw and Kim (1993) applied the fracture mechanics to study the effects of temperature on early crack formation. To properly control the occurrence of random cracking, saw-cut grooves are generally introduced at the earliest possible age of the concrete pavement. Adequate groove depth must be provided to ensure that the transverse cracks will be confined at the location of the groove. The cohesive crack model and finite element method are used, once knowing the expected temperature deferential and thickness of the pavement, they can determine the timing and groove depth. Based on their theory the spacing of saw-cut groove can not be determined.

It is reported by Federal Highway (FHWA, 1990) that thermal cracking of asphalt pavement continues to be a problem in many parts of the Unite States. The low-temperature shrinkage cracking is concerned in Canada and northern United States,

and thermal fatigue cracking is now recognized as a problem in more temperate climates. The early models to predict thermal cracking are based upon empirical or statistical relationships that relate cracking to various asphalt specification data and environmental parameters.

More recently, fracture mechanics theory was used to develop a computer-based model that can be applied to the thermal cracking problem. During the development of this model, it was necessary to resort to statistical regression equations to predict fracture properties, rather than to incorporate fundamental asphalt or mixture fracture properties into the model. Thus, neither the statistical based models nor the more recently developed fracture asphalt model is a completely mechanistic approach for relating fundamental asphalt or mixture properties to the incidence of thermal cracking.

The study of this dissertation treat asphalt concrete as a quasibrittle material with significant post-peak softening behavior. Actually asphalt concrete is more like a viscoelastic material in the warm temperature. However, during winter weather, viscosity of the asphalt concrete become less important, and as an approximation it can be reasonably excluded in our analysis. Although the materiel properties are temperature dependent, the dependence is not as pronounced if temperature is low.

The cracking of the asphalt pavement is sometimes measured by the number of cracks per mile. Some data are reported (Ruth, 1982) as to how this cracking index increases year by year for different type of asphalt concrete mix. However, in this report, only the cracks that cross the whole traffic lane are counted. Conceivably, if shorter cracks are also included, the value of the crack index should be multiplied by a factor of 2 - 4. Accordingly, the first year average crack spacing is about 30 meters if only full grown cracks are counted. If shorter cracks are also included, then the spacing is about 7 to 15 meters.

CHAPTER III

INITIATION THEORY — FOR BRITTLE MATERIALS

Because of cooling, externally applied loads, residual-stress build-up due to creep, loss of moisture and consequent shrinkage, or other natural of imposed processes, cracks often form from smooth surfaces. Problems of this kind include shrinkage cracks in drying concrete, Shrinkage cracks in polymers due to aging and loss of moisture, desiccation cracks in deserts and at the bottom of dried up lakes, to name just a few. The situation may be idealized as a system of parallel Mode I equaldistance cracks normal to the smooth surface of half-plane.

The crack propagation of a system of parallel cracks was studied in detail with respect to a proposed hot-dry-rock geothermal energy scheme in late '70s. The stability analysis of crack propagation was done by Bazant and Ohtsubo (1977), Bazant, Ohtsubo, and Aoh (1979) and Bazant and Wahab (1979) that they adopted the finite element approach; also by Nemat-Nasser, Keer, and Parihar (1978), Keer, Nemat-Nasser, and Oranratnachai (1979), Sumi, Nemat-Nasser, and Keer (1980) that they formulated the problem in terms of a singular integral equation. But most attention is focused on the problem of how cracks develop in structures that already have them (crack propagation happen after crack initiation). Although Keer, Nemat-Nasser (1978, 1979) gave some crack spacing estimate based on arbitrary assumption.

The purpose of this research is to provide a theoretical analysis and numerical approach for the crack initiation problem. The initiation of thermally induced equally spaced and equal lengths parallel cracks in a half-plane consisting of a homogeneous isotropic linearly elastic brittle material are studied. The problem is stated and basic model is outlined in section 1. In section 2 the basic three conditions for governing crack initiation of brittle material are cast. The corresponding thermoelasticity problem is formulated in the form of integral equations in section 3, and the numerical method of solution is outlined in section 4. Numerical results, relevant discussion and comparison with other theoretical results at limit cases are then presented in section 5. The experiment evident of glass comparing with the solutions are reported in section 6. Some comments and a few conclusions are presented in section 7. The possible experiment is suggested in the final section.

3.1 Statement of Problem

Consider an elastic half-plane of unit thickness that occupies the region $y \geq 0$ (Fig.3-1a) and is under plane stress. The material is homogeneous and isotropic. The half-plane is subjected to initial strain $\varepsilon_x = \varepsilon_0 f(y/d)$ which may be caused by cooling or drying of the surface; f is a given strain function and d is the penetration depth of cooling or drying. The initial stress is $\sigma_x = E\varepsilon_x = \varepsilon_0 E f(y/d)$. The general shape of function $f(y/d)$ is shown in Fig.3-1b. The initial strain profile may be considered either an error function (which is the exact solution of the linear diffusion problem) or a parabolic function (which is an often used approximation). These functions are

$$f(y) = 1 - \frac{2}{\sqrt{\pi}} \int_0^{\sqrt{3}y} e^{-u^2} du \quad \text{or} \quad f(y) = (1-y)^2 \quad 0 \le y \le 1 \qquad \textbf{(3-1)}$$

with maximum value $f(0) = 1$. We shall use both functions. Basically they give similar results.

The phenomena of crack formation are often complicated by the randomness of material inhomogeneity. The initial cracks rarely appear in a regular and systematic way. In the case of large concrete blocks, the cracks are never straight and the spacing between these cracks is hardly uniform. In the case of a drying lake bed, the crack pattern may not be exactly hexagon; it may be in the shape of a pentagon or heptagon. However, it is also true that hexagon is the most common shape, and the sizes of these hexagons are almost uniform. In the case of penetration of a sea ice plate, it is found that the total number of radial cracks varies from experiment to experiment, but generally larger punch sizes produce more radial cracks (Frankenstein, 1963). Despite the randomness, there must nevertheless be deterministic laws underlying these phenomena.

However, due to lack of information, and because of the accompanying analytical difficulty, we dramatically simplify the problem into the idealized case of cooling of a perfectly homogeneous and isotropic elastic half-plane, in which we expect the initial cracks to be straight, perpendicular to the free surface (system of parallel cracks), their spacing uniform and their pattern regular. The temperature profile in the solid is not altered by the formation and extension of these cracks. Moreover, to simplify the analysis further, we assume that the initial cracks are of equal length a in this chapter. Thus we may concentrate on one cell of width b as shown in Fig.3-1c.

The problem is first decomposed into two separate problems. The first is the structure without cracks with the initial (or residual) stresses applied. The second is the structure without initial stress, but with cracks and the crack surface traction that are equal in magnitude to the initial stresses but opposite in direction. The solution is obtained by the superposition of these two problems. Since there is no stress intensity factor in the first problem, we can, therefore, study only the second problem. This is the standard approach studying the fracture mechanics problem in elastic materials with residual stresses.

3.2. Conditions Governing Crack Initiation from Smooth Surfaces

It is well known from experience that the formation of initial macroscopic cracks from a smooth surface of brittle material is a sudden event. The phenomenon of crack initiation involves transition between two states: One is the initial equilibrium state in which there are no cracks. The other is the first state of stable equilibrium at which the cracks have formed and have come to a stop but are simultaneously in a critical state from which they can propagate further in a stable equilibrium manner. In between these two states, the cracks are unstable and grow dynamically. The reason that the transition is dynamic is that the energy release rate as a function of crack length begins increasingly from zero. At the same time, since we treat the problem according to linear elastic fracture mechanics (supplemented by the strength criterion), the fracture energy is constant and nonzero. This is what causes the initial instability of crack growth. In this study we are interested only in the two equilibrium states and the basic laws governing them. Because the material is considered to be elastic the response is path independent, and so the dynamic transition between these two states need not be analyzed in order to solve the crack spacing problem.

The first condition governing the crack initiation is a stress condition: The tensile stress caused by load before cracking must reach the tensile strength of the material at least at one point. For any load below this level the material simply can not start to break.

The second condition is that the final state, as we have defined it, satisfy the Griffith law that the energy release rate be equal to its critical value. If the energy release rate were above the critical value, then the cracks already formed would be unstable and would not stop at the final state. On the other hand, if the energy release rate were below the critical value, then the cracks would have had to stop earlier and that state would not represent the final state.

The third condition is provided by the law of energy conservation, which requires the potential energy of the structure released due to crack jump to be fully converted into surface energy of the newly formed cracks. Note that the Griffith law (the second condition) is also a statement of energy conservation which is however applied to an infinitesimal crack extension and is represented by a differentiation of the potential energy, whereas the third condition is energy conservation for a finite crack jump and is represented by a finite difference in potential energy.

The three conditions of crack initiation can simply be written as

$$\sigma_x(x,0) \geq f_t\,; \quad G(a,d;b) = G_f\,; \quad U(0,d;b) - U(a,d;b) = aG_f \tag{3-2}$$

where f_t = tensile strength of the material; G_f = fracture energy of the material defined as the energy required to open a unit crack fully, U = strain energy within the cell of width b. For simplicity, we use here for the stress condition the equality $\sigma_x = f_t$, and postpone the consideration of the case of inequality. In the following derivation, we will make use of Irwin's formula for energy release rate in terms of the stress intensity factor,

$$G = -\frac{dU}{da} = \frac{K^2}{E} \tag{3-3}$$

where K = mode I stress intensity factor at the crack tip , defined as $K = \lim \sigma_x [2\pi(y-a)]^{1/2}$,and E = Young's modulus of the elastic material. With this relation and based on the third condition, we can express the strain energy change as

$$(0,d;b) - U(a,d;b) = \frac{1}{E}\int_0^a K^2 da \tag{3-4}$$

Furthermore, by combining the second and third conditions and rearranging, we can cast the three basic conditions as:

$$\sigma_x = f_t\,; \quad K^2 = EG_f\,; \quad aK^2 = \int_0^a K^2 da \tag{3-5}$$

Since all the equations refer only to a unit cell of width b (crack spacing) the second condition of crack initiation furnishes a relation between the ratios of a/b and d/b. In this way, solution of the crack initiation problem yields K as a function of a/b and d/b for the given initial strain profile. In other words, there is a one-to-one correspondence between crack spacing b and the loading depth d. Once the penetration depth d is given, the crack spacing b and the initial crack length a can also be determined. We will come back to this point later.

3.3 Mathematical Formulation

Since all these quantities are complicated functions of the geometrical configuration and the loading profile, the solution has to be numerical.

The problem of a half space weakened by equidistant parallel surface cracks has been studied by Bazant et al. (1977, 1979) using the finite element method, by Nemat-Nasser, Keer and Parihar (1978) using the dislocation representation, and by Nied (1987) using the displacement jump as the basic unknown. The problem was also reviewed by Bazant and Cedolin (1991). The stresses for one normal surface crack in a half space were given by Keer and Chantaramungkorn (1975), and Nemat-Nasser, Keer and Parihar (1978) modified the expression to obtain the stresses for an array of equidistant cracks on the surface. When all cracks are of equal length, as assumed here, the equation can be simplified. The condition that stress at the surface reaches the tensile strength may be written as

$$\sigma_x(0,y) = \frac{\mathrm{E}}{4\pi}\int_0^a D(t)\sum_{n=-\infty}^{\infty} g(t,nb,y)dt = -f_t\, f(y/d) \tag{3-6}$$

where E is the Young's modulus for plane stress condition and changed to $E/(1-\nu^2)$ for plane strain condition, where ν is Poisson's ratio. Function $D(t)$ represent the dislocation density . The kernel function g can be expressed as

$$g(t,x,y)=\frac{2(y+t)}{(y+t)^2+x^2}-\frac{(y+3t)[(y+t)^2-x^2]}{[(y+t)^2+x^2]^2}+\frac{4ty(y+t)[(y+t)^2-3x^2]}{[(y+t)^2+x^2]^3}$$
$$-\frac{(y-t)[(y-t)^2+3x^2]}{[(y-t)^2+x^2]^2} \tag{3-7}$$

Since g is an even function of x, the series in (3-6) may be written as

$$\sum_{n=-\infty}^{\infty} g(t,nb,y)=g(t,0,y)+2\sum_{n=1}^{\infty} g(t,nb,y) \tag{3-8}$$

Using the following two formulae (Gradshteyn and Ryzhik, 1965, pp. 23, pp. 36),

$$\sum_{n=1}^{\infty}\frac{1}{x^2+n^2}=\frac{1}{2x^2}[\pi x\coth \pi x-1] \tag{3-9}$$

$$\sum_{n=1}^{\infty}\frac{x^2-n^2}{(x^2+n^2)^2}=\frac{\pi^2}{2}\operatorname{csc}h^2\pi x-\frac{1}{2x^2} \tag{3-10}$$

the infinite series can be summed into a finite expression:

$$2\sum_{n=1}^{\infty} g(t,nb,y)=\frac{t^2-y^2-4ty}{(y+t)^3}+\frac{2\pi}{b}\coth\pi\frac{y+t}{b}-\frac{(y+3t)\pi^2}{b^2}\operatorname{csch}^2\pi\frac{y+t}{b}$$
$$+\frac{4ty\pi^3}{b^3}\operatorname{csch}^2\pi\frac{y+t}{b}\coth\pi\frac{y+t}{b} \tag{3-11}$$
$$+\frac{1}{y-t}\left[1-2\pi\frac{y-t}{b}\coth\pi\frac{y-t}{b}+\pi^2\left(\frac{y-t}{b}\right)^2\operatorname{csch}^2\pi\frac{y-t}{b}\right]$$

Also from (3-7) we have

$$g(t,0,y)=\frac{1}{t-y}-\frac{t^2-y^2-4ty}{(y+t)^3} \tag{3-12}$$

It is further convenient to represent the kernel function in the following form

$$g(t,0,y)+2\sum_{n=1}^{\infty} g(t,nb,y)=\frac{\pi}{b}g_1\left(\frac{\pi t}{b},\frac{\pi y}{b}\right) \tag{3-13}$$

where the function g_1 can be written as

$$g_1(t,y) = \frac{1}{t-y} + 2\coth(y+t) - (y+3t)\operatorname{csch}^2(y+t) + 4ty\operatorname{csch}^2(y+t)\coth(y+t)$$
$$+\frac{1}{y-t}\left[1 - 2(y-t)\coth(y-t) + (y-t)^2\operatorname{csch}^2(y-t)\right]$$

(3-14)

Because function $D(t)$ is singular at the crack tip, it is now convenient to introduce a new unknown function $C(t)$:

$$D(t) = \left(\frac{a^2}{a^2-t^2}\right)^{\frac{1}{2}} C(t) \tag{3-15}$$

which is a smooth function. Equation (3-6) is thus transformed into the following equivalent integral equation for the unknown function $C(t)$:

$$\frac{\mathrm{E}}{4\pi}\int_0^a C(t)\left(\frac{a^2}{a^2-t^2}\right)^{\frac{1}{2}} \frac{\pi}{b} g_1\left(\frac{\pi t}{b},\frac{\pi y}{b}\right)dt = -f_t\, f\left(\frac{y}{d}\right) \qquad 0<y<a \tag{3-16}$$

Also the unknown function C is a bounded function. Once the unknown function is solved, the stress intensity factor can be calculated as

$$\begin{aligned} K &= \lim_{y\to a^+}\sqrt{2\pi(y-a)}\ \sigma_x(0,y) \\ &= \lim_{y\to a^+}\frac{\mathrm{E}}{4\pi}\sqrt{2\pi(y-a)}aC(y)\left\{\frac{-i\pi}{\sqrt{a^2-y^2}}\right\} = -\frac{\mathrm{E}}{4}\sqrt{a\pi}C(a) \end{aligned} \tag{3-17}$$

The detail proof can be found in appendix 1.

3.4 Numerical Method

Since the first term of the expression of function g_1 is 1/(t-y), (3-16) is actually a Cauchy's singular integral equation. To solve it numerically, we first normalize the interval (0,a) by defining

$$s = t/a, \quad x = y/a, \quad C(as) = B(s) \tag{3-18}$$

Now the singular integral equation (3-16) can be written in the form

$$\frac{\mathrm{E}}{4\pi}\int_0^1 \frac{B(s)}{\left(1-s^2\right)^{1/2}} \frac{\pi a}{b} g_1\left(\frac{\pi as}{b}, \frac{\pi ax}{b}\right) ds = -f_t f\left(\frac{ax}{d}\right), \qquad 0 < x < 1 \tag{3-19}$$

Next, (3-16) is extended into the interval (-1, 1) by an even continuation:

$$B(-s) = B(s) \qquad 0 < s < \tag{3-20}$$

In this way, (3-16) can be equivalently expressed as

$$\frac{1}{2}\frac{\mathrm{E}}{4\pi}\int_{-1}^1 \frac{B(s)}{\left(1-s^2\right)^{1/2}} \frac{\pi a}{b} g_1\left(\left|\frac{\pi as}{b}\right|, \frac{\pi ax}{b}\right) ds = -f_t f\left(\frac{ax}{d}\right), \qquad 0 < x < \tag{3-21}$$

With the Gauss-Chebyshev quadrature and the collocation technique as described by Erdogan, Gupta and Cook (1972, pp. 380-381, where n is replaced here by 2n+1), we can convert the singular integral equation into a discrete form as

$$\begin{aligned} -f_t f\left(\frac{ax_j}{d}\right) &= \frac{1}{2}\frac{\mathrm{E}}{4\pi}\sum_{i=1}^{2n+1} \frac{\pi}{2n+1} B(s_i) \frac{\pi a}{b} g_1\left(\left|\frac{\pi as_i}{b}\right|, \frac{\pi ax_j}{b}\right) \\ &= \frac{\mathrm{E}}{4\pi}\sum_{i=1}^{n} \frac{\pi}{2n+1} B(s_i) \frac{\pi a}{b} g_1\left(\frac{\pi as_i}{b}, \frac{\pi ax_j}{b}\right), \qquad j = 1, 2, \ldots., n \end{aligned} \tag{3-22}$$

where n is the number of integration points and

$$s_i = \cos\left(\frac{2i-1}{4n+2}\pi\right), \qquad x_j = \cos\left(\frac{j\pi}{2n+1}\right) \tag{3-23}$$

let

$$\begin{aligned} e &= \frac{a}{b}, \qquad \Delta = \frac{d}{b}, \\ t_i &= \pi e s_i, \quad y_j = \pi e x_j. \end{aligned} \tag{3-24}$$

then equation (3-22) may be written as

$$\frac{\mathrm{E}}{4\pi}\sum_{i=1}^{n}\frac{\pi}{2n+1}B(s_i)H(t_i,y_j;e) = -f_t f\left(\frac{1}{\pi\Delta}y_j\right), \qquad j = 1,2,\ldots,n \quad \textbf{(3-25)}$$

where

$$H(t,y;e) = \pi e\{4t + 2\coth(y+t) - (y+3t)\coth^2(y+t)$$
$$+4ty\coth(y+t)[\coth^2(y+t)-1] - 2\coth(y-t) + (y-t)\coth^2(y-t)\}. \quad \textbf{(3-26)}$$

If we introduce

$$A(s_i) = -\frac{\mathrm{E}}{4(2n+1)}\frac{1}{f_t}B(s_i), \qquad i = 1,\ldots,n, \quad \textbf{(3-27)}$$

Then (3-25) become

$$\sum_{i=1}^{n}A(s_i)H(t_i,y_j;e) = f\left(\frac{1}{\pi\Delta}y_j\right), \qquad j = 1,2,\ldots,n \quad \textbf{(3-28)}$$

Such a system of linear equations can be easily solved, for example, by the method of triangular factorization. Once we know A, we can calculate the stress intensity factor K in the form of dimensionless stress intensity factor N as

$$N = \frac{K}{f_t\sqrt{2\pi b}} = -\frac{\frac{\mathrm{E}}{4}\sqrt{a\pi}C(a)}{f_t\sqrt{2\pi b}} = (2n+1)\sqrt{\frac{e}{2}}A(1) \quad \textbf{(3-29)}$$

Note that the numerical solution does not yield directly $A(1)$. The closest data point on which the unknown function is defined is $s_1 = \cos(\pi/(4n+2))$. In theory, an extrapolation, for instance a quadratic extrapolation, is needed to find $A(1)$. However, when n is large enough (for instance, $n = 50$), the difference between $A(1)$ and $A(s_1)$ is in the third of fourth digit, and thus is negligible.

The stress intensity factor, either in the form of K or the dimensionless form N, is obviously a function of a/b and d/b as well as the initial strain profile $f(y/d)$. Our purpose in the next section will be to find the relation between these geometric characteristics.

In terms of dimensionless stress intensity factor N, we can rewrite the last equation in (3-5) as

$$\int_0^e N^2(x,\Delta)dx = eN^2(e,\Delta) \tag{3-30}$$

Note that this equation is purely geometric, that is independent of the material properties. From this equation, we can establish a relationship, which turns out to be one-to-one, between e and Δ. Furthermore, let

$$l_0 = \frac{G_f E}{f_t^2} \left(or \frac{K^2}{f_t^2} \right) \tag{3-31}$$

This frequently used material characteristic, which will be called the effective length (or characteristic length), is an important quantity in this analysis. (For the concrete with Young's modulus E = 4.2 x 10^6 psi, fracture Energy G_f = 85 N/m = 0.485 lb/in, and the tensile strength f_t = 3.45 Mpa = 500 psi, the effective length l_0 would be 8.15 inches.) All the lengths characterizing the geometry will be normalized with respect to l_0. The second equation of (3-5) can now be converted to the form:

$$N^2(e,\Delta) = \frac{l_0}{2\pi b} = \frac{1}{2\pi b^*} \tag{3-32}$$

where $b^* = b/l_0$ is the dimensionless crack spacing. Also, the dimensionless crack length and loading depth can be defined as

$$a^* = \frac{a}{l_0} = \frac{a}{b} b^* = e\, b^* \qquad d^* = \frac{d}{l_0} = \frac{d}{b} b^* = \Delta\, b^* \tag{3-33}$$

In the calculations, the ratio Δ is given as an input. Then, using (3-30) we can solve for e. After e and Δ are known, the value of b^* is determined from (3-32). The dimensionless quantities a^* and d^* can be determined using (3-33). In this way, the problem is solved accurately and efficiently.

The detailed procedure are given step by step as :

(1). give ratio Δ (penetration depth d over crack spacing b);

(2). select ratio e (crack length a over crack spacing b);

(3). solve for $A(1)$ through eq.(3- 28) and calculate N by eq. (3-29);

(4). check equation (3-30). If N^2 satisfy it go to next step otherwise go back to step 2;

(5). determine b*, a* and d* by using eqs. (3-32), (3-33).

3.5 Analysis of Numerical Results

Fig.3-2 shows the relation between a^* and d^*, as well as between b^* and d^*. It should be emphasized that the relation plotted in Fig.3-2 between the penetration depth d^* and the crack spacing b^* (as well as the initial crack length a^*) does not apply for the subsequent crack evolution. Rather, each point in Fig.3-2 represents an event of crack formation. After the crack is formed, there are other laws that govern the further growth of the crack system, which have been discussed in detail by Bazant et al. (1977, 1979, 1991) and Nemat-Nasser et al. (1978, 1979).

The solid curve shows the error function and the dashed curve the parabolic function. As can be seen from Fig.3-2, the difference in the final results between these two profiles is not significant. Thus, all the following analysis refers to the parabolic profile only. As the dimensionless loading depth d^* increases, the spacing b^*, starting from a very large value (which is actually infinite), decreases monotonically. However, the initial crack length first decreases. After it reaches its minimum value, it increases with d^* towards infinity. Such a behavior must reflect the requirement of energy balance. The crack driving force is controlled by the loading depth d^*. For small d^* there is only a small amount of energy available, and so the cracks must be very sparse, crack spacing b^* must be very large and the crack length a^* must be very small. On the other hand, a larger d^* provides a larger amount of energy, and therefore a smaller crack spacing. Because the rate of decrease of b^* is initially dramatic, the energy available for each crack must be reduced. That is why initially the crack length must decrease with the loading depth. After the rate of decrease of b^* becomes less dramatic, the energy availability for each crack somehow catches up, and then the crack length a^* begins to increase monotonically with d^*.

For very large d^*, the crack length a^* is also very large. Therefore, for the crack tip, the free surface at $y = 0$ is no longer important. In addition, when the loading depth increases unboundedly, the initial strain distribution becomes uniform. The problem is thus transformed into an array of semi-infinite cracks under the uniform surface pressure f_t. The stress intensity factor for this problem can be solved analytically using Fourier transformation method (Tada, 1985), and the result is:

$$K = f_t \sqrt{b/2} \qquad \textbf{(3-34)}$$

Substituting this solution into the second equation of (3-5), we obtain the theoretical result for the lower limit of crack spacing $b^* = 2$. Such a limit serves as a check for our numerical calculation. Specifying a large value of d/b, we can solve for b^*, which is found to be always larger, but very close to 2. For example, when $d^* = 10^4$, b^* =2.026. If $d^* = 10^5$, then $b^* = 2.013$. For the concrete with the effective length l_0 = 20cm = 7.8 inches, the lower limit of crack spacing would be 15.6 inches.

The other limit corresponds to a small d^* value when the spacing is infinitely large. Since the interaction between the cracks can be neglected, the problem can be transformed into a single crack in an elastic half-plane. The numerical method described in the previous section can certainly be modified to solve for the stress intensity factor for this configuration, but we decide to use a simpler and more explicit approach. According to Tada (1985) (page 8.3a), the stress intensity factor can be expressed as

$$K = \frac{2f_t}{\sqrt{\pi a}} \int_0^a \frac{F(y/a)}{\sqrt{1-(y/a)^2}} f\left(\frac{y}{d}\right) dy \tag{3-35}$$

where $F(x) = 1.3 - 0.3x^{5/4}$. This formula has an error less than 0.5%.

Let

$$\frac{K}{f_t} = \frac{2}{\sqrt{\pi a}} \int_0^a \frac{F(y/a)}{\sqrt{1-(y/a)^2}} f\left(\frac{y}{d}\right) dy = \overline{K} \tag{3-36}$$

By introduce dimensionless variables

$$s = y/a, \quad z = y/d \text{ and } t = a/d \tag{3-37}$$

and dimensionless function

$$\Phi(t) = \int_0^1 \frac{F(s)}{\sqrt{1-s^2}} f(st)\,ds \tag{3-38}$$

thus

$$\overline{K}^2 = \frac{4}{\pi} a\Phi^2(t) = \frac{4d}{\pi} t\Phi^2(t) \tag{3-39}$$

The term $\overline{K}^2$ must satisfy the third condition of crack initiation in the form

$$\int_0^a \overline{K}^2 dy = a\overline{K}^2$$

It can be transfer to the following form by using the relation (3-38)

$$\int_0^t z\Phi^2(z)\,dz = t^2\Phi^2(t) \tag{3-40}$$

We can define another dimensionless function

$$\Psi(t) = \int_0^t z\Phi^2(z)\,dz \tag{3-41}$$

and rewrite (3-40) as

$$\Psi(t)/t = t\Phi^2(t) \tag{3-42}$$

Also according to (3-31) and (3-39)

$$l_0 = \overline{K}^2 = \frac{4d}{\pi} t\Phi^2(t)$$

so two following equations are obvious existed

$$t\Phi^2(t) = \frac{\pi}{4d^*} \qquad \Psi(t)/t = \frac{\pi}{4d^*} \tag{3-43}$$

To achieve adequate precision, Gauss-Chebyshev quadrature must be employed to calculate the function Φ. First we extend the integration interval to (-1, 0) as

$$\Phi(t) = \frac{1}{2}\int_{-1}^{1} \frac{F(|s|)}{\sqrt{1-s^2}} f(t|s|)\,ds \tag{3-44}$$

We now use the integration formula corresponding to the weight function $(1-s^2)^{-1/2}$ and obtain

$$\begin{aligned}\Phi(t) &= \frac{1}{2}\sum_{i=1}^{2n+1}\frac{\pi}{2n+1}F(|s_i|)f(|ts_i|)\\ &= \frac{\pi}{2n+1}\sum_{i=1}^{n}F(s_i)f(ts_i)\end{aligned} \tag{3-45}$$

where s_i has the same definition as one in (3-23).

We can determining the ratio *a/d* from equation (3-42). Then, through either of equations in (3-43), we can determine the value of d^*. This value of d^* is found to be approximately 2.281, and the corresponding crack length a^*=1.411 (when the initial strain profile is taken as a parabolic function). This result is also used as another check on our numerical calculations. The difference between the values just calculated and the extreme values of our previous numerical results is less than 0.4%.

The function $t\Phi^2(t)$ and $\Psi(t)/t$ is plotted in Fig.3-3. Note that, away from the origin, there is only one point at which these two curves intersect. Such a point happens to be the maximum point of function $\Psi(t)/t$, which is the dimensionless form of the total energy released due to the crack formation. This property can easily be verified by the definition (3-38) and (3-41) of these two functions. The ratio t = *a/d* = 0.6186 is such that the total energy released is maximized among all the other ratios. As a result, the penetration depth is minimized.

One is naturally led to the question: what will happen when the maximum tensile stress exceeds the tensile strength of the material while the penetration depth d^* is still much less than the minimum value 2.281? Such a situation can happen, for instance, when the half plane represents a very hot object, and the surface of which is suddenly brought into contact with a very cold medium. The surface stress quickly rises to $E\alpha(T_1 - T_0)$ (where α is the coefficient of thermal expansion and $T_1 - T_0$ is the temperature difference), but the penetration depth is initially very small because there is not enough time for the conduction of heat into the material.

According to our theory, when d^* is smaller than the lower limit value, there will not be enough energy available to open a crack, although the stress level is already high enough to break the material. As a result, the maximum tensile stress can rise above the tensile strength while the material retains its integrity. Now we can replace the stress condition with

$$\sigma_x(0,y) = \gamma f_t f(y/d) \qquad \gamma \geq 1 \tag{3-46}$$

Then, equations (3-40) and (3-44) will change to

$$\overline{K}^2 = \frac{4d\gamma^2}{\pi} t\Phi^2(t), \quad t\Phi^2(t) = \frac{\pi}{4d^*\gamma^2}, \tag{3-47}$$

When the stress condition is changed, the energy balance laws are also changed accordingly. In fact, the altered system will be the same as the equations in (3-42) except that the dimensionless loading depth d^* has to be replaced with $\gamma^2 d^*$. As a result, the critical ratio *a/d* is the same and the minimum penetration depth becomes $2.281/\gamma^2$, which is still finite, although smaller than the original minimum depth.

3.6 Experimental Evidence

The present theory appears to be compatible with the existing experiment evidence. In Geyer's experiment (Geyer et.al., 1982), a uniformly heated (at about 200

$^{\circ}C$) glass plate was put into contact with dry ice (at -78 $^{\circ}C$). Seconds after contact, a few cracks suddenly shot up in a dynamic manner. Since the paper did not report what kind of glass is used in the test, we assume that it was soda-lime glass. For this kind of glass, the tensile strength is typically 70 *MPa* (Bansal, 1986). The typical standard deviation in the glass tensile strength is about 20%. The Young's modulus reported in the paper is $E = 69\ GPa$. The thermal expansion coefficient is $8.5 \times 10^{-6}\,^{\circ}C$. The initial tensile stress caused by the temperature difference is calculated to be of $60 MPa$, which is larger than the tensile strength. If the fracture energy G_f is taken as 3.6 N/m as reported in the paper, the effective length of material l_0 is about $5 \times 10^{-2} mm$. With such a small reference length, only the part of the solution for small d^* and big b^* is relevant to this experiment.

It is observed that cracks do not form immediately after the hot glass is in contact. Rather, a few seconds are usually needed. This can also be explained by our theory: the penetration depth needs to reach a certain length (a process that takes time) before the cracks can form. The average spacing is about 1 to 2 *cm*, which is sufficiently large for b^* to be regarded as infinity. In this experiment, the maximum stress is larger than the tensile strength (λ is about 2). An over stressed plate can be highly unstable. For instance, any disturbance supplying energy (such as kinetic energy) can make the energy sufficient for crack formation. If this condition is met, the crack could form suddenly and probably in a dynamic manner. Another possible cause, for dynamic crack growth, probably more important, is the fact that the tensile strength decreases with an increase of temperature. Although the fracture energy also decreases with temperature, the rate of decrease is not as significant as the tensile strength. In the case of Geyer's test, the cold side of the glass plate is much stronger, therefore requires a higher level of stress to break the glass. However, once the cracks are formed and enter the zone of higher temperature, where the glass is less tough, then there is a surplus of crack driving force (that is, energy release rate). Such a surplus of driving force would certainly cause cracks to grow in an uncontrolled dynamic way.

3.7 Additional Comments and Brief Summary

Which d^* should be used depends on the loading method? Imagining that both the maximum value of the initial strain and the loading depth grow with time, one should take the loading depth at the moment when the maximum strain reaches the tensile strength. It is this loading depth that determines the initial crack spacing and the initial crack length. However, if the loading depth is still smaller than the minimum value, then the critical penetration depth will be the depth that first satisfies the relation $d^* = 2.281/\gamma^2$.

Nemat-Nasser et al. (1978), (1979) and gave an estimate of the lower limit of crack spacing by energy consideration. The idea is that the fraction of total strain energy before cracking should be used to generate new surfaces. From which , using our notation, the minimum crack spacing in the form of $b^* > 1/(\gamma^2 K_0)$. K_0 is an empirical coefficient depending on the initial strain loading profile, the ratio *a/d* and a parameter θ representing the fraction of strain energy to be used in creating new crack surfaces. However, neither *a/d* nor θ can be determined in their analysis, as is admitted by Nemat-Nasser (1979). In Geyer's paper, this factor is taken as 0.1. Therefore, their estimate of lower limit is 5 times larger than here. Bazant et al. (1979) also gave a similar estimate, and the value of a/d is considered to be at least 1.5, which is also larger than our result $a/d = 0.62$ (see Fig.3-3). An adequate experiment is needed to verify these theoretical predictions. Glass is probably not the best choice for the test, because its effective length is so small. Crack sizes in the range of 1 to 10 times of l_0 are very hard to observe by the naked eyes. Brittle materials with l_0 in the range of millimeters or even centimeters are preferable.

For small d^*, the initial crack length is of the same order as the effective length l_0. Note that l_0 is of the same order as the process zone length, which is a zone that contains highly nonlinear deformation. When the crack length is of the same order as the process zone length, the nonlinear effects are no longer negligible. The crack initiation theory, which is mainly based on linear elastic fracture mechanics, should be only regarded as the first approximation. The problem of determine the initial crack spacing in a material with a large nonlinear process zone is to be studied in the chapter V.

The crack initiation theory proposed herein is more general than either homogeneous isotropic materials or a half-plane problem. For example, for orthotropic or anisotropic material you may find a suitable representation for the components of stresses or the stress intensity factor (as a function of crack length, loading depth and crack spacing), then the problem can be solved in the same way as for isotropic material . For the purpose of applying the theory to more practical engineering problems and also checking the correctness of the initiation theory, the crack initiation of concrete pavements is to be studied in the next chapter.

The main contribution done in this chaper van be briefly summarized as follows:

1. The initial spacing and initial stable equilibrium length of parallel equidistant cracks emanating from the surface of a brittle elastic half plane can be determined from three conditions: (1) The stress at the surface reaches a given strength limit. (2) After the initial cracks form, the energy release rate equals its given critical value. (3) The finite energy release due to the initial crack jump equals the energy needed to form the crack (according to the given fracture energy of the material or fracture toughness).

2 The problem can be solved if the stress intensity factor as a function of loading depth, crack length and the crack spacing is known. The stress intensity factor can be solved using Cauchy's integral equation. For the limiting cases of infinite initial crack length and of infinite large crack spacing, the correct limiting values are approached, which provides a check for the accuracy of the numerical solutions.

3. The results of analysis compares favorably with available experimental evidence on thermal cracks in glass. However, this comparison is valid only in the range of very large initial crack spacing. For a complete check of the validity of the solution, further experimental studies are needed.

3.8 Outline of a Proposed Experiment

For a complete check of the validity of the solution, further experimental studies are needed. The following experiment may be conducted in a laboratory.

The brittle material suggested for experiment is gypsum, which is cheap and its characteristic length l_0 is suitable for a limit sized spacemen simulating a half-plane. Glass's l_0 is too small the naked eye may not observe crack forming. On contrary concrete's l_0 is too large, required size of specimen would be beyond our laboratory ability.

It is important to evaluate the material fracture properties. Beam specimens can be used for three-point bending tests. The dimensions of the beam specimen could be 12 inches long, 3 inches high, and 1 inch thick. During three-point beam test, the applied load, the CMOD (crack mouth opening displacement), and the load-point deflection (δ) should be monitored and stored in a digital form. The rate of loading is controlled by a constant increment of CMOD. The suggested loading rate is 0.01 in./min. The typical load-load line deflection (P - δ) and load-CMOD (P - CMOD) curves can be obtained from the test data. From these two curves, Young's modulus and fracture energy (G_f) can be evaluated. The Young's modulus value calculated from the load-CMOD curves are usually higher than those obtained from the load-deflection curves, as reported by other researchers. Fracture energy is defined as the area under the load-line deflection curve divided by the initial uncracked ligament area. Although the area under the load-CMOD curve does not have a direct physical meaning, the fracture energy calculated from it is comparable with that obtained from load-deflection curves. Since CMOD value is less sensitive to support settlements, the P-CMOD curve should be used to determine the fracture energy.

For determining the tensile strength , splitting tension tests can be conducted, which is carried out on a standard cylinder, tested on its side in diametral compression. The dimensions of the cylinder specimen could be 3 inches in diameter and 6 inches long. The test could be performed under displacement control at a rate of 0.005 in./min or under load control at a rate of 50 to 150 lb/in.^{2}/min. The tensile strength then can be calculated as $f_t = \frac{2P}{\pi LD}$, where P is the applied compressive load, L the cylinder length, D the cylinder diameter.

To observe the phenomena of crack initiation due to drying shrinkage the following experiment may be conducted in some laboratory. The top opened rectangle box, which inside dimension may be three feet width, one inch thick and two feet high (the final size should depend on the fracture material properties), can be made by concrete or some hard material because the deformation in width direction is not allowed. Two side panel in thickness direction should be greased, it would allow free movement along these panel surfaces. The moisture measure meters may be installed in the middle section distributed from top to bottom of box. The prepared gypsum paste then can fully fill the box. Keep the top of box open to evaporate water from this top surface.

The moisture record every certain period of time until the shrinkage cracks appear. Measure the crack spacing and depth and draw a moisture distribution curve, it can be modified as a drying profile. The results from the experiment and from the initiation theory can be compared and reported.

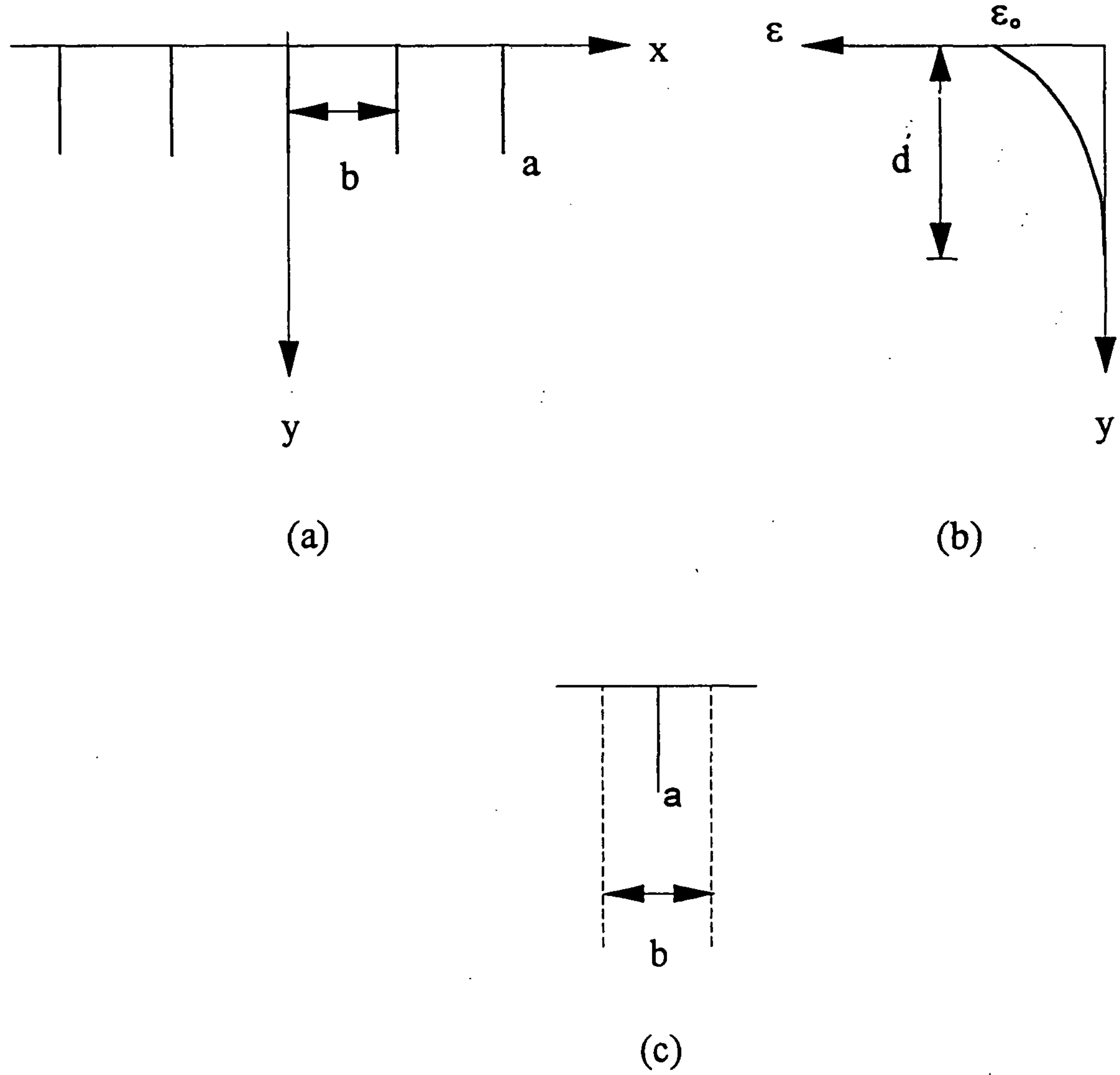

Fig. 3-1(a) Geometry definition of parallel crack system;

(b) Initial strain profile;

(c) Unit cell of width b.

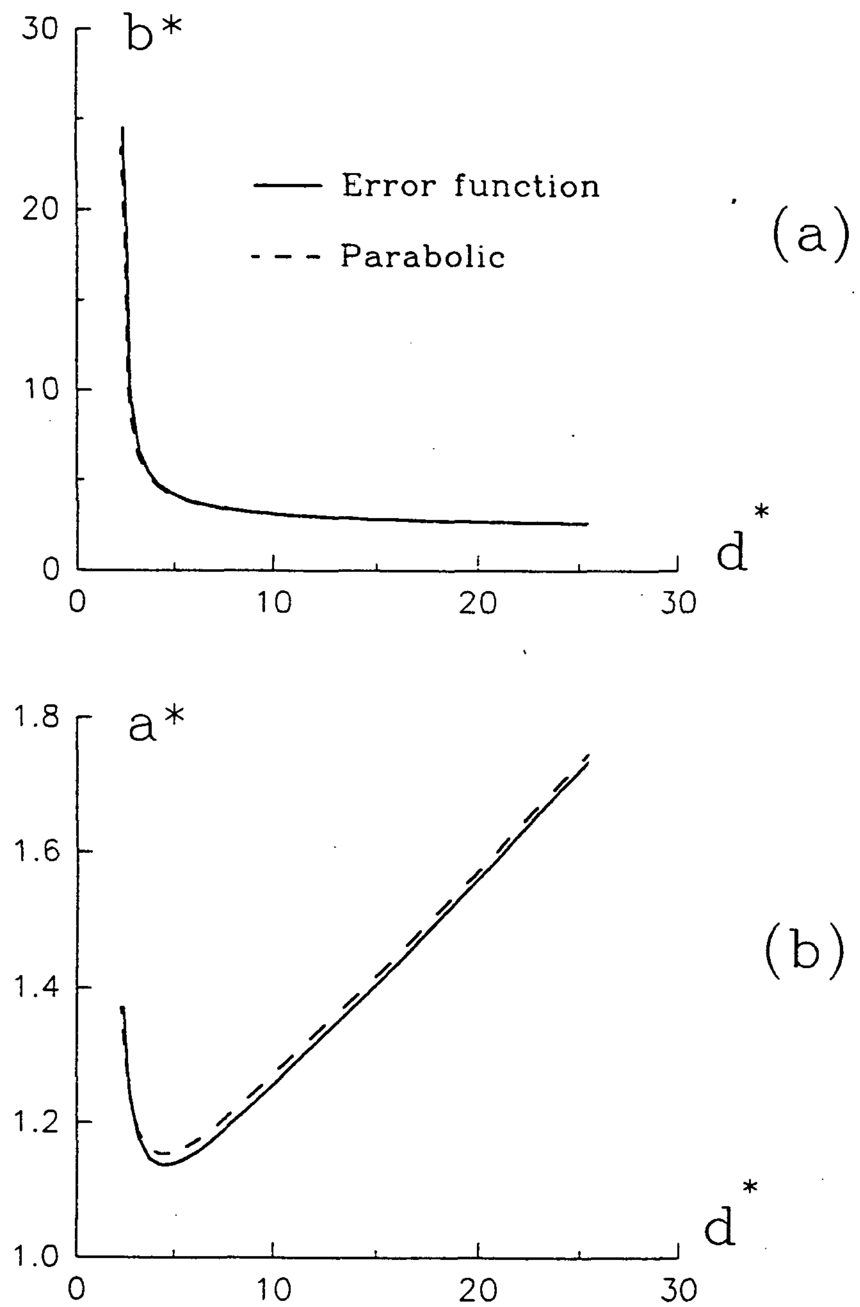

Fig.3–2 (a) Crack spacing versus load depth;
(b) Initial crack length versus load depth.

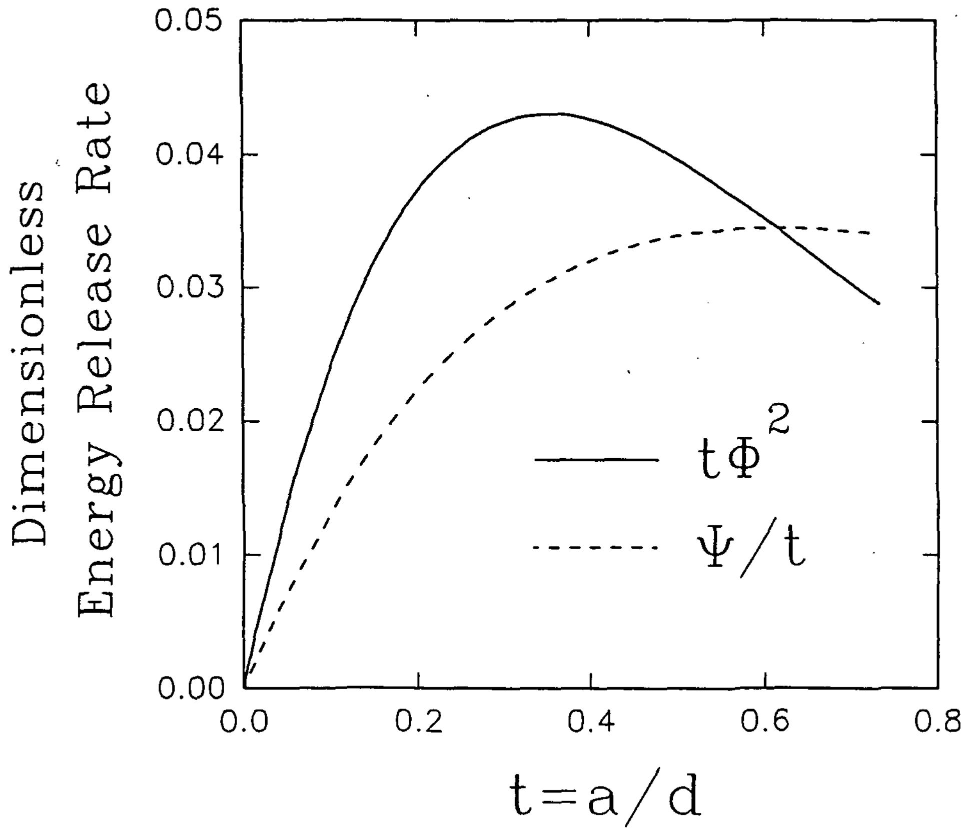

Fig.3−3 Energy release rate and average energy release rate as a function of a/d in the limit case

CHAPTER IV

CRACK INITIATION IN CONCRETE PAVEMENTS

It has been known that joints must be placed in Portland cement concrete pavement to control cracking that is caused by environmental changes. By providing joints, cracks either do not develop or develop only in a controlled manner related to the location of the joint. The cost of construction increases and the ride quality decreases if the spacing between the joints are short. Selection of joint spacing is motivated by above requirement. Many states have developed standards for joint spacing through experience. No rational procedure exists to determine the "correct" joints spacing. However, due to paucity of general understanding of the crack spacing phenomena, the best guideline, at the present time, is still the local road service record or certain rule of thumb. For instance, it is advised that the joints spacing (in feet) should not greatly exceed the slab thickness (in inches). It is therefore important to understand the basic physical mechanism of pavement crack spacing.

For asphalt concrete pavement, thermal cracking is one of the main causes of quality deterioration. Each seasonal cycle brings about new cracks in the surface course, and the extent of cracking is usually measured by the cracking index, which is the length of cracks in each unit area. The theory proposed in this paper is relevant when pavement surface is free of cracks, or when the cracks are still very sparse.

This dissertation aims to establish a simple mechanical model of concrete pavement that can be used to predict the spacing in pavement due to temperature differential. Crack spacing due to moisture change can be discussed in the same way if the coefficient of expansion due to moisture change is known for the material. The main purpose of this study is to identify the basic laws that govern the cracking phenomena in pavement, and using these basic laws to relate causes to their consequences. With these knowledge, it may improve our capability to extrapolate the experimental findings in one locality to another and thus reduce the cost and time required for repeated field tests on different geographical locations. The model proposed hopefully can serve as a theoretical foundation for pavement joint design.

Cracking in pavement is an example of a special class of mechanical problems in which a system of cracks suddenly occurs on a smooth surface under the action of temperature and moisture change. The problem of crack initiation from the surface of an elastic half-plane has been studied in the previous chapter. However, the problem of crack initiation in pavement has its own rights because of the following reasons. First, the pavement is very different from a homogeneous half-plane, the material property is dramatically different between the pavement and its foundation (or subbase). Second, the pavement material is not perfectly brittle so linear elastic fracture mechanics cannot be applied. As a result, a new modeling must be devised to take advantages of the structures main feature, and the crack initiation theory must also be modified to take into account of the influence of large process zone.

4.1 Mechanical Modeling of Pavement

The pavement is structurally modeled as an elastic plate sitting on a Winkler foundation(Fig.4-1a). To focus on the main issue, only transverse cracking will be considered in this paper. Therefore, we can take a slice of plate of unit width together with its supporting foundation in the longitudinal direction from the plate. Since we are only interested in the average behavior of cracking spacing in pavement, the crack spacing $2l$ and crack depth a are assumed to be uniform. Following the treatment of Okamura (1973, 1975) and also that of Rice and Levi (1972), the effect of cracks in a beam is represented by the increase in its compliance. Let Δ_t and θ_t be the total elongation and rotation of an elastic beam with an edge crack at the center (Fig.4-2) loaded by bending moment M (moment per unit width) and axial tension N (force per unit width) at both ends. M and N are reaction forces from adjacent plates. The positive M is defined as it would open the crack (top of beam in tension). The total deformation can be expressed as the sum of the deformation of the beam without a crack and the additional ones due to the crack, that is,

$$\Delta_t = \Delta_0 + \Delta_c \text{ and } \theta_t = \theta_0 + \theta_c \tag{4-1}$$

where subscript "0" denotes deformations of the beam without a crack, and "c" additional deformations due to a crack. These deformations also are corresponding to the whole beam, which are the sum of both ends deformation. The additional deformations can be related to these nominal forces as:

$$\theta_c = \lambda_{MM} M + \lambda_{MN} N, \quad \Delta_c = \lambda_{NM} M + \lambda_{NN} N \tag{4-2}$$

where λ represents the increments of the compliance functions caused by the existence of a crack, namely, λ_{MM} = additional rotation due to an unit bending moment, λ_{NN} = additional elongation due to an unit axial tension force, $\lambda_{MN} = \lambda_{NM}$ (due to reciprocity of linear elasticity) = elongation or rotation due to a unit value of M or N respectively. These additional compliances would be defined in section 4.

The basic equation of lateral equilibrium of plate resting on Winkler foundation can be written as

$$D\frac{d^4 w}{d x^4} + k_v bw = 0 \tag{4-3}$$

where $D = Ebh^3/12(1-\nu^2)$ = plate stiffness and k_v = the coefficient of subgrade vertical reaction; E =Young's modulus of pavement, ν = Poisson's ratio of pavement, b = plate's width, and h = plate's thickness. This equation is the same as that for an elastic beam in the plane strain condition. The external load need not be considered because only thermal effect is of concern. Also because the self weight of pavement only produce uniform downward movement and increase the magnitude of the contact stress, thus, the flexure of the beam is unaffected by effects of self-weight. We need not to consider it either.

The temperature vary through the thickness of pavement but not in planes parallel to the surface of the pavement. For simplicity the temperature distribution through the thickness of the pavement is assumed to be linear. This assumption is without significantly affecting the accuracy of the computations., as Armaghani, Larsen and Smith (1987) pointed.

The pavement is stressed by temperature differential, with T_t = the temperature differential at the top of the beam and T_b = the temperature differential at the bottom. Denote

$$M_T = \frac{E\alpha}{1-\nu}\frac{T_t - T_b}{2}\frac{h^2}{6}, \quad N_T = \frac{E\alpha}{1-\nu}\frac{T_t + T_b}{2}h, \tag{4-4}$$

as the moment and tension that the beam would experience if the corresponding deformation is restrained, α = thermal expansion coefficient of pavements.

4.2 Structural Analysis

The structure can be solved by the compatibility condition at the cracked section. Due to symmetry, only one half of the beam needs to be considered (Fig.4-1c). The elastic solution of equation (4-3), found from Selvadurai's book (1979), pp.84, is

$$w(x) = e^{\lambda x}(C_1\cos\lambda x + C_2\sin\lambda x) + e^{-\lambda x}(C_3\cos\lambda x + C_4\sin\lambda x) \tag{4-5}$$

where $\lambda^4 = k_v/4D$, λx is a dimensionless parameter. The constants C_i, (i=1,2,3,4) are to be determined by the boundary conditions of the beam.

From the homogenous solution (4-5) the slope , bending moment and shear force of the beam are given by

$$\theta(x) = \frac{dw}{dx}; \quad M(x) = D*\frac{d^2w}{dx^2} - M_T; \quad V(x) = -D*\frac{d^3w}{dx^3} \tag{4-6}$$

Boundary conditions $\theta(0) = 0$, $V(0) = 0$ and $V(l) = 0$ yield

$$C_1 = C_3; \quad C_2 = -C_4; \quad C_1 = QC_2$$

Then the solution can be written in the forms:

$$\theta_0 = 2\theta(l) = 4C_2\lambda\Psi(\lambda l), \quad M(l) = 4DC_2\lambda^2\Phi(\lambda l) - M_T \tag{4-7}$$

Where Φ and Ψ are dimensionless functions given as

$$\Phi(x) = \cos x \cosh x - Q(x) \sin x \sinh x \qquad \textbf{(4-8)}$$

$$\Psi(x) = Q(x)(\cos x \sinh x - \sin x \cosh x) + \cos x \sinh x + \sin x \cosh x \qquad \textbf{(4-9)}$$

and

$$Q(x) = \frac{\cos x \sinh x - \sin x \cosh x}{\cos x \sinh x + \sin x \cosh x} \quad , \qquad \textbf{(4-10)}$$

By eliminating C_2 from (4-7), we can obtain the following relation:

$$\theta_0 = \frac{\Omega(\lambda l)}{\lambda D}(M + M_t) \quad with \quad \Omega(\lambda l) = \frac{\Psi(\lambda l)}{\Phi(\lambda l)} \qquad \textbf{(4-11)}$$

The rotational compliance of beam can be defined as

$$C_{MM} = \frac{\theta_0}{M + M_t} = \frac{\Omega(\lambda l)}{\lambda D} \qquad \textbf{(4-12)}$$

The function Ω is plotted in Fig.4-3. As can be seen, when the nondimensional length λl becomes larger about 1.8, Ω starts to fluctuate and eventually approaches to 4. However, this behavior is not desirable from physical point of view, because it amounts to say that the bending compliance is bounded from above, while in reality the bending compliance must increase with beam length.

The assumption that the reaction from the foundation is proportional to deflection is reasonable when the beam deflection is downward. It becomes meaningless if the deflection is upward. A small portion of upward deflection is acceptable because the self-weight always produce uniform downward movement that keeps the beam in contact with the foundation, but if there are significant uplifting of the beam, then the compliance formula must be modified. The simplest remedy is to assume that the stiffness of the foundation can be neglected, one can use the simple beam theory to obtain

$$C_{MM} = \frac{2\theta(l)}{M(l)} = \frac{2l}{D} \qquad \textbf{(4-13)}$$

this compliance formula is proportional to the beam length. It will be seen later that (4-12) and (4-13) yields very close solutions for a small crack spacing, (4-13) is more reasonably behaved if the crack spacing is large. Therefore, the compliance function defined in (4-13) is preferable.

The elongation is related to the elastic normal force and thermal force through the following relation

$$\Delta_0 = C_{NN}(N + N_T), \quad C_{NN} = \frac{2l(1-\nu^2)}{Eh} \qquad \textbf{(4-14).}$$

Now the total deformations at the ends of beam can be expressed as

$$\theta_t = C_{MM}(M + M_T) + (\lambda_{MM} M + \lambda_{MN} N) \qquad \textbf{(4-15)}$$

$$\Delta_t = C_{NN}(N + N_T) + (\lambda_{NM} M + \lambda_{NN} N) \qquad \textbf{(4-16)}$$

The final equation for solving the bending moment and axial force depends on additional assumptions regarding the constraint in the longitudinal direction.

Case I. The full constraint at the ends of beam : $\theta_t = 0$ and $\Delta_t = 0$.

This case reflects that for an infinite long pavement , the ends of any unit beam are the surface of symmetry, at which above constrains conditions established. Through Eqs.(4-15) and (4-16), the bending moment and axial tension force can be solved from a set of coupled equations:

$$(C_{MM} + \lambda_{MM})M + \lambda_{MN} N + C_{MM} M_T = 0 \qquad \textbf{(4-17)}$$

$$\lambda_{NM} M + (C_{NN} + \lambda_{NN})N + C_{NN} N_T = 0 \qquad \textbf{(4-18)}$$

As we will see later, the crack spacing will be very sensitive to the thermal contraction, which is presented in the equation in terms of N_T.

Case II. Constraint only on rotation but not in axial direction: $\theta_t = 0$.

If there is no bonding or friction between the pavement and its subgrade, then the beam can expand freely in axial direction and the axial force N is zero consequently. We obtain an equation to determine the total moment as

$$(C_{MM} + \lambda_{MM})M + C_{MM} M_T = 0 \tag{4-19}$$

Case III. The same constraint condition as Case II and plus friction force.

If there is friction between the pavement and its subgrade, then during contraction the friction would act against the relative movement to prevent the contraction. Across the center of the beam the frictional force must change sign because of symmetry. The axial force at the end of the beam, denoted as N_f must be the total fractional force on one half of the beam span. Equation (4-17) must be modified as

$$(C_{MM} + \lambda_{MM})M = -C_{MM} M_T - \lambda_{MN} N_f \tag{4-20}$$

The simple formula of friction force (lb.) proposed by Friberg (1954) was $N_f = \int_0^l \frac{(l-x)F}{12}dx = \frac{Fl^2}{24}$ for a slab with length $2l$ inches, concrete weight of 1/12 lb. per cu. in., and average frictional coefficient F. According to his paper, the range of the ratios between elastic modulus and friction coefficient might be from $10^6/0.33$, to $4.5\text{x}10^6/1.5$. For the typical concrete system, with $E = 4.2\text{x}10^6$ psi, the friction coefficient F should be taken as 1.4, thus the friction force $N_f = 7l^2/120$.

The frictional force acts to enhance the effect of thermal loading in the pavement. This is in agreement with the engineering experience that the joint spacing must decrease for an increase of frictional coefficient. . However, according to our calculation, the effect of friction force on the crack spacing is practically negligible.

Subbases used many years ago were soft, loose and unbounded, such as sand, gravel and clay. Today stabilized agents, such as cement, lime and asphalt, are added to subbase materials, which lead to a strong bonding between the pavement and subbase in the tangential direction. As demonstrated by Wesevich (1987), the horizontal force is basically proportional to displacement for concrete slab placed on cement or lime treated clay subbases, suggesting that the interaction may be modeled as bonding rather than friction. For further increase of horizontal displacement, the resisting force approaches a constant. If that is the case, equation (4-18) should be used instead of the model to be proposed as follows. However, as will be seen later, neither bonding nor frictional forces seem to be important for determining the crack spacing in the pavement.

Case 4. The pavement is bonded to the subbase and full constrain (as Case I) at the ends.

If the pavement is assumed to be bonded to the subbase and the tangential force at the bottom is assumed to be proportional to the horizontal displacement, then the proportional constant, denoted as k_h and representing another elastic modulus of the properties of the subbase, must also be given. The equilibrium equation for a slice of pavement (of unit width) in the axial direction can be expressed as

$$\frac{Eh}{1-\nu^2}\frac{d^2u}{dx^2}-k_h u=0 \tag{4-21}$$

The solution that satisfies the condition $u(0) = 0$ can be written as

$$u(x)=C\sinh\mu x,\quad N(x)=C\frac{E\mu h}{1-\nu^2}\cosh\mu x \tag{4-22}$$

where $\mu^2 = (1\text{-}\nu^2)k_h\,/Eh$ and C is an arbitrary constant. The compliance function at the end of the beam is obtained as

$$C_{NN}=\frac{2u(l)}{N(l)}=2\frac{1-\nu^2}{Eh\mu}\tanh\mu l \tag{4-23}$$

It is straightforward to show that when k_h becomes vanishingly small, the compliance function increases and approaches the limit value $C_{NN}=2\,l(1\text{-}\nu^2)/Eh$. Therefore, bonding compliance reduces the axial compliance only, as our intuition would expect. The total axial force and bending moment must be solved by Eqs. (4-17) and (4-18) with C_{NN} being calculated according to (4-23). The moment contribution of this bonding force is neglected for the benefits of simplicity of the formulation.

Before we proceed further, it is important to note that in the above discussion, the thermal load is calculated on the assumption that the subbase dose not contract or expand with temperature. If the thermal deformation of subbase is also considered, then the thermal loads defined by (4-4) must be modified accordingly.

4.3 Stress Intensity Factors and Additional Compliance Functions

The stress intensity factors at crack tip caused by an axial force and bending moment, according to Tada's handbook (1985), can be represented respectively as:

$$K_N = \frac{N}{\sqrt{h}} k_N(e), \quad K_M = \frac{M}{h\sqrt{h}} k_M(e) \tag{4-24}$$

where $e = a/h$ = relative crack length and

$$k_N(x) = \sqrt{2\tan\frac{\pi x}{2}} \frac{0.752 + 2.02x + 0.37(1 - \sin\frac{\pi x}{2})^3}{\cos\frac{\pi x}{2}}, \tag{4-25}$$

$$k_M(x) = 6\sqrt{2\tan\frac{\pi x}{2}} \frac{0.923 + 0.199(1 - \sin\frac{\pi x}{2})^4}{\cos\frac{\pi x}{2}} \tag{4-26}$$

The total stress intensity factor $K = K_N + K_M$.

The elastic strain energy of structure due to cracking (also substituting the eqs (4-2) into expression) is

$$\begin{aligned} \Pi_c &= \frac{1}{2} N\Delta_c + \frac{1}{2} M\theta_c \\ &= \frac{1}{2}\lambda_{NN} N^2 + \lambda_{MN} MN + \frac{1}{2}\lambda_{MM} M^2 \end{aligned} \tag{4-27}$$

The energy release rate in terms of stress intensity factors by Irwin's formula can be expressed as

$$\begin{aligned} G &= (K_N + K_M)^2 (1 - \nu^2) / E \\ &= \frac{1-\nu^2}{E h^3}\left(h^2 N^2 k_N^2 + 2hNM\, k_N k_M + M^2 k_M^2 \right) \end{aligned} \tag{4-28}$$

Also
$$G = \frac{d\Pi}{da} = \frac{1}{2} N^2 \frac{d\lambda_{NN}}{da} + NM \frac{d\lambda_{NM}}{da} + \frac{1}{2} M^2 \frac{d\lambda_{MM}}{da} \tag{4-29}$$

By comparing above two expressions of G the following relations established between compliance functions and stress intensity factors as:

$$\frac{d\lambda_{NN}}{da}=\frac{2(1-\nu^2)}{Eh}k_N^2,\quad \frac{d\lambda_{NM}}{da}=\frac{2(1-\nu^2)}{Eh^2}k_N k_M,\quad \frac{d\lambda_{MM}}{da}=\frac{2(1-\nu^2)}{Eh^3}k_M^2 \quad \textbf{(4-30)}$$

By integrating them the compliance functions can be expressed as

$$\lambda_{ij}=\frac{2}{h^\eta}\frac{1-\nu^2}{E}\int_0^e k_i(e')k_j(e')de' \qquad \textbf{(4-31)}$$

where i, $j = M$ or N, $\eta = 0$ for λ_{NN}, $\eta = 1$ for λ_{NM} and $\eta = 2$ for λ_{MM}. The compliance function can be calculated according to these formulas using numerical integration method. In fact, the expression for λ_{MM} and λ_{NN} can be obtained directly from the fracture mechanics handbook compiled by Tada et al. (1985), only λ_{MN} needs to be calibrated according to (4-31) using numerical integration, see Appendix 2.

4.4 Crack Initiation Theory

The previous structural analysis allows us to calculate the internal bending moment and axial force once the crack spacing $2l$ and crack depth a are known. If there are no initial cracks in pavement, the internal moment and axial force can also be obtained using the method discussed in the previous section by letting the compliance of the cracked section being zero. As the thermal loading continues to increase, the tensile strength of the pavement is reached, and the necessary condition for crack initiation is satisfied. However, the strength criterion cannot determine what is the average crack spacing, nor can it determine the average depth of the cracks.

The energy release rate can be related to the net (total) stress intensity factor K by the Irwin formula as $K^2(1-\nu^2)/E$, the total stress intensity factor can be expressed as

$$K = K_N + K_M = \frac{N}{\sqrt{h}} k_N(e) + \frac{M}{h\sqrt{h}} k_M(e) \tag{4-32}$$

where N and M is determined by the method discussed in the previous section. Although the function k_N and k_M increases with relative crack length a/h, N and M decreases with a/h because if the section is totally severed N and M becomes zero due to loss of constraint. Once cracks start to gain enough lengths, the crack will stop growing when Griffith condition $G = G_f$ is satisfied. During the crack growth, the total energy needed to form new crack surfaces, which is aG_f for each crack, must be equal to the energy released by the structure, which is the shaded area under the curve in Fig.4-3. This is the very condition that determines the crack spacing.

The process of crack initiation consists a transition from the pre-initiation state, at which the strength criterion is satisfied, to the post-initiation state, at which the Griffith criterion is satisfied. More specifically, the proposed initiation theory in Chapter III can be restated as

(1) The maximum tensile stress must be equal to the tensile strength of the pavement at the pre-initiation state;

(2) The energy release rate of the structure must equal to the pavement toughness G_c at the post-initiation state;

(3) The total energy must conserve during the initiation process.

These three conditions play different roles in the solution procedure. The first condition determines the critical value of temperature differential, but it is not related to the cracked configuration. The temperature profile is considered fixed during the initiation process. The rest of the two conditions must be solved together to determine the crack spacing and crack depth for the post-initiation state.

Mathematically, with the temperature profile determined by the first condition, the axial force *N* and the moment *M* can be solved as functions of half crack spacing *l* and crack depth *a*. *l* and *a* can be determined by the second and the third condition, which are

$$G(a) = G_f, \quad \Pi(0) - \Pi(a) = a G_f \tag{4-33}$$

where P is the elastic strain energy of the structure. According to the definition of the energy release rate, the third condition can also be expressed as

$$\int_0^a G(a')da' = a G_c \tag{4-34}$$

The integral usually must be evaluated by numerical quadrature.

In the previous discussion, the material is assumed to be perfectly brittle. In terms of fracture mechanics analysis, brittleness means that the nonlinear process zone around the crack tip is negligible compared to characteristic structural dimension. It is widely known that Portland cement concrete is not a perfectly brittle material, its nonlinear process zone is often of several inches in size (Bazant, 1986a). To take the nonlinear behavior of the material into consideration, one must perform fracture mechanics analysis according to, for instance, the cohesive crack model (Hillerborg, 1976) with the softening stress described by the crack opening displacement, or equivalently, a crack band model (Bazant and Oh, 1983). The crack initiation theory based on nonlinear fracture mechanics theory, although extremely interesting and will be pursued in a future study, is too complex for the purpose of this study.

To obtain a simpler model, one should be cognizant of the difference between the fracture energies obtained using different methods of calibration. Based on the cohesive crack model, one can obtain fracture energy based on the work of fracture, as is shown schematically in Fig.4-4. The total work W_{total} done by the load P during a displacement controlled experiment is assumed to be totally transformed into creating new crack surfaces, which is equal to $2B(h-a)$, where B = the beam width, therefore the total fracture energy $G_f = W_{total}/2B(h-a)$. For Portland cement concrete, it is typically 80 ~ 120 N/m.

There are many other methods to calibrate the toughness of concrete on the basis of maximum load capacity, among them we mention the size-effect approach proposed by Bazant and Pfeiffer (1987) and the two-parameter model proposed by Jenq and Shah (1985). These methods are based on the peak load value of the experimental measurement. The fracture energy so obtained would be denoted as G_f^{eff}, which is usually in the range of 30 ~ 60 N/m.

The difference in the values of fracture energy can be understood from the point of view of the cohesive crack model. The maximum load that a structure can sustain, according to the cohesive crack model, depends on the slope of the softening curve, not the total area under the softening curve. This is because that the crack tip opening displacement at the peak load is less than its threshold value w_c. For concrete slab with thickness around 10 inches, the crack tip opening displacement at peak load is typically less $w_c/3$. In other words, the shape of the softening curve that corresponds to values larger than $w_c/3$ is irrelevant for the purpose of maximum load determination. In other words, the softening curve for the purpose of maximum load can be effectively replaced with a linear softening law with its slope corresponds to certain average slope of the original nonlinear softening law in its small crack opening displacement range. The total area under this linear softening law is denoted as G_f^{eff}. As shown by experimental studies, G_f^{eff} is typically 1/2 ~ 1/3 of G_f, which is the total area of the original nonlinear softening law, as is shown schematically in Fig.4-4.

The second condition of crack initiation is concerned with the load bearing capacity of the structure in the post-initiation state, therefore it seems appropriate to use G_f^{eff} as a measure of material toughness. The third condition is a statement of energy conservancy, therefore G_f appears to be more relevant as a measure of material toughness. It should be noted that the difference between the two measure is size-dependent, and G_f^{eff} would approach G_f if the characteristic size of structure becomes very large. Thus, the crack initiation theory given previously is correct if the material is perfectly brittle. But for pavement, the difference between G_f^{eff} and G_f must be reflected in the crack initiation theory. To this end, the second condition of the crack initiation theory may be written, mathematically, as

$$G = G_f^{eff} = \beta G_f, \quad \beta = G_f^{eff} / G_f \tag{4-35}$$

where the typical value of β ranges from 1/2 to 1/3. The third condition remains the same. In this way, the nonlinearity of the pavement material can be approximately accounted. As will be seen later, the modification dose not have significant influence on the final crack spacing and crack depth. The nonlinear effect of the material, therefore, does not seem to be consequential by this approximation.

4.5 Numerical Method

It is useful to use a non-dimensional form to understanding the dependence of the solution on various material properties. For this purpose, the following non-dimensional nominal stresses can be introduced

$$\sigma_N = \frac{N}{f_t\, h}, \quad \sigma_M = \frac{6M}{f_t h^2} \tag{4-36}$$

where f_t is the tensile strength of the material. With these notations the first condition of crack initiation theory can be simply expressed as

$$\sigma_N + \sigma_M = 1 \tag{4-37}$$

while the second condition becomes

$$\left(\sigma_N k_N(e) + \frac{\sigma_M}{6} k_M(e)\right)^2 = \frac{\beta l_0}{h} \tag{4-38}$$

where $l_0 = E\, G_f /(1-\nu^2) f_t^2$ = the effective length of the pavement. The third condition becomes

$$\frac{1}{e}\int_0^e \left(\sigma_N k_N(e') + \frac{\sigma_M}{6} k_M(e')\right)^2 de' = \frac{l_0}{h} \tag{4-39}$$

It should be emphasized that, although not explicitly written in (4-38) and (4-39), σ_N and σ_M depends on the relative crack depth as well as crack spacing.

Also the equations for solving bending moment and axial force can be written in nondimensional form. By defining the nominal thermal bending stress as $\sigma_M^T = 6M_T / h^2 f_t$ and nominal thermal normal stress as $\sigma_N^T = N_T / h$, the basic coupled equations (4-17) and (4-18) (in Case I) in the nondimensional form are

$$(C^*_{MM} + \lambda^*_{MM})\sigma_M + \lambda^*_{MN}\,\sigma_N \; + C^*_{MM}\,\sigma^T_M = 0 \tag{4-40}$$

$$\lambda^*_{MN}\,\sigma_M/6 + (C^*_{NN} + \lambda^*_{NN})\sigma_N + C^*_{NN}\,\sigma^T_N = 0 \tag{4-41}$$

where the non-dimensional compliances due to a crack are defined as

$$\lambda^*_{MM} = \lambda_{MM}\frac{h^2}{6}\frac{E}{1-\nu^2} = \frac{1}{3}\int_0^e k^2_M(e')de' \tag{4-42}$$

$$\lambda^*_{MN} = \lambda_{MN}\frac{Eh}{1-\nu^2} = 2\int_0^e k_N(e')k_M(e')de' \tag{4-43}$$

$$\lambda^*_{NN} = \lambda_{NN}\frac{Eh}{1-\nu^2} = 2\int_0^e k^2_N(e')de' \tag{4-44}$$

and their empirical expression are presented in appendix 2.

The non-dimensional compliance functions are defined as

$$C^*_{NN} = C_{NN}\frac{E}{1-\nu^2} = \frac{2\lambda l}{\lambda h}, \quad C^*_{MM} = C_{MM}\frac{h^2}{6}\frac{E}{1-\nu^2} = \frac{2\Omega(\lambda l)}{\lambda h} \tag{4-45}$$

Since the compliance function due to cracks is zero if the crack length is zero, the nominal stresses at pre-initiation state can be simply solved as $\sigma_M = -\sigma_M{}^T$ and $\sigma_N = -\sigma_N{}^T$. Therefore the first condition, the necessary condition for crack initiation, becomes

$$\sigma^T_M + \sigma^T_N = -1 \tag{4-46}$$

which becomes a condition to determine the critical temperature deferential. When the distribution of the thermal stress is far from being linear, then (4-46) should be disregarded in favor of the condition expressed in (4-37).

Combining (4-38) and (4-39), we obtain the following equation:

$$\frac{\beta}{e}\int_0^e \left(\sigma_N k_N(e') + \frac{\sigma_M}{6}k_M(e')\right)^2 de' = \left(\sigma_N k_N(e) + \frac{\sigma_M}{6}k_M(e)\right)^2 \qquad (4\text{-}47)$$

For a given reasonable value of crack spacing l, one can always determine e from (4-47). To prove this, one needs to know that the net stress intensity factor K is zero when e approaches 0 or 1. The first zero is due to the fact that stress intensity factor approaches zero as $e^{1/2}$ when $e \to 0$. The second zero is due to the fact that the total stress intensity factor K also approaches zero when e approaches 1. This is because that the compliance functions due to crack approaches infinity as $1/(1-e)^2$, forcing the nominal stresses due to tension or bending approaches zero as $(1-e)^2$. Although the stress intensity factors due to unit load approaches infinity as $1/(1-e)^{3/2}$, thus the total stress intensity factor K must approach zero like $(1-e)^{1/2}$ when e approaches 1. Translated into the language of energy release rate, we know that G approaches zero like $1-e$ when e approaches 1.

The actual structure of K is more complex. Depending on the tensile component of thermal stress σ_N^T, K can be negative for a significantly large crack length, with the negative portion of K is deliberately cut off, see Fig.4-5. This phenomena is particularly obvious for large compressive axial thermal stress σ_N^T (negative values in the plot). Although K becomes positive again for even larger crack length, this region cannot be reached unless additional energy is available to assist the crack to jump through the valley of negative K. Although the energy release rate is still positive for negative K, this value does not represent the energy that can be released from the structure by crack propagation. For this reason, it is necessary to ensure, by means of numerical algorithm, that the solution of crack depth does not cross the valley of negative K values.

Based on these observations, we know that G must be an increasing function initially and becomes a decreasing function eventually. When G is an increasing function, its average value from 0 to e must be smaller than the current value. Since β is less than 1, the left hand side of (4-47) must be less than the right hand side of (4-47) for small e value. For e closes to 1, the average value of energy release rate must be a positive number while the energy release rate approaches zero, thus the left hand side of (4-47) must be larger than the right hand side of (4-47). Consequently, there must be a relative crack length e between 0 and the boundary of negative-K value that satisfies (4-47). This property is essential to design a successful numerical algorithm to solve the unknown crack spacing and crack depth. Once the crack depth is solved as a function crack spacing, one can use the second condition (4-38) to determine the crack spacing. This is the main feature of the numerical method used in this study.

4.6. General Behavior of the Model

In the following numerical examples, the thickness of the concrete slab is taken as 10 inches, which is a typical value in the pavement design. The material properties used in these calculation is $E = 4.2*10^6$ psi, $\nu = 0.18$ and $k_v = 400$ lb/in^3. With these parameter, $\lambda =$ 0.0293 (1/in.). The parameter β is chosen to be 1/3. For typical Portland cement concrete the material length is about 7 inches, in which the toughness of the material must be defined by the work-of-fracture method. The tensile strength f_t and thermal expansion coefficient α need not to be specified at this point because these parameters do not enter into equations (4-38) or (4-39). They will determine the critical value of temperature differential.

The simplest case is the pure bending without axial constraint (case II). The crack spacing and crack depth in inches are plotted in Fig.4-6 as a function of material length l_0, which is also measured in inches. The effect of different compliance functions is clearly demonstrated. If C_{MM} is defined by (4-12), that is, if the pavement is modeled as a beam resting on a Winkler foundation, then there is a upper limit for l_0 beyond which there is no solution for the crack initiation problem. This upper limit is obviously related to the upper bound of the compliance function, as explained in the previous discussion. On the other hand, the crack spacing is basically a linear function if C_{MM} is defined by (4-13), which appears more reasonable from physical point of view. When l_0 is small, both compliance functions yield very similar results.

When the axial deformation is constrained (case I), crack opening is restrained by the compressive force it generates, the crack depth is smaller whereas crack spacing is larger for the same l_0., as can be seen from Fig.4-7. The crack spacing approaches infinity when l_0. approaches certain finite value. One may argue that the extreme sensitivity of the crack spacing when l_0 is close to its upper limit value is not reasonable from the physical point of the view. For small l_0. values, these two compliance functions again yield very similar results. Therefore, only the compliance function defined in (4-13) will be used in further discussion.

The bonding between the pavement and foundation is plotted in Fig.4-8 with the l_0. fixed 3 and 7 in., respectively. Adequate data for the k_h value are difficult to find in the open literature. If we assume $k_h = k_v$, then $\mu \approx 3\text{x}10^{-3}$ (in.$^{-1}$). At this magnitude, the tangential bonding is not particularly important if l_0 is 7 inches. It can be important for larger value of

l_0 though. For smaller l_0 value this bonding effect can be neglected for all practical purposes.

The effect of β is plotted in Fig.4-9 with no tangential bonding but with axial deformation constrained. Although it may come as a surprise, the influence of β is not important at all. The most substantial influence on crack spacing, in addition to the material length l_0, comes from the thermal stress distribution. As shown in Fig.4-10, if there is a substantial tension component in the thermal loading, then the spacing is significantly reduced. If there is a compressive component, then the spacing is dramatically increased.

It is instructive to know what will happen when there is only uniform temperature drop when the axial deformation is constrained. Since there is no bending, the beam would simply break into segments. The average length of these segments would be the crack spacing in this limiting case. Because the beam is totally severed, the crack depth $a = h$, the beam depth. Therefore the second condition is nullified, and only the first and the third conditions remain. The third condition can be written as $2lh\sigma^2/2E' = hG_f$. The conversion must occur at $\sigma = f_t$. As a result, one obtains that the minimum crack spacing $2l = 2l_0$. It can be seen from this analysis that l_0 is simply the ratio of specific elastic energy to fracture energy, which is why l_0 is one of the main factors that determine the crack spacing. This minimum value of crack spacing was also obtained in the previous study of spacing of parallel cracks initiated from the surface of an elastic half plane.

For more general loading configuration, the elastic energy that can be stored, as well as the fracture energy needed, depend on the crack depth. This is why the second condition of the initiation theory must be employed. However, the main picture is still the global energy conservancy. The more elastic energy is stored per unit length, the smaller the crack spacing will be; and vice versa. For instance, the elastic energy per unit length would be smaller if the restraint by the foundation is considered. That is why the spacing predicted with a Winkler foundation in effect is generally larger than the spacing without a foundation. For the same reason, the axial constraint leads to larger crack spacing because the deformation is constrained, thus less elastic energy is stored in the beam per unit length. The effect of axial thermal loading can also be explained. As can be seen from Fig.4-5, with a uniform contraction in thermal loading, the overall K value(and thus the total energy that can be released from the structure) is increased, thus smaller crack spacing. On the other hand, with uniform thermal expansion, the energy that can be released from the structure becomes smaller, thus larger crack spacing becomes necessary.

4.7 The Effect of Nonlinear Temperature Distribution

As was shown by Armaghani et al. (1987) that the nonlinear temperature distribution caused by daily temperature fluctuation is not very significant. In other words, the thermal load calculated according to (4-4) is a good approximation if we are only concerned with the thermal stress caused by daily temperature changes. However, any pavement structures with adequate design should not develop cracks under normal daily temperature changes. It is very likely that the critical condition is met when unusual weather conditions occur. For instance, a rainstorm in a hot summer afternoon will bring drastically cool off the temperature in the top layer of the pavement, as shown in Fig.4-11a.

The temperature distribution becomes very different from a linear distribution, thus the thermal loads calculated according to (4-4) is no longer appropriate. Asphalt concrete pavement invariably develops thermal cracks in northern American states during winter season when the temperature drops rapidly in the night. The temperature profile is schematically plotted in Fig.4- 11b. In these cases (4-4) must be modified.

Let $T(z)$ be the temperature increment (that is, the measured temperature minus the reference temperature at which there is no thermal stress) along the pavement depth. The thermal stress is $E\alpha T/(1-\nu)$. The critical temperature distribution is determined by the condition that the stress at the top surface is equal to the tensile strength of the material. The thermal bending and thermal tension can be calculated as

$$M_T = \frac{E\alpha}{1-\nu}\int_{-h/2}^{h/2} T(z)z\,dz, \quad N_T = \frac{E\alpha}{1-\nu}\int_{-h/2}^{h/2} T(z)\,dz \qquad \textbf{(4-48)}$$

The nondimensional nominal thermal stresses $\sigma_M{}^T$ and $\sigma_N{}^T$ are, again, defined according to (4-36). The crack initiation condition on the nominal thermal stresses (4-46), which is established on the assumption of linear temperature profile, must be discarded.

It is assumed that the elastic bending and tensile stresses can still be determined by (4-40) and (4-41) during crack propagation. This is because once cracks occur, only the bending and tension is the dominant deformation modes away from the cracked cross section, which are captured by our mechanical model. As a result, cracks are initiated with lower level of elastic energy per length stored in the pavement, which in turn causes larger crack spacing. This effect can be important when theoretical predictions are to be compared with field observations.

As a demonstrative example, let's estimate the crack spacing in the asphalt concrete pavement. In the state of Illinois, the crack spacing developed in the pavement, after first winter, is about 8 to 12 meters on the average. Similar value of the first year crack spacing can be also deducted from the data given by McLeod (in the discussion of the paper by Ruth et al. 1982). The asphalt concrete is a very complex material, with material properties vary strongly with temperature. Asphalt concrete becomes quite brittle under low temperature, especially under temperature below freezing point. Although the experimental data of material length l_0 is not available, we take $l_0 = 10$ in. for asphalt concrete, which is believed to be a reasonable value, judging from the fact that Portland cement concrete typically has $l_0 = 7$ in. Assume also that the critical thermal stress $\sigma_M^T = 0.7$ and $\sigma_N^T = 0$ during a rapid temperature drop in a winter night. Furthermore, it is assumed that the pavement thickness is 10 in. and the effect of foundation can be neglected (i.e. the elastic bending compliance is calculated according to (4-13) and tangential bonding between the pavement and its subgrade is considered). Under these assumptions, the calculated crack spacing is $2l = 388$ in., which is approximately 10 meters and is very realistic in comparison with the field observation. If the nonlinear critical temperature yields $\sigma_M^T = 0.5$, then the crack spacing would become more than 800 in., or 20 meters, which is still reasonable. The actually values of these parameters must be determined by experiment.

4.8 Discussion and Conclusions

In this chapter, a simple mechanical model for predicting the crack spacing in concrete pavement is proposed. The pavement is modeled as a simple beam with or without a foundation, and the influence of cracks in the pavement is simulated by the increase of the compliance. As a result, a simple yet effective analytic model is obtained. It is emphasized that the occurrence of cracking in pavement is determined by the strength criterion, and no attempt is made to improve the strength criterion. Our model is aimed at predict the average crack spacing and crack depth after the strength criterion is satisfied. Therefore, the proposed model complements the existing knowledge on the phenomena of pavement cracking.

The main contribution can be summarized as follows:

1. The crack spacing can be influenced by many different factors. The most important factors are the material length l_0 and the distribution of thermal stress. The effect of the foundation can be important only under extraordinary condition, such as perfect strong bonding.

2. For nonlinear material, a distinction must be made among the concepts of fracture energy. The effective fracture energy, which is defined on the basis of load capacity, can be as little as 1/3 of the total fracture energy, which is defined by the work of fracture method. The effective fracture energy must be used with the second condition of crack initiation theory, while the total fracture energy must be used with the third condition.

3. It is demonstrated that the most main mechanism that controls the crack spacing in the pavement is energy conservancy. If the elastic energy per length that can be released by crack propagation is large, then the crack spacing is small, with $2l_0$ being the smallest possible value. This relation can probably be developed into an experimental procedure to determine the material length l_0 directly

4. Thermal cracking usually occurs during extreme weather conditions, in which the thermal stress distribution can be far from linear. When such a thermal stress becomes critical, meaning that the maximum tensile stress reaches the tensile strength of the material, the crack will initiation under rather small stress level, causing larger crack spacing.

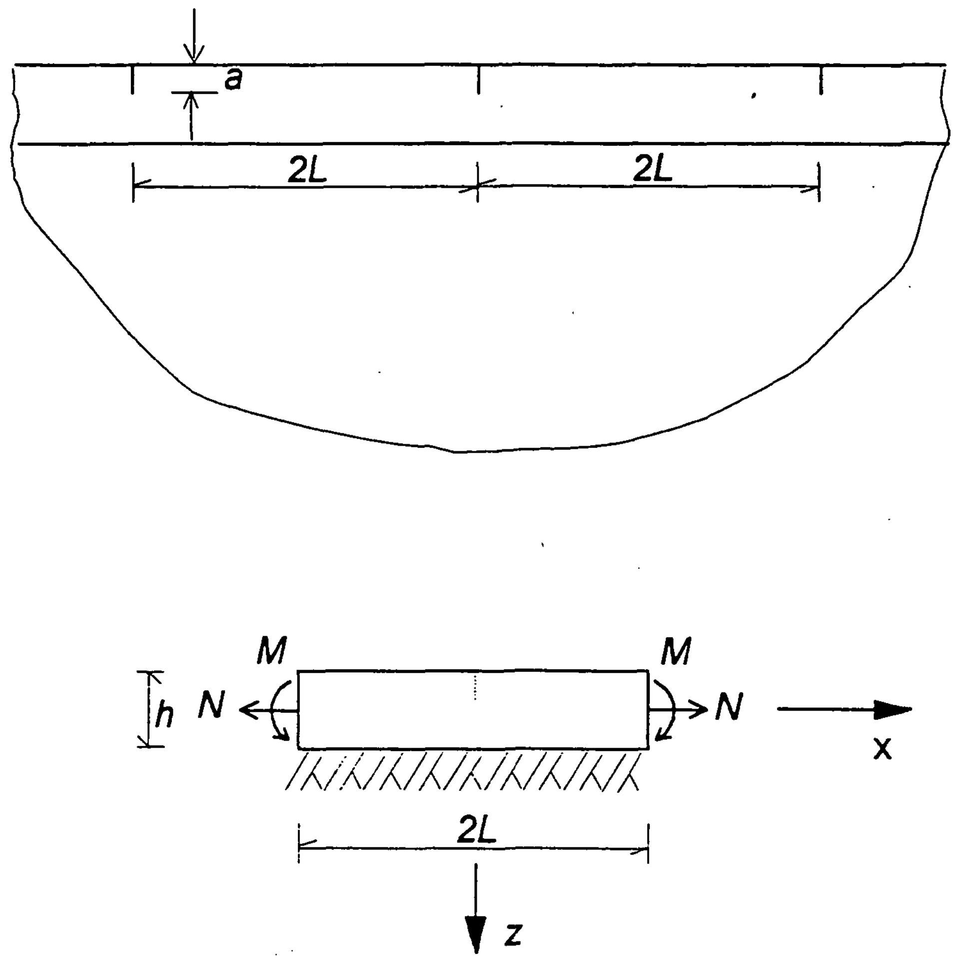

Fig.4-1 Geometry definitions for
(a) pavement on an elasic foundation;
(b) a unit cell with an edge crack in the center.

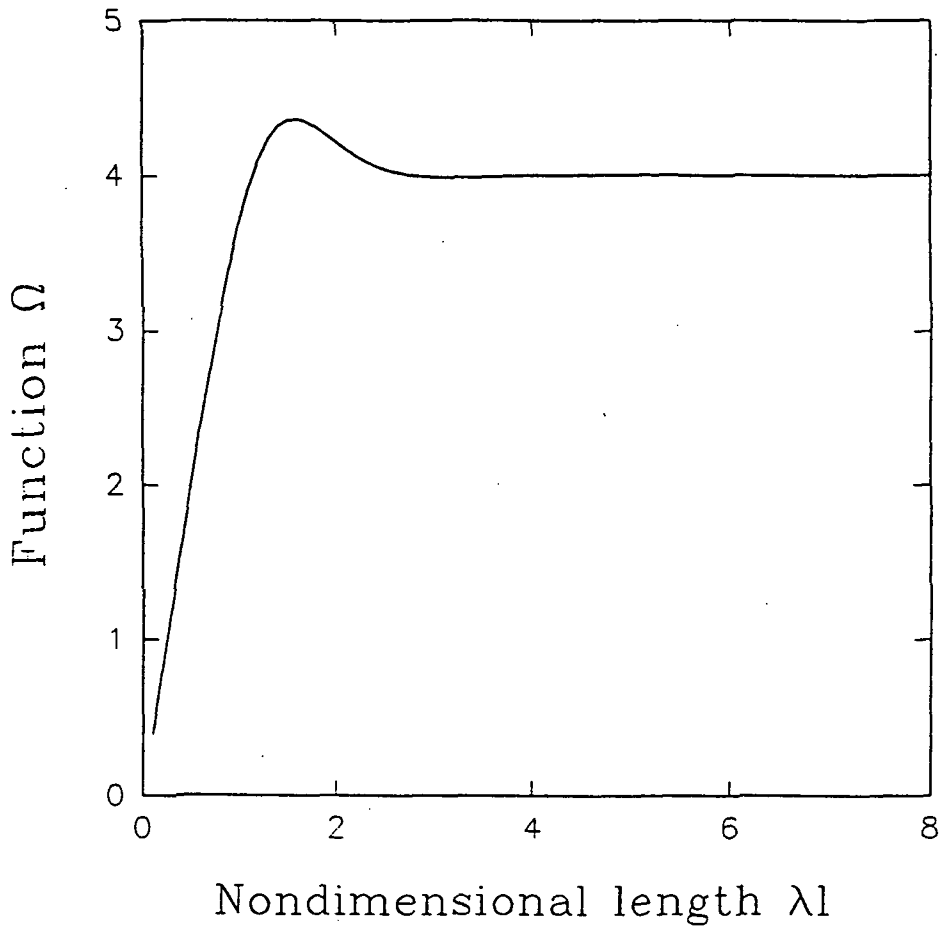

Fig 4-2 The length-dependent bending compliance of a beam on Winkler foundation

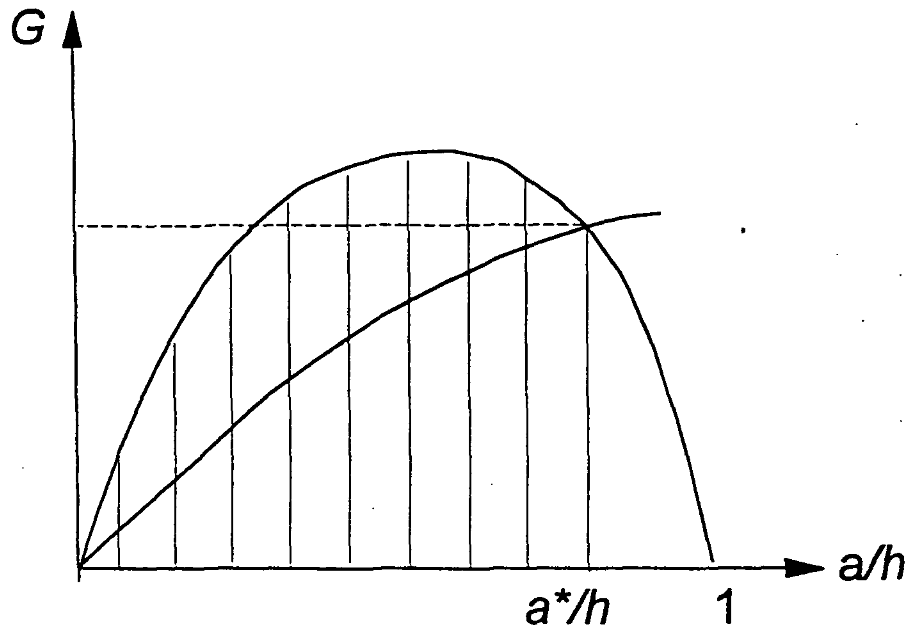

Fig.4-3 Schematic of crack initiation theory

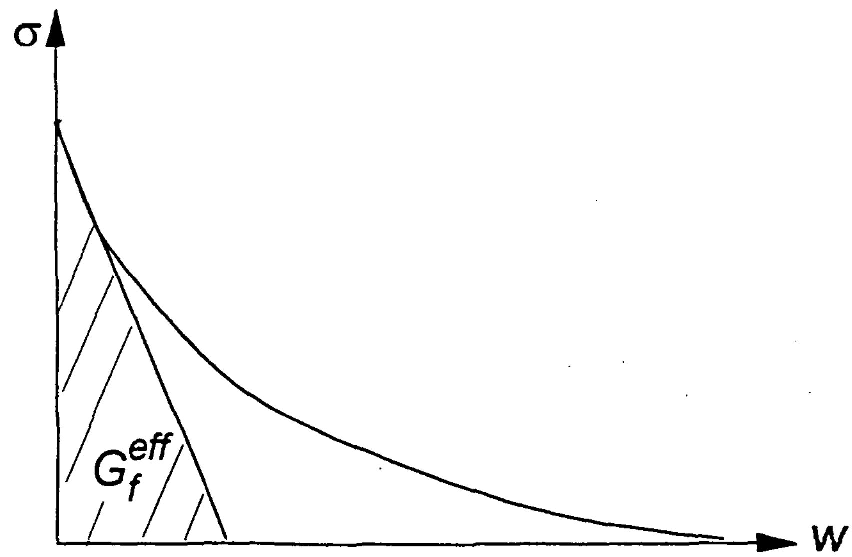

Fig.4-4 Definitions of effective fracture energy
and total fracture energy

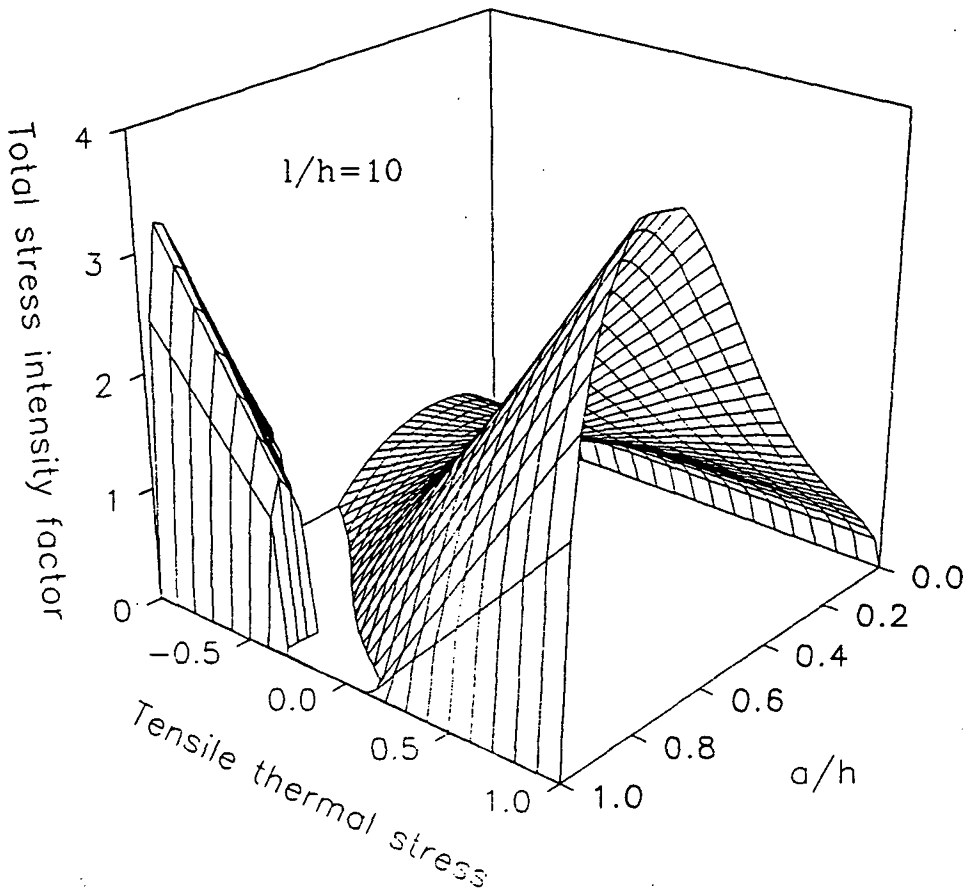

Fig.4-5 Total stress intensity factor as a function of crack length and loading configuration

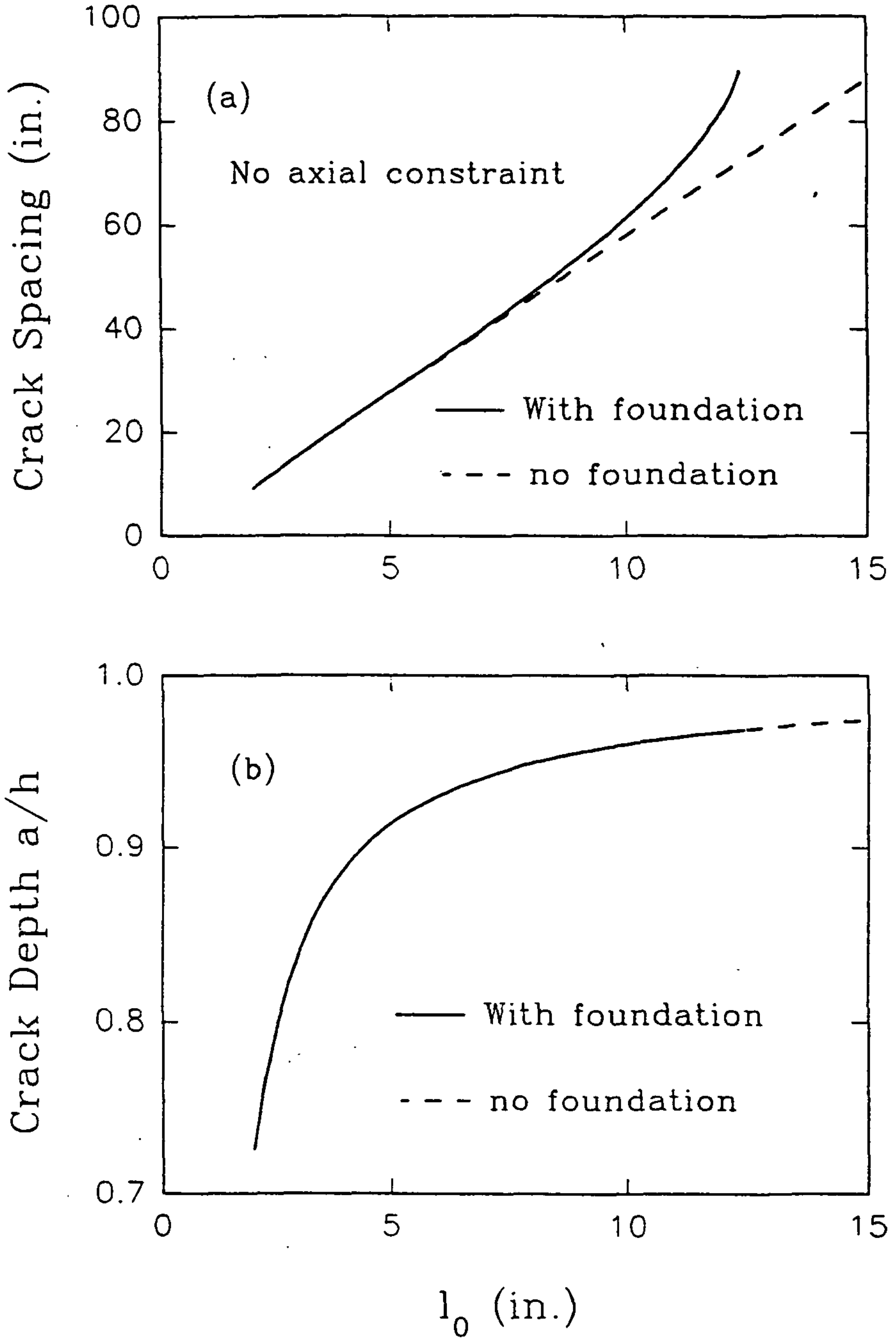

Fig.4–6 Crack spacing as a function of l_0 without axial constraint

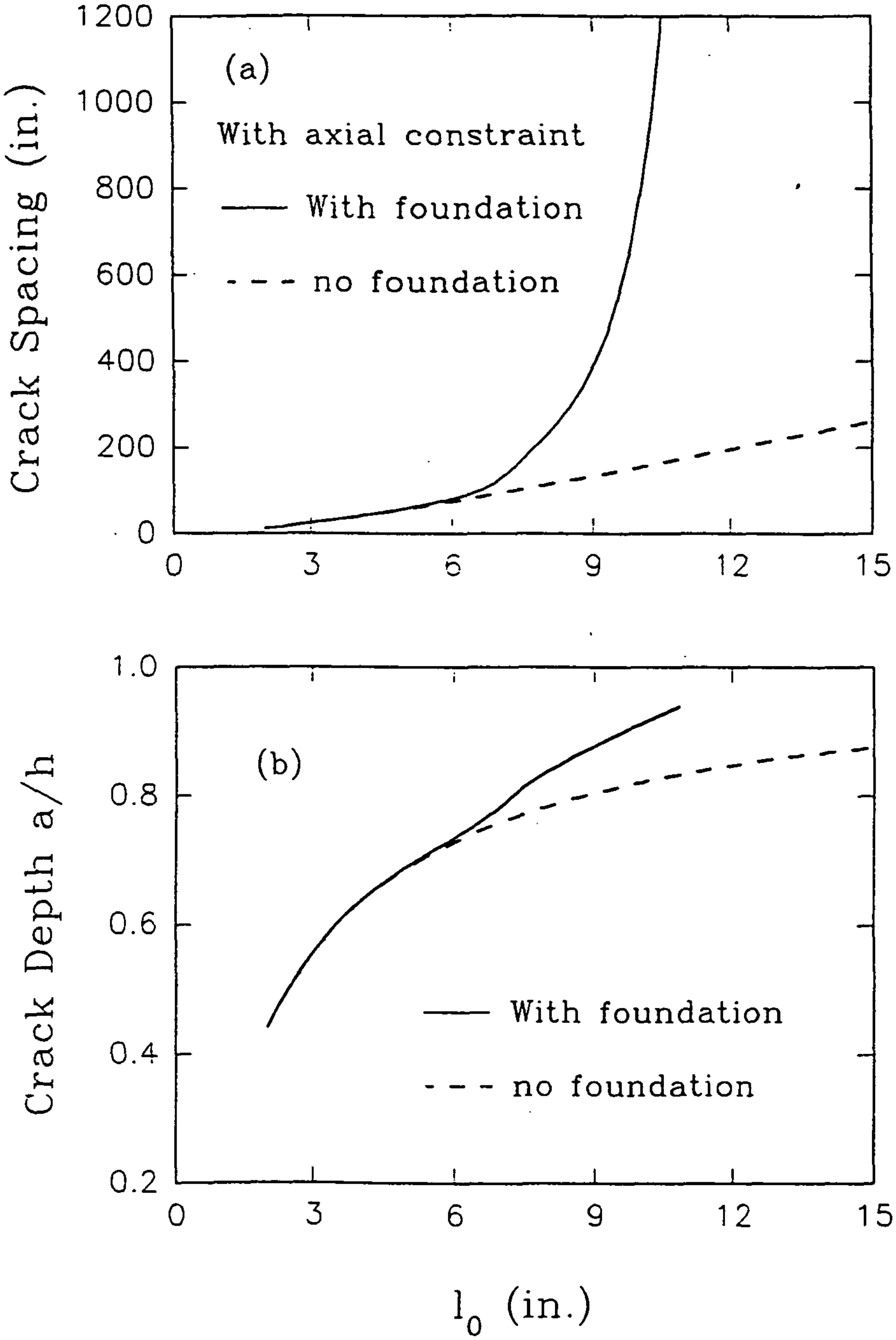

Fig.4–7 Crack spacing as a function of l_0 with axial constraint

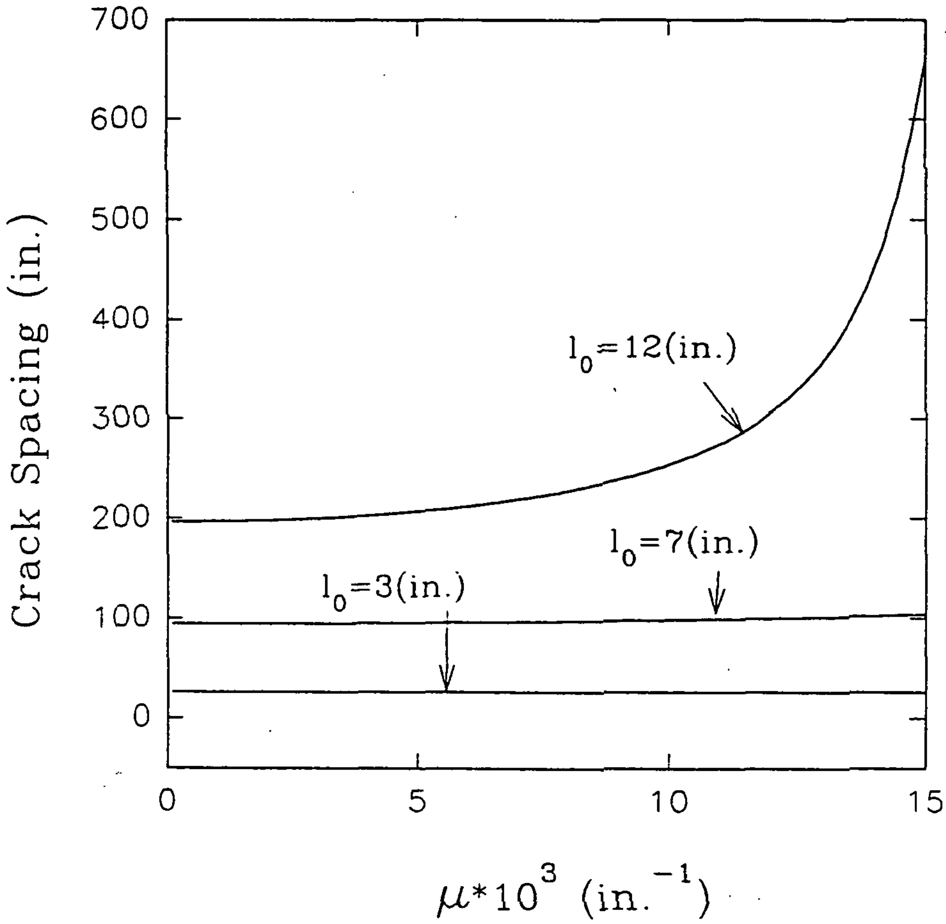

Fig.4–8 Crack spacing with tangential bonding

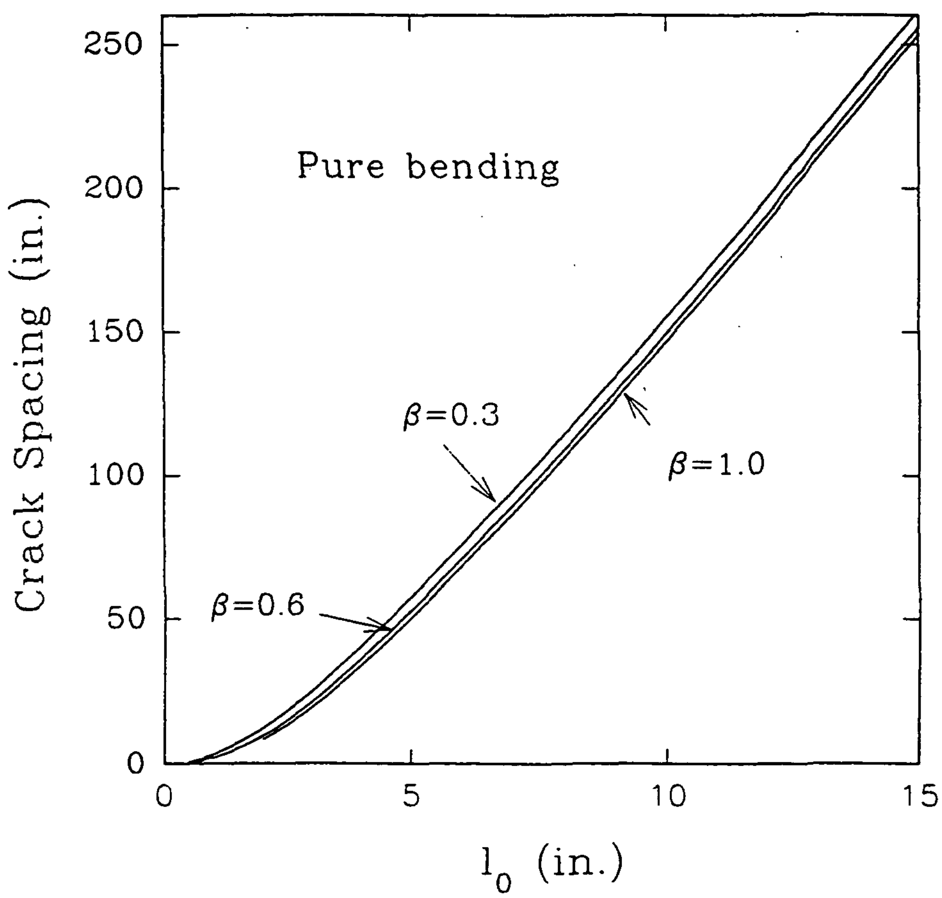

Fig.4–9 The effect of nonlinearity coefficient β on crack spacing

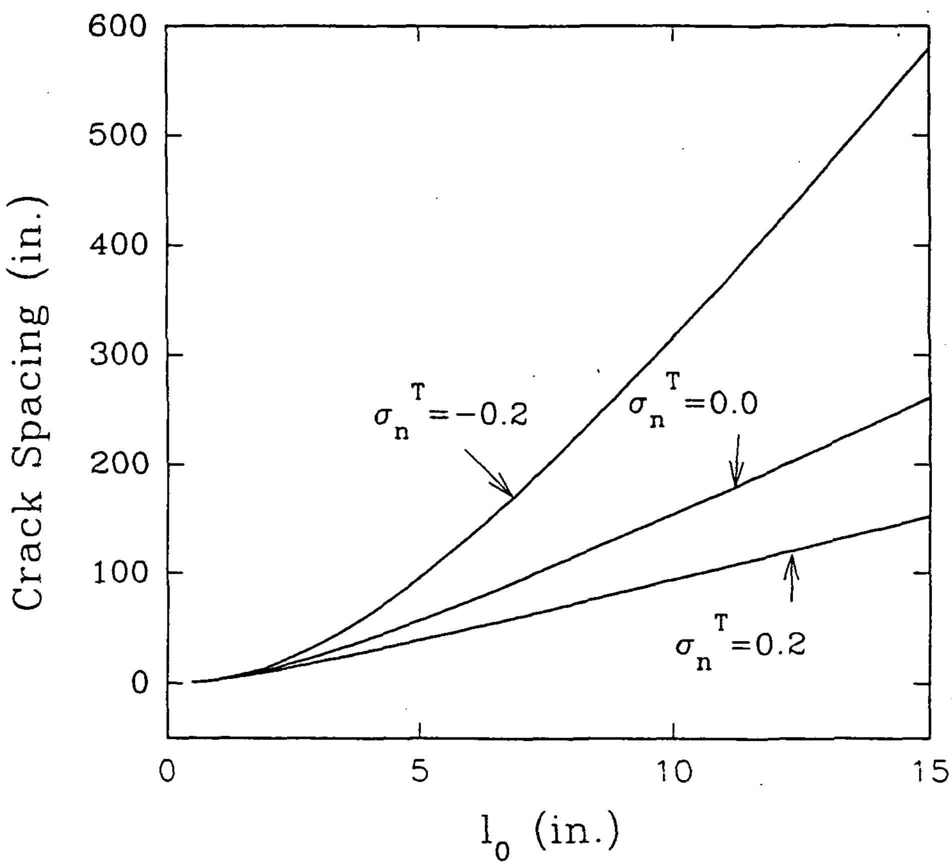

Fig.4-10 The effect of axial thermal stress

C-2

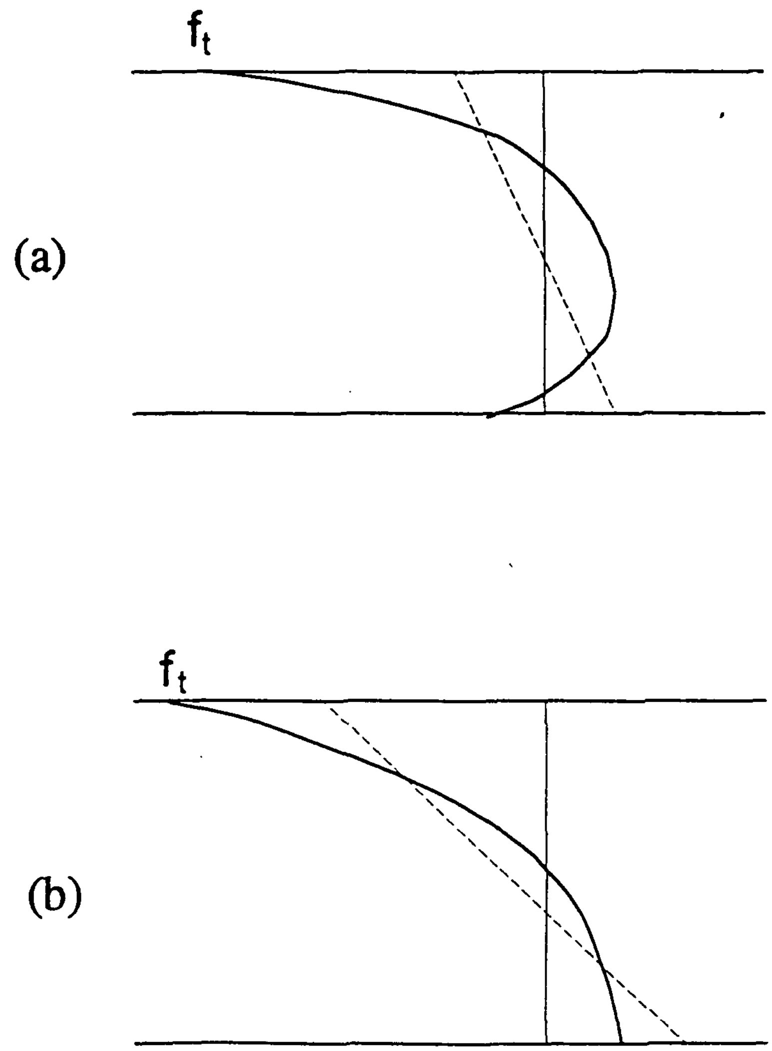

Fig.4-11 Schematic of nonlinear distribution of thermal stress

CHAPTER V

INITIATION THEORY — FOR QUASI-BRITTLE MATERIALS

In the previous discussion, the material is assumed to be perfectly brittle, so that the linear elastic fracture mechanics can be utilized to describe the fracture behavior. Although the nonlinear process zone is taken into account for the concrete material used in highway pavement, the treatment is only approximate. In reality no material can be regarded as perfectly brittle. Perfectly brittle material is an idealization of the so-called quasi-brittle material when the nonlinear process zone is very small compared to crack length. In quasi-brittle materials fracture is preceded by a fracture process zone. It mainly consists of microcracking or other material defects. Experiment observations of concrete indicate that within this zone, fracture is manifested in the form of aggregate debonding and overlapping micro-cracks, mainly parallel to each other, with some intact grain bridges between them (Mier, Rots and Bakker, 1991). For illustration purposes this region is portrayed in Fig 5-1(a). The cohesive crack model describes the region as a process zone (or a fictitious crack) where the material can still transfer stresses which decreases with increasing crack opening. In the crack initiation problem, the initial crack length is zero, therefore the process zone length is always important to be included in the analysis. The theory of cohesive crack model to be employed in this dissertation is a nonlinear fracture mechnics theory, which was proposed by Hillerborg et al. (1976) for concrete material.

When a structure contains more than one crack, the question of how cracks interact must be answered. These cracks may grow simultaneously, or some cracks may close during certain stages of crack growth. In the framework of linear fracture mechanics, Bazant et al. (1977, 1978), Nemat-Nasser et al.(1978) studied the interaction of equidistant parallel surface cracks. The problem of cohesive crack model with multiple cracks does not seem to be studied before.

In this chapter the basic concept of the cohesive crack model and basic conditions governing the cohesive crack initiation will be introduced first. The crack initiation is more complex in cohesive crack model because it may involve the crack bifurcation, crack growth and crack closure. In particular, we propose the concept of unloading of a cohesive crack model to describe the crack closure. The half-plane with a system of alternative surface cracks is still formulated as a singular integral equation. The basic behavior of cohesive crack model with alternative crack lengths are discussed. To study the solution behavior, the rate equations (rate form of the basic equations) are developed. Based on the rate equations, the critical condition of CCM with interactive cracks can be reduced to an eigenvalue problem. Through it the maximum load and the bifurcation point can be directly found. The post-critical behavior is also discussed. It is very interesting that the lower limit of crack spacing in cohesive crack model is same as the one obtained for brittle materials.

5.1. Basic Conditions and Definitions

In the theory of the cohesive crack model, it is assumed that fracture under monotonically increasing mode-I loading occurs when the maximum (tensile) principal stress reaches the tensile strength of the material f_t. It is further assumed that fracture is localized in the so-called process zone such that there is no energy dissipation in the bulk of the structure. The process zone (Fig.5-1(b)) is modeled by a displacement discontinuity (a crack opening displacement) with the proviso that the faces of the discontinuity are capable of transmitting certain cohesive stresses, less than f_t, such that $\sigma = \sigma(w)$ with $\sigma(0) = f_t$, and $\sigma(w) \geq 0$, where $\sigma(w)$ describes the tensile softening behavior. In practice, $\sigma(w)$ was approximated by a linear or bi-linear relation and was assumed to vanish when the crack opening displacement w reached a certain critical value w_c. The fracture response in this model is characterized by fracture energy G_f defined as the energy required to open a unit crack fully, or in other words as the area under the strain-softening curve between $w = 0$ and $w = w_c$. In particular, we employ the linear softening law in which the cohesive stress in the crack surface can be expresses as

$$\sigma = f_t(1 - \frac{w}{w_c}), \qquad w \leq w_c \tag{5-1}$$

where $w_c = 2G_f / f_t$ is the threshold value of crack opening beyond which $\sigma = 0$.

The stress distribution on the crack surface should include this cohesive stress that opposites to thermal loading stress and push the crack closure. Now the total stress distribution on the crack surface can be expressed as

$$-F(\xi)+\sigma(w(\xi)) \tag{5-2}$$

where $F(\xi)=\gamma f_t f(\xi/d)$ is the thermal loading stress due to temperature penetration. For satisfying the strength condition the loading parameter $\gamma \geq 1$ is added here because this thermal loading stress must overcome the opposite effect of the cohesive stress. Actually the thermal loading have two parameters: the maximum loading stress γ and the loading depth d. They may grow simultaneously with time or only one of them grows. For simplicity, we choose γ as loading parameter because F is the explicit function of γ.

In the previous work, we proposed the three governing conditions for brittle elastic solid. The first one, the strength condition, can still be used in CCM for the initiation of process zone. The crack initiation in quasi-brittle structure is a continue process in which the stress equilibrium condition will be the governing condition instead of the strength condition. It should be pointed out that the process zone initiation is not the same as the crack initiation. The second one is replaced by the condition of finite stress, which is discussed below. The third one is no longer applicable for the cohesive crack model.

The stress in the cohesive crack model is finite everywhere, thus the total stress intensity factor at crack tip, which is the sum of stress intensity factor due to the external load and due to the cohesive stress, must be equal to zero:

$$K(a)=0 \tag{5-3}$$

This condition is initially introduced by Barenblatt (1959, 1962), and is the fundamental feature of any cohesive crack models. Compared to our previous study with linear fracture mechanics, equation (5-3) corresponds to the Griffith theorem, that is, the energy release rate due to incremental crack growth must be equal to the fracture energy of the material. Furthermore, equation (5-3) implies that the total energy release rate is zero, because the energy release rate is proportional to the square of the total stress intensity factor. The condition that the energy release rate is equal to zero means that during crack growth (or to be more precise, process zone growth) all energy released from the deformation energy in the bulk of the structure is transformed, completely, to the formation of crack surfaces or overcome the work of the cohesive stress. (Although in linear elastic fracture mechanics the energy is also require to be converted into surface energy, the process of conversion is not included in the analysis. In cohesive crack model, the conversion of energy is realized by the work of the cohesive stress, which is a function of crack opening displacement, in the process zone ahead of the stress-free crack tip.)

In our previous analysis, the Griffith theorem is not satisfied during the crack jump, therefore this condition must be supplemented by the condition that the total energy released during the crack jump must totally converted into the surface energy of newly created cracks, which is an independent condition. In the case of cohesive crack model, however, (5-3) is always satisfied. It implies that the third condition is no longer an independent condition. This difference in the energy consideration makes the initiation theory based on cohesive crack model fundamentally different from the initiation theory based on linear elastic fracture mechanics. In the cohesive crack model, we need to extend our understanding and concept of crack initiation, and find a new approach to describe the process of crack initiation. This is the main goal of this proposed research.

For quasi-brittle materials, the cracking of the material is a gradual process, the crack opening involves a large process zone in which the microcracks exist. If there is still cohesive stress acting across the crack surfaces, the crack should not be regarded as completely opened. In other words, we define that a crack surface is fully created if the corresponding crack opening displacement exceeds the threshold value w_c. Also we need to define the crack initiation of the cohesive crack model at the condition of crack opening. In other words, if crack surface be fully occupied by cohesive zone, the crack have not initiated yet.

5.2 Cohesive Crack Model with Interactive Cracks

So far we have only considered the case where all cracks grow in equal rate. If the load can only increase to certain level which has not sufficient energy for all cracks to initiate, we want to know whether all these cracks stop growing or some cracks stop or even close in favor of other cracks to grow in a faster rate, resulting in larger crack spacing. To study this type of crack behavior, it is necessary to study a cohesive crack model with interactive cracks. In other word, we must study the cohesive crack model in which different cracks can have different lengths. These cracks may grow simultaneously, or some cracks may close in favor of other's growth. For simplicity we assume the every another crack has the same length, see Fig 5-2(a).

When a structure contains more than one crack, the question of how cracks interact must be answered. In the framework of linear fracture mechanics, Bazant (1977, 1979), Nemat-Nasser et al. (1978) have studied the alternative crack growth by differentiating the stress intensity factors with respect to crack lengths. However, the cohesive crack model with multiple interactive cracks has not been studied. The method mentioned above by other authors is no longer useful in cohesive crack model because the stress intensity factors equal zero. Two basic conditions: the stress equilibrium condition and crack tip conditions are the basic tools to probe the phenomena and help us to find out new condition in our problem.

The crack initiation of cohesive crack model is a complicate problem that may involve crack growth, crack bifurcation and crack jump.

Also we need define the crack unloading condition to discuss the phenomena of the crack closure. A cohesive crack is called in loading condition if its crack opening displacement increases, otherwise it is called in unloading condition. For simplicity it is assumed that all cracks are in loading condition in the preceding discussions. It is usually sufficient for CCM to study the load-deflection curve with a single growing cohesive crack. This is perhaps the main reason why there is little study about the unloading behavior of CCM. When there are more than one cracks, it is possible that some cracks are in loading condition while the other in unloading condition, even when the applied load increases.

When a cohesive crack is in unloading condition, the cohesive stress does not follow function σ to increase when the crack opening displacement w decreases. The material in the process zone is partially damaged, and the damage can not be reversed by crack closure. While the actual behavior of the unloading stress-displacement relation is a subject of experimental study, a simple relation is proposed as shown in Fig.5-1(b). Upon closing, the stress reduces linearly back to the origin. If the crack is reopened, the stress increases along the unloading line until the softening curve f is reached, then it decreases again following the softening curve σ. This relation implies that the material can close perfectly to its original position. In reality the fractured surfaces are rough, the crack opening displacement may be unable to return to zero. One may need to use more sophisticated unloading relation to describe the immature crack closure. However, the precise nature of the unloading is beyond the my research.

The cohesive stress at the crack unloading condition (in the linear assumption) is calculated as

$$\sigma(w_u) = \frac{\sigma(w^*)}{w^*} w_u \tag{5-4}$$

where w^* denotes the crack displacement at the bifurcation point and w_u of unloading cracks. This formulation insure the cohesive stresses linearly return to zero when the crack is finally closed.

A loading crack implies a propagating crack. When a crack propagates, one requires that the total stress intensity factor be zero. The position of the process zone tip is unknown for a propagating crack, so the condition of zero stress intensity factor can be viewed as a condition to determine the crack tip position. On the other hand, if a crack is unloading, it no longer propagates. The process zone tip position of an unloading crack is thus not a variable, and its correspondent crack tip equation is redundant. Consequently, whenever a crack is in unloading condition, the corresponding component in the crack tip equations must be discarded so that the number of equations and the number of unknowns match.

5.3 Mathematical Formulation and Numerical Method

The problem of a half-plane weakened by a system of equidistant parallel surface cracks with alternative lengths a_1 and a_2 can still be formulated in terms of a system of singular integral equations. The stress equilibrium conditions may be written as follows:

$$\begin{aligned}\sigma_x(0,y) &= \frac{E}{4\pi}\int_0^{a_1} D_1(t)\sum_{n=-\infty}^{\infty} g(t,2nb,y)dt + \frac{E}{4\pi}\int_0^{a_2} D_2(t)\sum_{n=-\infty}^{\infty} g(t,b+2nb,y)dt \\ &= -\gamma f_t f\left(\frac{y}{d}\right) + \sigma_1(y) \qquad for \quad 0<y<a_1\end{aligned} \tag{5-5}$$

and

$$\begin{aligned}\sigma_x(b,y) &= \frac{E}{4\pi}\int_0^{a_1} D_1(t)\sum_{n=-\infty}^{\infty} g(t,b+2nb,y)dt + \frac{E}{4\pi}\int_0^{a_2} D_2(t)\sum_{n=-\infty}^{\infty} g(t,2nb,y)dt \\ &= -\gamma f_t f\left(\frac{y}{d}\right) + \sigma_2(y) \qquad for \quad 0<y<a_2\end{aligned} \tag{5-6}$$

where $\sigma_1(y), \sigma_2(y)$ are cohesive stresses at corresponding crack surfaces. The function $D_1(t), D_2(t)$ represent dislocation densities and the kernel g is given by

$$\begin{aligned}g(t,x,y) &= \frac{2(y+t)}{(y+t)^2+x^2} - \frac{(y+3t)[(y+t)^2-x^2]}{[(y+t)^2+x^2]^2} + \frac{4ty(y+t)[(y+t)^2-3x^2]}{[(y+t)^2+x^2]^3} \\ &\quad - \frac{(y-t)[(y-t)^2+3x^2]}{[(y-t)^2+x^2]^2}\end{aligned} \tag{5-7}$$

Since g is an even function of x, the series in (5-5) and (5-6) may be written as

$$\sum_{n=-\infty}^{\infty} g(t,2nb,y) = g(t,0,y) + 2\sum_{n=1}^{\infty} g(t,2nb,y) \tag{5-8}$$

$$\sum_{n=-\infty}^{\infty} g(t,b+2nb,y) = 2\sum_{n=1}^{\infty} g(t,(2n-1)b,y) \tag{5-9}$$

The above series can be summed in closed form by using same technique in chapter III and written as

$$\begin{aligned} 2\sum_{n=1}^{\infty} g(t,2nb,y) = {} & \frac{t^2-y^2-4ty}{(y+t)^3} + \frac{\pi}{b}\coth\pi\frac{y+t}{2b} - \frac{(y+3t)\pi^2}{4b^2}\operatorname{csch}^2\pi\frac{y+t}{2b} \\ & + \frac{ty\pi^3}{2b^3}\operatorname{csch}^2\pi\frac{y+t}{2b}\coth\pi\frac{y+t}{2b} \\ & + \frac{1}{y-t}\left[1-\pi\frac{y-t}{b}\coth\pi\frac{y-t}{2b} + \pi^2\left(\frac{y-t}{2b}\right)^2\operatorname{csch}^2\pi\frac{y-t}{2b}\right] \end{aligned} \tag{5-10}$$

$$\begin{aligned} 2\sum_{n=1}^{\infty} g(t,(2n-1)b,y) = {} & \frac{\pi}{b}\tanh\pi\frac{y+t}{2b} + \frac{(y+3t)\pi^2}{4b^2}\operatorname{sech}^2\pi\frac{y+t}{2b} \\ & - \frac{ty\pi^3}{2b^3}\operatorname{sech}^2\pi\frac{y+t}{2b}\tanh\pi\frac{y+t}{2b} \\ & - \frac{\pi}{4b}\left[4\tanh\pi\frac{y-t}{2b} + \pi\frac{y-t^2}{b}\operatorname{sech}^2\pi\frac{y-t}{2b}\right] \end{aligned} \tag{5-11}$$

It is further convenient to represent the kernel function as

$$g(t,0,y) + 2\sum_{n=1}^{\infty} g(t,2nb,y) = \frac{\pi}{b} g_1\left(\frac{\pi t}{b},\frac{\pi y}{b}\right) \tag{5-12}$$

$$2\sum_{n=1}^{\infty} g(t,(2n-1)b,y) = \frac{\pi}{b} g_2\left(\frac{\pi t}{b},\frac{\pi y}{b}\right) \tag{5-13}$$

where the function g_1, g_2 can be written as

$$g_1(t,y) = \frac{1}{t-y} + 2\coth(y+t) - (y+3t)\,\mathrm{csch}^2(y+t) + 4ty\,\mathrm{csch}^2(y+t)\coth(y+t)$$
$$+\frac{1}{y-t}\left[1 - 2(y-t)\coth(y-t) + (y-t)^2\,\mathrm{csch}^2(y-t)\right]$$

(5-14)

$$g_2(t,y) = 4t + 2\tanh(y+t) - (y+3t)\tanh^2(y+t) - 4ty\tanh(y+t)\{1-\tanh^2(y+t)\}$$
$$-2\tanh(y-t) + (y-t)\tanh^2(y-t)$$

(5-15)

The crack opening displacements can be represented by the dislocation density D(y) [Keer et al. 1975] as

$$w_1(y) = \int_y^{a_1} D_1(t)dt \quad , \qquad 0 \le y \le a_1$$
$$w_2(y) = \int_y^{a_2} D_2(t)dt \quad , \qquad 0 \le y \le a_2 \qquad \textbf{(5-16)}$$

Thus cohesive stresses at crack faces then can be expressed as

$$\sigma_1(y) = f_t\{1 - \frac{1}{w_c}\int_y^{a_1} D_1(t)dt\} \quad , \qquad y_{c_1} \le y \le a_1$$
$$\sigma_2(y) = f_t\{1 - \frac{1}{w_c}\int_y^{a_2} D_2(t)dt\} \quad , \qquad y_{c_2} \le y \le a_2 \qquad \textbf{(5-17)}$$

Because function D_1, D_2 are singular at crack tips, it is now convenient to introduce new unknown function C_1, C_2 :

$$D_1(t) = \left(\frac{a_1^{\,2}}{a_1^{\,2} - t^2}\right)^{\frac{1}{2}} C_1(t), \quad D_2(t) = \left(\frac{a_2^{\,2}}{a_2^{\,2} - t^2}\right)^{\frac{1}{2}} C_2(t), \qquad \textbf{(5-18)}$$

which are smooth functions. Equations (5-5), (5-6) are thus transformed into the following equivalent integral equations:

Next, extending the interval into (-1, 1) and employing the same technique used in chapter III we can convert the singular integral equations into discrete forms as

$$\frac{\mathrm{E}}{4\pi}\sum_{i=1}^{n_1}\frac{\pi}{2n+1}B_1(s_i)\frac{\pi a_1}{2b}g_1\left(\frac{\pi a_1 s_i}{2b},\frac{\pi a_1 x_k}{2b}\right)+\frac{\mathrm{E}}{4\pi}\sum_{j=1}^{n_2}\frac{\pi}{2n+1}B_2(s_j)\frac{\pi a_2}{2b}g_2\left(\frac{\pi a_2 s_j}{2b},\frac{\pi a_1 x_k}{2b}\right)$$
$$=-\gamma f_t f\left(\frac{a_1 x_k}{d}\right)+f_t\{1-\frac{a_1}{w_c}\sum_{i=1}^{k}v_i B_1(s_i)\},\qquad k=1,2,\ldots,n_1$$

(5-24)

$$\frac{\mathrm{E}}{4\pi}\sum_{i=1}^{n_1}\frac{\pi}{2n+1}B_1(s_i)\frac{\pi a_1}{2b}g_2\left(\frac{\pi a_1 s_i}{2b},\frac{\pi a_2 x_l}{2b}\right)+\frac{\mathrm{E}}{4\pi}\sum_{j=1}^{n_2}\frac{\pi}{2n+1}B_2(s_j)\frac{\pi a_2}{2b}g_1\left(\frac{\pi a_2 s_j}{2b},\frac{\pi a_2 x_l}{2b}\right)$$
$$=-\gamma f_t f\left(\frac{a_2 x_l}{d}\right)+f_t\{1-\frac{a_2}{w_c}\sum_{i=1}^{l}v_i B_2(s_i)\},\qquad l=1,2,\ldots,n_2$$

(5-25)

where v_i are integral coefficients corresponding integral point i (because of the integral interval is not (-1, 1) we can't use Erdogan's integration formula for this part). Where

$$s_i=\cos\left(\frac{2i-1}{4n_1+2}\pi\right),\qquad x_k=\cos\left(\frac{k\pi}{2n_1+1}\right)$$
$$s_j=\cos\left(\frac{2j-1}{4n_2+2}\pi\right),\qquad x_l=\cos\left(\frac{l\pi}{2n_2+1}\right)\qquad\textbf{(5-26)}$$

let

$$e_1=\frac{a_1}{b},\quad e_2=\frac{a_2}{b},\qquad \Delta=\frac{d}{b},$$
$$t_{1i}=\pi e_1 s_i,\quad t_{2j}=\pi e_2 s_i,\quad y_{1k}=\frac{\pi e_1}{2}x_k,\quad y_{2l}=\frac{\pi e_2}{2}x_l.\qquad\textbf{(5-27)}$$

and introduce

$$A_1(s_i) = -\frac{\mathrm{E}}{4(2n_1+1)}\frac{1}{f_t}B_1(s_i), \qquad i = 1,\ldots.,n_1,$$
$$A_2(s_j) = -\frac{\mathrm{E}}{4(2n_2+1)}\frac{1}{f_t}B_2(s_j), \qquad j = 1,\ldots.,n_2. \tag{5-28}$$

then equation (5-24) and (5-25) may be written as

$$\sum_{i=1}^{n_1} A_1(s_i)H_1(t_{1i}, y_{1k}; e_1) + \sum_{i=1}^{n_2} A_2(s_j)H_2(t_{2j}, y_{1k}; e_2) = \gamma f\left(\frac{2}{\pi\Delta}y_{1k}\right) - 1 - 2a_1 {}^*(2n_1+1)\sum_{i=1}^{k} v_i A_1(s_i),$$
$$k = 1,2,\ldots.,n_1 \tag{5-29}$$

$$\sum_{i=1}^{n_1} A_1(s_i)H_2(t_{1i}, y_{2l}; e_1) + \sum_{i=1}^{n_2} A_2(s_j)H_1(t_{2j}, y_{2l}; e_2) = \gamma f\left(\frac{2}{\pi\Delta}y_{2l}\right) - 1 - 2a_2 {}^*(2n_2+1)\sum_{i=1}^{k} v_i A_2(s_i),$$
$$l = 1,2,\ldots.,n_2 \tag{5-30}$$

where

$$H_1(t,y;e) = \frac{\pi e}{2}\{4t + 2\coth(y+t) - (y+3t)\coth^2(y+t)$$
$$+4ty\coth(y+t)[\coth^2(y+t)-1] - 2\coth(y-t) + (y-t)\coth^2(y-t)\} \tag{5-31}$$

and

$$H_2(t,y;e) = \frac{\pi e}{2}\{4t + 2\tanh(y+t) - (y+3t)\tanh^2(y+t)$$
$$+4ty\tanh(y+t)[\tanh^2(y+t)-1] - 2\tanh(y-t) + (y-t)\tanh^2(y-t)\}. \tag{5-32}$$

and in deriving the last terms of these two equations the expressions for w_c and l_0 have been taken into account of.

Also it is convenient to write the stress equilibrium condition in the matrix form as:

$$[\mathbf{H}]\{\mathbf{A}\} + a_1^*[\mathbf{V}]\{\mathbf{A}\} = \{\mathbf{F}\} \tag{5-33}$$

where

$$[\mathbf{H}]=\begin{bmatrix}\mathbf{H}_{11} & \mathbf{H}_{12}\\ \mathbf{H}_{21} & \mathbf{H}_{22}\end{bmatrix},\quad [\mathbf{V}]=\begin{bmatrix}\mathbf{V}_1 & 0\\ 0 & \dfrac{a_2*}{a_1*}\mathbf{V}_2\end{bmatrix},\quad [\mathbf{F}]=\gamma\begin{Bmatrix}\mathbf{f}_1\\ \mathbf{f}_2\end{Bmatrix}-\begin{Bmatrix}\mathbf{I}_1\\ \mathbf{I}_2\end{Bmatrix},\quad \{\mathbf{A}\}=\begin{Bmatrix}\mathbf{A}_1\\ \mathbf{A}_2\end{Bmatrix}. \tag{5-34}$$

Note that only at $a_1 = a_2$ $(or\ e_1 = e_2)$ and $n_1 = n_2$

$$\mathbf{H}_{11}=\mathbf{H}_{22},\ \mathbf{H}_{12}=\mathbf{H}_{21},\ \mathbf{V}_1=\mathbf{V}_2,\ \mathbf{f}_1=\mathbf{f}_2 \tag{5-35}$$

In the cohesive crack model the stress intensity factor K is always zero. This crack tip condition is equivalent to

$$A_1(1)=0 \tag{5-36}$$

and

$$A_2(1)=0 \tag{5-37}$$

This is our second condition that should be satisfied. $A_1(1)$ and $A_2(1)$ can be obtained by extrapolating the $A(s_i)$. The equations (5-33) and one of (5-36), (5-37) can be arranged as a system of equations from which one can solve for $A(s_i)$ and the loading parameter γ. And rest one of equation of (5-36), (5-37) can be used as a checking condition.

5.4 Computational Procedure and Observation

Through these two conditions or four governing equations we can find some very interesting phenomena and fracture behavior.

To solve the problem, the following procedure are used:

(1) give value of space $b*$ and load depth $d*$;

(2) Select a value of crack one length a_1*;

(3) For a guessed value of crack two length a_2* solve the Eqs.(5-33) and (5-36) for {A} and the loading parameter γ.

(4) Adjusting a_2* to satisfy the equation (5-37) based on the solution obtained in step (3), go back to (3). Repeat this loop until all the equations are satisfied.

(5) Choose another value of a_1* and go back step (3).

We did check the crack opening displacement of crack two at every step in the unloading condition and see if it gradually close when crack one still keep growth.

In practice we use the same number of integral points on each crack surfaces, thus $n_1 = n_2 = m$. Also the size of the system of equations (5-33) is denoted as n, which is equal to 2m. The initial results are plotted in Fig.5-3 The following phenomena are observed:

(1). In the range from the origin to point C_{bif} (a) cracks grow stably at the same length with increasing of load and (b) no crack closure is observed. The solution (a) is checked by setting cracks at different lengths. They come out to be the same and satisfy all four conditions. (b) is checked by setting crack two unloaded. But the crack opening displacement at crack two still keep growth after the unloading. It means that the crack two cannot stop growing at this range.

(2). After point B the crack growth has at least the two possible paths: top one from point C_{bif} to C_{max} in which cracks grow in same lengths and bottom one from C_{bif} to C_{ml} in which one of cracks, say, crack two, stop growing at point C_{bif} and start to gradually close up thereafter, while the crack one continues to grow (possibly at a faster rate). It is a possible that crack two unloading at any point between C_{bif} and

$C_{max.}$ The upper curve corresponds to the condition that the applied load is maximized when the crack length is equal to the given value for a given crack spacing. Obviously the load required for the unloading path right at bifurcation point (bottom one) is less than anyone else. One can easily understand why one crack unloading is more likely to happen in the real situation.

(3). When we solve the system of equation (5-33) we actually first triangulate **[H]** as **[Q][P]**, where **[Q]** is lower triangle matrix and **[P]** is upper triangle matrix with $P_{ii} = 1$. So one can obtain the determinant of [H] by multiplying all Q_{ii}. Instead of checking det.**[H]** one only need to check Q_{ii}. It is observed that all Q_{ii} are positive before point C_{bif}, Q_{nn} is almost zero at point C_{bif} then changes to negative sign after Point C_{bif}. That means det.**[H]** becoming negative. From C_{bif} to C_{max} the negative Q_{ii} moves up from bottom position. When reaching point C_{max} there are two Q_{ii} becoming negative but det**[H]** change back to the positive sign.

On the contrast, det$\mathbf{[H]}_b$ (take unloading equation (5-4) into account) is positive between C_{bif} and C_{ml} until reaching C_{ml} where Q_{mm} starts become negative.

Mathematically there must be a some equation, which can decide the position C_{bif}, C_{max} and C_{ml} where det.**[H]** change its sign. This work will greatly simplify the fracture analysis. We no longer need step-by-step to search these critical points.

5.5 Rate Equation of CCM

To study these solution behavior, one needs to study the rate form of the basic equations. For developing the rate equation of CCM in the initiation problem with two cracks the stiffness influence functions will be utilized in our basic conditions. The stress equilibrium conditions at crack faces can be written in terms of stiffness function as

$$\begin{aligned} -F(x_1)+\sigma(w_1(x_1)) &= \int_0^{a_1} S_{11}(x_1,x_1')w_1(x_1')dx_1'+\int_0^{a_2} S_{12}(x_1,x_2')w_2'(x_2')dx_2' \\ -F(x_2)+\sigma(w_2(x_2)) &= \int_0^{a_1} S_{21}(x_2,x_1')w_1(x_1')dx_1'+\int_0^{a_2} S_{22}(x_2,x_2')w_2(x_2')dx_2' \end{aligned} \qquad \textbf{(5-38)}$$

where x_i (i = 1,2) are the coordinates measured along crack one and crack two. The stiffness functions $S_{ij}(x_i, x_j)$ (force at x_i generated by a unit displacement at x_j.) is symmetric with respect to i and j due to the assumption of linear elasticity in the bulk material. The above conditions can be simplified by using the summation convention as

$$G_i = F(x_i) - \sigma(w_i(x_i)) + \int_0^{a_j} S_{ij}(x_i,x)w_j(x)dx = 0 \qquad \textbf{(5-39)}$$

where i =1, 2. The summation convention in this section only apply to the repeated subscript j.

The total stress intensity factor in each crack tip must be zero, which can be expressed as

$$\begin{aligned} K_1 &= \int_0^{a_1} k_{11}(x)w_1(x)dx + \int_0^{a_2} k_{12}(x)w_2(x)dx = 0 \\ K_2 &= \int_0^{a_1} k_{21}(x)w_1(x)dx + \int_0^{a_2} k_{22}(x)w_2(x)dx = 0 \end{aligned} \qquad \textbf{(5-40)}$$

where $k_{ij}(x_j)$ = stress intensity factor at the tip of crack i due to a unit displacement at the position x_j. Also crack tip conditions can be simplified in same way as

$$K_i = \int_0^{a_1} k_{ij}(x)w_j(x)dx = 0 \qquad \textbf{(5-41)}$$

Equation (5-39) and (5-41) are the basic equations of CCM with two cracks. If there are more than two cracks, one can simply extend the range of index j. If the range of j is from 1 to n, then i = 1,2,...,2n, so there are just enough number of equations to solve the unknown crack opening displacement w_j and crack length a_j, It is useful to call $q_i = (w_i, a_i)$ the state variables, for the system is totally determined once the state variable is specified.

The rate equations can be obtained by considering the basic unknown variables to be the function of time t, which is only for the purpose of keeping the sequences of the system development. When a_i changes the stiffness functions also change.

The derivatives of the stiffness functions with crack length a_i can be expressed in terms of stress intensity factors as

$$\frac{\partial S_{ij}(x_i, x_j)}{\partial a_m} = -\frac{2}{E} k_{mi}(x_i) k_{mj}(x_j) \tag{5-42}$$

No summation over m is implied. This relation is given, for instance, by Okamura (1975), and (5-42) is simply a generalization to the case of multiple cracks.

The time derivative of (5-39) can be expressed as

$$\begin{aligned}\frac{dG_i}{dt} &= -\sigma' \dot{w}_i(x_i) + \int_0^{a_j} S_{ij}(x_i, x) \dot{w}_j(x) dx \\ &+ \dot{a}_m \int_0^{a_j} \frac{\partial S_{ij}(x_i, x)}{\partial a_m} w_j(x) dx + a_j S_{ij}(x_i, a_j) w_j(a_j) = 0\end{aligned} \tag{5-43}$$

where a dot denotes derivative with respect to time t. σ' denotes the derivative of softening function σ with respect to its argument w. However, at crack tip displacement w_j is zero, thus the last term can be dropped. The next last term can be changed due to (5-42) and (5-41) as

$$\dot{a}_m \int_0^{a_j} \frac{\partial S_{ij}(x_i, x)}{\partial a_m} w_j(x) dx = -\frac{2}{E} \dot{a}_m k_{mi}(x_i) \int_0^{a_j} k_{mj}(x) w_j(x) dx = -\frac{2}{E} \dot{a}_m k_{mi}(x_i) K_m \quad \text{(5-44)}$$

This term is also equal to zero due to $K_m = 0$.

Thus, equation (5-43) reduces to the form

$$\frac{dG_i}{dt} = -\sigma^t \dot{w}_i(x_i) - \int_0^{a_j} S_{ij}(x_i, x) \dot{w}_j(x) dx = 0 \quad \text{(5-45)}$$

which is still independent of $\dot{a}_m$. If there are unloading cracks, the rate equations should be modified accordingly. In other words, σ^t should be calculated according to unloading curve.

The time derivative of (5-41) can be expressed as

$$\frac{d}{dt} K_i = \int_0^{a_1} k_{ij}(x) \dot{w}_j(x) dx + \dot{a}_m \frac{\partial}{\partial a_m} \int_0^{a_1} k_{ij}(x) w_j(x) dx = 0 \quad \text{(5-46)}$$

In calculating the last term, we deliberately avoid expanding the derivative into the sum of the derivative with respect to the integral limit and the derivative of k_{ij} with respect to a_m, because each term will be unbounded. However, since we expect the final result to be bounded these singular terms must cancel each other to yield a bounded value.

Equations (5-45) and (5-46) are the rate equations of CCM for the thermal loading problem. They depend on the state variable q_i, but is linear in the rate of state variables. When the system is normal, there is only zero solution to the rate equation. When a system is critical, there can be a non-zero solution to the rate equation. In this way, one can study the behavior of CCM by study the behavior of its rate equation.

One can find the rate equations (5-45) in the matrix form as

$$[\mathbf{H}]\{\dot{\mathbf{A}}\} + a_1^*[\mathbf{V}]\{\dot{\mathbf{A}}\} = \{\mathbf{0}\} \tag{5-47}$$

To solve it for a non-zero solution is a difficult task. However, the problem is simplified if (5-47) is viewed as an eigenvalue problem. In particular,,we are interested only in the smallest eigenvalue of a_1^*.

5.6 Maximum Load and Bifurcation

A symmetric solution, in which the two cracks are of equal length and same crack displacement, was plotted in Fig.5-3 as the curve on top. The system is at critical condition when the applied load is at its maximum, and the corresponding crack length is denoted as C_{max}, which is smallest eigenvalue that corresponds to the eigenvector $\{\dot{\mathbf{A}}_1\} = \{\dot{\mathbf{A}}_2\}$ (equivalent to $\dot{w}_1 = \dot{w}_2$). For different crack spacing these crack lengths, at which the applied load is at its maximum, compose a right curve in Fig 5-4.

The maximum load can be calculated directly using the eigenvalue solution. It is obtained by multiplying the stress equilibrium condition (5-39) with eigenfunction and integral it along the crack surface as

$$\int_0^{a_1} \left[\gamma f_t f(x_i/d) - f_t(1 - \frac{w_1}{w_c}) + \int_0^{a_1} S_{ij}(x_i, x) w_j(x) dx \right] \dot{w}_i(x_i) dx_i = 0 \tag{5-48}$$

By changing the integral order and using the rate equation (5-46) to cancel relevant two terms, we find that the loading parameter can be computed from the expression

$$\gamma = \frac{\int_0^a \dot{w}(x) dx}{\int_0^a \dot{w}(x) f(x/d) dx} \tag{5-49}$$

In deriving this equation, we have utilized the critical condition (5-46) and the symmetric property of the stiffness functions, as well as the symmetry condition of the eigenfunction. This solution is useful if one need to know the maximum load as a function of crack length.

The left curve in Fig.5-4 corresponds to the bifurcation point for a given crack spacing, and the corresponding crack length is denoted as C_{bif} in Fig.5-3. This curve corresponds to the eigenvector $\{\dot{\mathbf{A}}_1\} = -\{\dot{\mathbf{A}}_2\}$(equivalent to $\dot{w}_1 = -\dot{w}_2$), so the corresponding load parameter cannot be calculated using a relation similar to (5-49). The symmetric solution is the unique solution if a_l is less than the bifurcation length. When passing the bifurcation length, one of the cracks may unloading, leaving only the other one to grow in response to the loading. Consequently, the solution lost its symmetry. The load required to propagate only one crack is usually less than that of a symmetric solution. Although both solution are stable , the asymmetric solution is more likely to be actually followed.

5.7 Maximum Load with One Crack Unloading

The unloading stress-displacement equation (5-4) need to be used in crack unloading condition. The solution procedure must be modified because zero K condition for unloading crack must be discarded. The load parameter as a function of the active crack length is shown in Fig.5-3 as the curve in the bottom.

With one of the cracks unloading and the other growing, load reaches a maximum value, which corresponds to yield another critical condition. The critical condition can again be characterized by the rate equation (5-45) or its matrix form (5-47), in an expanded form, as

$$[\mathbf{H}_{11}]\{\dot{\mathbf{A}}_1\}+[\mathbf{H}_{12}]\{\dot{\mathbf{A}}_2\}=-a_1^*[\mathbf{V}_1]\{\dot{\mathbf{A}}_1\} \tag{5-50}$$

$$[\mathbf{H}_{21}]\{\dot{\mathbf{A}}_1\}+[\mathbf{H}_{22}]\{\dot{\mathbf{A}}_2\}=a_1^*[\mathbf{V}^*_2]\{\dot{\mathbf{A}}_2\} \tag{5-51}$$

where $[\mathbf{V}^*_2]$ is modified according the unloading stress-displacement equation (5-4).This system equation cannot be simplified into a proper linear eigenvalue problem, because there is a negative sign in right hand side. But one can eliminate $\{\dot{\mathbf{A}}_2\}$ from (5-51)

$$\{\dot{\mathbf{A}}_2\}=-([\mathbf{H}_{22}]-a_1^*[\mathbf{V}^*_2])^{-1}[\mathbf{H}_{21}]\{\dot{\mathbf{A}}_1\}=-[\mathbf{Q}]\{\dot{\mathbf{A}}_1\} \tag{5-52}$$

$[\mathbf{Q}]$ can be solved from the following equation

$$([\mathbf{H}_{22}]-a_1^*[\mathbf{V}^*_2])[\mathbf{Q}]=[\mathbf{H}_{21}] \tag{5-53}$$

substituting the (5-52) into (5-50), a well-posed eigenvalue equation for solving $\{\dot{\mathbf{A}}_1\}$ can be obtained as

$$([\mathbf{H}_{12}][\mathbf{Q}]-[\mathbf{H}_{11}])\{\dot{\mathbf{A}}_1\}=a_1^*[\mathbf{V}_1]\{\dot{\mathbf{A}}_1\} \tag{5-54}$$

The solution strategy is: (1) assume initial a_1^*; (2) calculate [Q] from (5-53); (3) solve the eigenvalue problem through (5-54), and corrected value of a_1^* obtained; (4) use this new a_1^* and repeat step (2) and step (3) until the value a_1^* is converged. This procedure usually takes only very few steps, typically 2 or 3 for 4 digit accuracy in a_1^*. Since the singularity condition is mainly determined by crack one and the influence of crack two on crack one is not very substantial.

The smallest eigenvalue of the singularity condition yields yet another critical crack length for crack one, which corresponds C_{ml} in Fig.5-3 and the curve plotted in the middle of Fig.5-4. It is interesting to note that this curve is virtually the same as the right curve if its crack spacing $b*$ is multiplied by a factor of 2. In fact, the crack spacing should be doubled when the crack one keeps growing and the crack two unloads at early stage. I would explain it later. The corresponding maximum load can also be obtained by multiplying the eigenfunction to the equilibrium equations and integrating along the crack surface

$$\gamma = \frac{\int_0^{a_1} \dot{w}_1(x)dx}{\int_0^{a_1} \dot{w}_1(x) f(x/d)dx + \int_0^{a_2} \dot{w}_2(x) f(x/d)dx} \tag{5-55}$$

In above section, we have assumed that crack two starts to unloading right at the point of bifurcation. Although this is most likely the case, it does not have to be this way. Actually, a_2 can be any value between C_{bif} and C_{max}. In this sense, the solution is not unique once the crack lengths exceed the bifurcation point. This is very similar to the case of the buckling of an elastoplastic column (Bazant and Cedolin, 1991): once the applied load exceeds the tangent modulus load, there are more than one solutions bifurcating from the original symmetric solution.

5.8 Post-critical Behavior and Lower Crack Spacing Limit

We are also interested in the crack growth after these critical points. From Fig.5-5a the view is very clear that, there will be a jump in crack growth if every another crack is unloaded at the bifurcation point. Note that the crack opens fully at

$a_1* = 0.734$, which is half way during the jumping, therefor it cannot stop at that point. The crack length at the post-initiation state should be measured from the surface to the point C_{ini}, where the load once again becomes the same value as the peak load. Before this point crack would not stop and after this point the crack would not grow without further increase of load level. The crack mouth opening displacement of crack two is reduced to below 0.1 while that of crack one is increased to 2, see Fig.5-5(b). When crack two is compared with crack one, both crack length and crack opening displacement are very small. This means that practically the cracking spacing is doubled. The equal length cracks (upper curve) will grow slowly and require much higher level of load to initiate the cracks will not actually happen.

When the crack spacing is small, like the previous example, the cracks become highly interactive, and some cracks stop while the others grow at a much faster rate. When the cracks are far apart, say b*>20, their interaction is weak and , therefore, they grow at equal rates. A question therefore naturally arises: does the crack spacing have a lower limit? The lower limit is defined as the least crack spacing the cracks can initiate. In other words, even denser cracks may exist in initial stage, some of them will stop in the process of crack initiation and thus should not be counted when measuring the spacing in the final stage of crack initiation.

The lower limit of crack spacing is found to be 2, as can be seen from Fig.5-4. This lower limit for quasi-brittle material in cohesive crack model is the same as the one for brittle material discussed in the previous chapter. The reason is as follows. The process zone length, although varies with structure size, has an upper limit. When a crack length is very long and the relative process zone becomes vanishing small. As a result, the behavior of the cohesive crack model converges to that described by linear elastic fracture mechanics when the crack length becomes very long. For the lower limit, the crack depth approaches infinity, that is why both theories have the same lower limit value for crack spacing.

5.9 Concluding Remarks

The crack initiation is a complicated problem. Although we have established a theory to determine initial crack spacing based on linear fracture mechanics, such a theory cannot be applied when material is not perfectly brittle. In real world, there is no perfectly brittle material. Cohesive crack model is the simplest possible nonlinear fracture mechanics available to study this problem. With cohesive crack model, the crack tip is replaced by a nonlinear process zone and the concept of fracture is extended. With such a model it is possible to treat the initiation problem at a more realistic level.

It is observed that there is always a considerable amount of randomness associated with initial crack spacing. In reinforced concrete, the crack spacing is described, not by a determined value, but by a lower limit. In the light of cohesive crack, the initial development of the nonlinear process zone obviously will start from the weakest point of material. Those weakest point of the material are, usually called the defects, are randomly distributed. Such a point of view is adopted by Weibull (1951) in his analysis of statistical behavior of material strength. However, as we have known from our preliminary study, not all defects will develop into macrocracks. The geometry as well as the loading process has an effect on which defect will become activated. Our main goal is to understand the basic mechanisms of this selection process and find a way to model these mechanisms.

The crack initiation described by the cohesive crack model with alternative crack length is much more complicated than the one for brittle materials. It is a gradual process that may involve propagation as well as crack closure. In the example problem, both bifurcation and stability limit can happen before the crack mouth opening exceeds the threshold value w_c. Based on the rate equations of the cohesive crack model, mathematically it is shown that the critical conditions of the cohesive crack model can be determined by considering only the homogeneous rate equation of the stress equilibrium equation.

The external loading providing the energy for crack initiation includes two parameters. They adjust each other: the longer the penetration depth d, the less the maximum loading stress γ. Because the homogeneous rate equation does not include the external loading, crack lengths of bifurcation, critical points determined by the rate equation depend only on the crack spacing, except when there is an unloading crack (but the effect due to the external loading in the unloading crack has negligible influence on the crack spacing, as has been mentioned before).

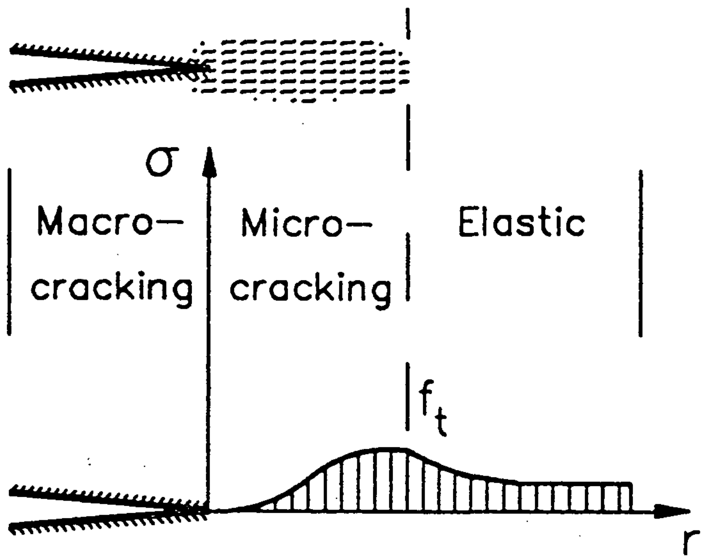

Fig.5-1 (a) Cracking of quasi-brittle materials

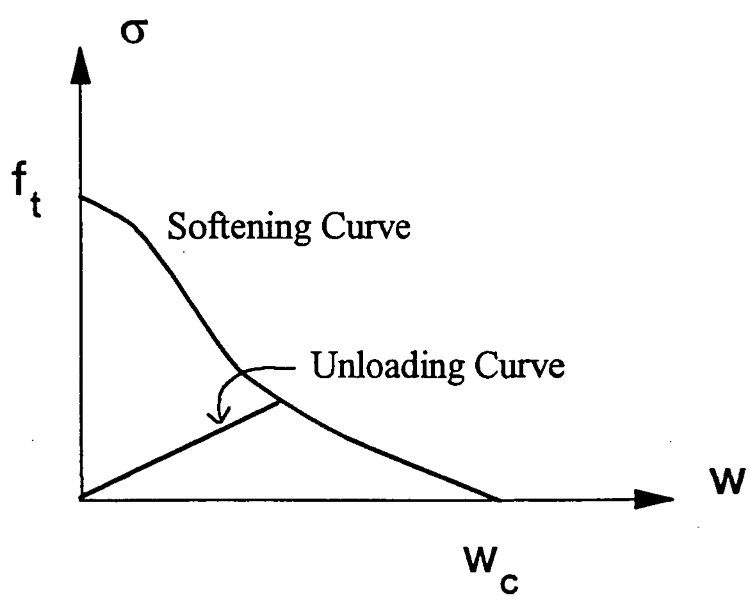

Fig.5-1(b) The cohesive crack model

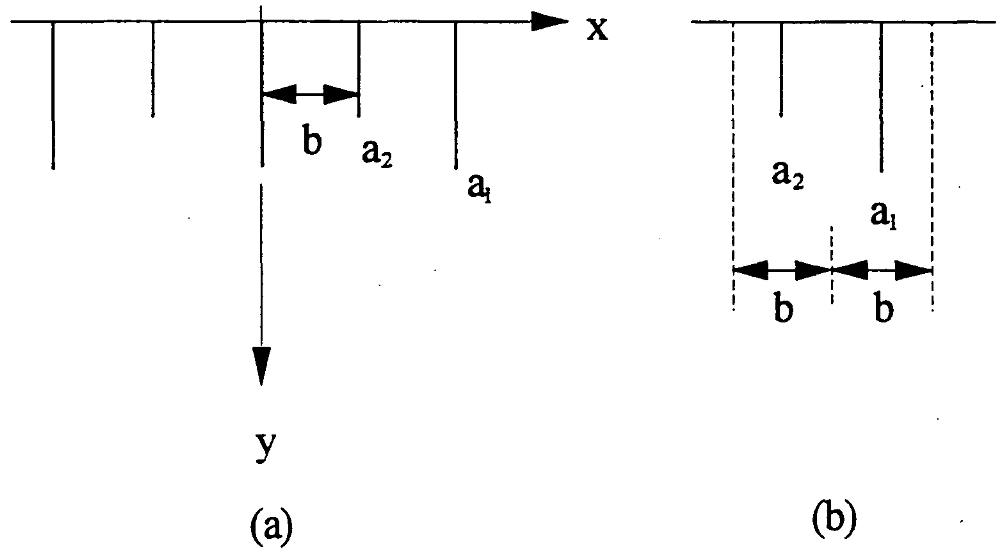

Fig. 5-2 (a) Geometry difinition of parallel crack system with alternative lengths;
(b) Unit cell of width 2b.

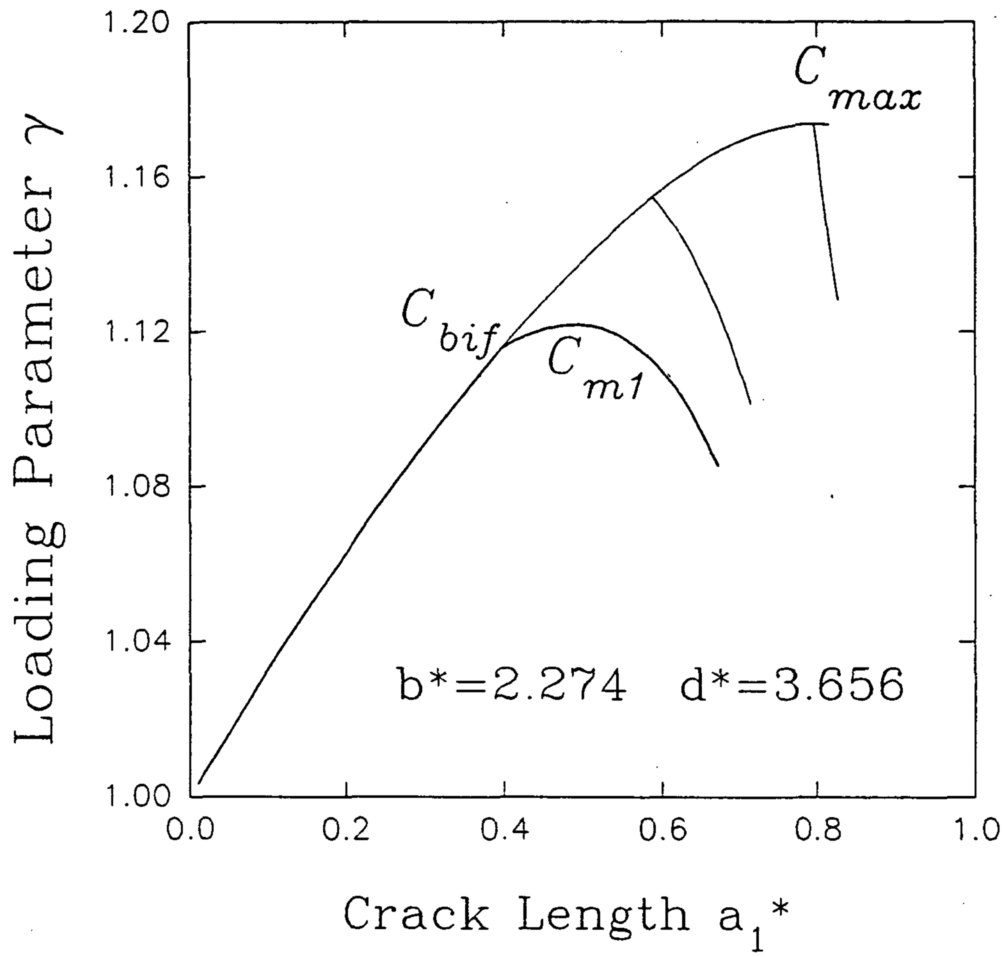

Fig.5-3 Possible crack initiation paths

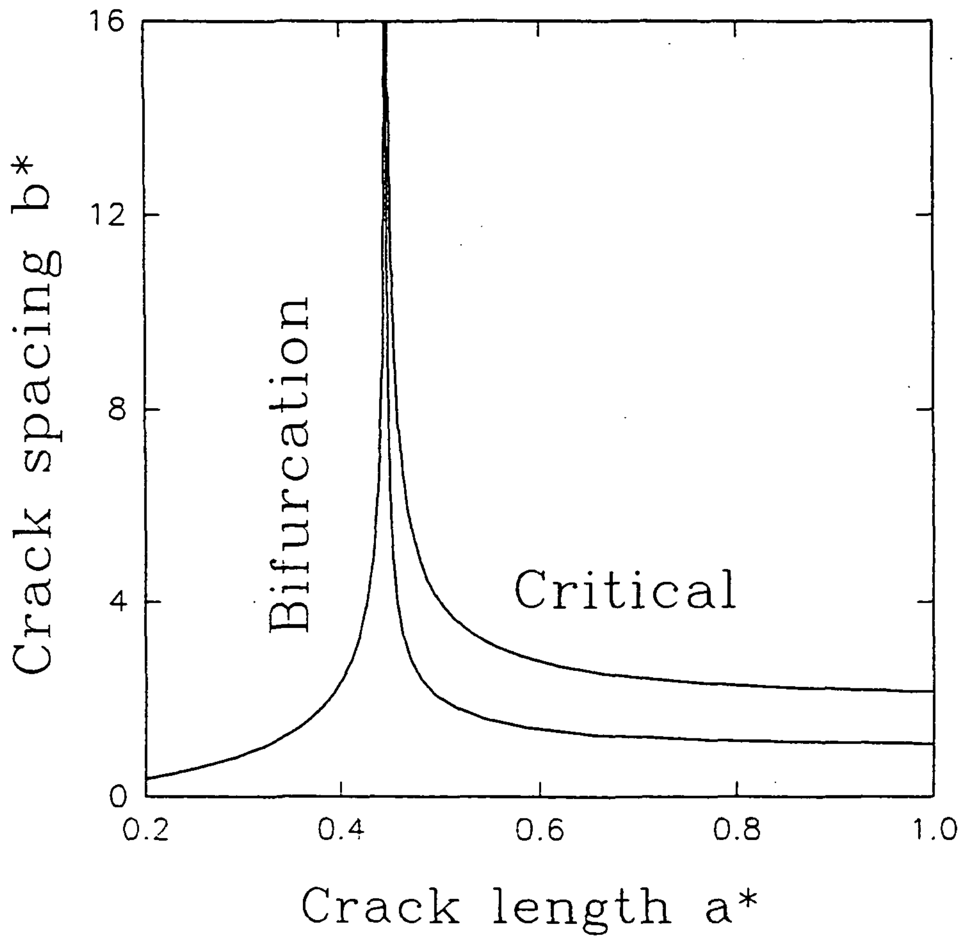

Fig.5–4 Bifurcation and critical curves

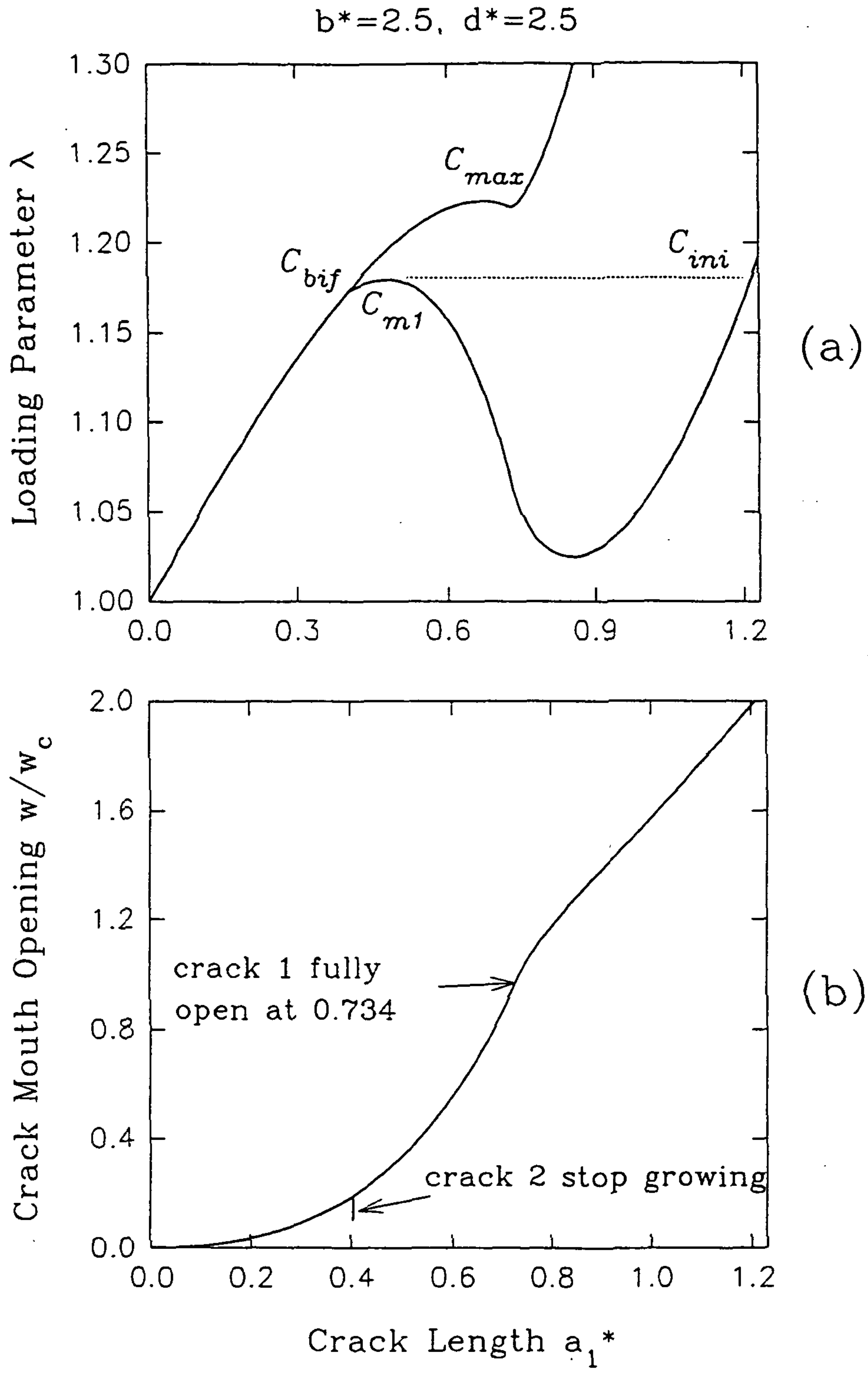

Fig.5–5 Post–critical behavior of crack initiation

CHAPTER VI

CONCLUSIONS AND FUTURE RESEARCH

The study of crack initiation from a smooth surface is still at its infant stage, many problems are still not fully understood and require further researches. However, now it has been established in this study that in order to describe the initiation, the strength criterion and the fracture mechanics theory must be combined. Strength theory can only mark the starting point of cracking, while the fracture mechanics determines what would happen after the cracking is started. In the general situation, the material under consideration always have defects to begin with, so the strength of the material varies from point to point, and cracks of small sizes will start where the strength criterion is first reached. In this sense, the crack initiation is a random phenomena. However, not every small crack develops into a crack of macroscopic sizes, most cracks will be unloaded and yield themselves to a few cracks of larger sizes. In other words, the structure appears to have the ability to select, from a large number of cracks of microscopic sizes, a few cracks that will eventually grow into macroscopic sizes. Although the overall initiation process is random, this structural effect is deterministic in nature and is the main reason why its average behavior can be studied by a deterministic approach.

If the material can be modeled as linear elastic and perfectly brittle, the crack initiation can be summarized as three conditions between the two states of the initiation process. The first condition is the strength criterion, which determines the stress level at which the pre-initiation state. This stress level is assumed to be kept constant during the whole the initiation process. The second is the condition that the Griffith condition be satisfied at the post-initiation state. This condition is important not only because it marks the end of the initiation process, but also because it determines the total amount of the elastic strain energy the structure can release. The third condition is required due to the fact that the crack initiation is not an equilibrium state. Cracks are often occur suddenly, indicating the process is more like a jump than gradual growth. In fact, because the energy release rate is a linear function of crack length if the length is very small, the Griffth condition cannot be satisfied during the early stage of the crack initiation. That is why it is essential to supplement the condition that the total energy released during the process of crack initiation must be converted into surface energy.

The study of crack initiation from the surface of an elastic half plane is related to the crack initiation from the surface of a large structure, such as the top surface of a large concrete block. The solution can be related to the spacing and the depth of cracks that are some distance away from the side wall. It is interesting that the crack spacing has a lower limit of $2l_0$. The same lower limit of crack spacing can be obtained by using just the first and the third condition. This result should be explored further. The case of infinite crack spacing warrants further attention. According to our assumption, the crack will not propagate if the loading depth is very short, even though the stress level may exceed the tensile strength. Further experimental study is needed to clarify the situation.

The problem of crack initiation in the pavement is interesting not only from mechanics point of view, but also from the practical point of view. Cracking is one of the main factors that cause damage to the highway pavement. The study represents the first step to a better understanding of the behavior of cracking in the pavement. For Portland concrete pavement, joints must be provided in the pavement so that random cracking can be controlled. The theoretical result may help engineers to design the joint placement on a physically sound basis.

From the mechanics point of view, pavement is a non-homogeneous structure: the material properties of the top layer is quite different from its subbase. Therefore, the half-space solution cannot be directly applied. However, since the typical crack spacing is large compared to the pavement thickness, the plate assumption can be advantageously be used to simplify the analysis. The nonlinear process zone is important because the zone size is not small compared to the pavement thickness. As an approximation, it is assumed that in the third condition, the fracture energy should be determined by the work-of-fracture method, while in the second condition, the effective fracture energy. The modification is necessary because the effective fracture energy is usually significantly different from the fracture energy calibrated by the work-of-fracture method for pavement material.

This brings us to the discussion of crack initiation by the cohesive crack model. Concrete and asphalt concrete are classified as quasibrittle materials, meaning that cracking is the main failure mechanism. In the cohesive crack model, the crack is a gradual process. Once the tensile stress reaches the tensile strength of the material, the process zone, where bridging stress decreases with increasing crack open displacement, starts to elongate until some limit size is reaches which corresponds to the maximum loading value. The first condition remains the same if one assumes that the pre-initiation state can be marked by the starting of the process zone. The second condition is essential unchanged, except now it is in the form of the condition of zero total stress intensity factor at the tip of process zone. The third condition can also be translated into the language of the cohesive crack model if we could define the total energy of the cohesive crack model. However, the total energy cannot be meaningfully introduced if there is crack closing. This is perhaps the main reason why more study is needed along this direction. Nevertheless, the cohesive crack model can successfully be used to identify the moment when uniform cracks growing bifurcate to only every another crack grow while the rest stop and unloading. Such phenomenon is believed to be important to fully understand the crack initiation process with more realistic detail. When the loading depth is increased, it is seen that both cohesive crack model and the theory of linear elastic fracture mechanics yields the same lower limit for crack spacing, no matter whether unloading is considered or not.

For further research directions, we may note that the crack initiation theory has not been established, as yet, for the cohesive crack model. The difficult lies in the fact that the very concept of initiation becomes blurred once the cohesive crack model is introduced. Because the material is still stable when the process zone is just started, the stress level must be raised further to make the cracks to grow. In other words, there is no jump of crack propagation before the maximum load is reached. Since there is no stage during which the incremental energy balance condition is violated, the third condition of the crack initiation theory may not be an independent condition, at least from the physical point of view.

In addition to the problems that related to the cohesive crack model, the theory still needs to be further generalized to cover more complex situations, among them the following can be mentioned:

1) The crack initiation theory of composite material. One of the main energy absorption mechanism is multiple lateral cracking along the fiber-matrix interface. Dense multiple cracking is a desirable phenomena in certain applications. It seems that the research idea developed here can also find application in that area. The main modification would be the consideration of the shear force that is transferred from fiber to matrix or vice versa. The crack initiation problem in reinforced concrete belongs to the same category.

2) In this study we have only considered the solution of one dimensional crack initiation pattern. The pattern in two-dimensional plane is known to hexagonal, but the proper equation has yet been set up for this interesting problem.

3) Another generalization is the problem of non-uniform solution. We have been able to obtain the uniform solution as the average behavior of cracking pattern, but it will be a big step further if we can also know something about the non-uniformity of the crack pattern, and understand what we can do to control the situation.

4) The problems discussed in this study is defined on a surface extending infinitely in both direction. If there is boundary that ends the extension of the free surface, then the crack initiation theory developed here must be modified, because the crack pattern may not be uniform any more. This problem is thus also connected to the previous problem. For a non-uniform pattern of cracks, the parameters that characterize the pattern is more than two, so the theory developed herein is not sufficient to determine any crack pattern that needs more than two parameters to define. This seems to be the most urgent problem that must be solved.

5) At present research stage only mode-I crack is considered. For mixed-mode cracking (for example, half-plane with a system of parallel incline cracks) the shear cohesion should also be included. The stress-displacement relation for the shear cohesion may have a similar form as the one for the tensile cohesive stress. The number of the basic equations are doubled but the solution procedure remains the same. However, since shear deformation is often associated with friction, which consumes the released energy, the energy conservation equation must be modified accordingly.

BIBLIOGRAPHY

"AASHTO Guide for Design of Pavement Structures 1993", Published by the American Association of State Highway and Transportation Officials.

Armaghani, J.M., Larsen, T.J. and Smith, L. L. (1987) "Temperature response of concrete pavements", Transportation Research Record 1121, pp.23-33.

Bansal, N.P. and Doremus, P.H. (1986) "Handbook of glass properties", Chapter 12, Academic Press, New York.

Barenblatt, G.I. (1959a) "The formation of equilibrium cracks during brittle fracture. General ideas and hypotheses. Axially-symmetric cracks", J. Appl. Math. Mech. Vol.23, pp.622-636.

Barenblatt, G.I. (1959b) "Equilibrium cracks formed during brittle fracture. Rectilinear cracks in plane plates", J. Appl. Math. Mech. Vol.23, pp.1009-1029.

Barenblatt, G.I. (1962) "The mathematical theory of equilibrium cracks in brittle fracture", Adv. Appl. Mech. 7, 55-129.

Base, G.D. and Murray, M.H. (1982) "A new look at shrinkage cracking", Civil Engrg Transactions, 171-176.

Bazant, Z.P. and Ohtsubo, H. (1977) "Stability conditions of a system of cracks in a brittle solid", Mech. Res. Comm., Vol.4(5), 353-366.

Bazant, Z.P. And Ohtsubo, H. and Aoh, K. (1979) "Stability and post-critical growth of a system of cooling or shrinkage cracks", Int. J. Fracture Vol.15(5), 443-456.

Bazant, Z.P. and Wahab, A.B. (1979) "Instability and Spacing of Cooling or Shrinkage Cracks", J. Engrg Mechanics Division, ASCE, Vol.105, No.EM5, 873-889.

Bazant, Z.P. and Wahab, A.B. (1980) "Stability of parallel cracks in solids reinforced by bars", Int. J. Solids Structures, Vol.16, 97-105.

Bazant, Z.P. and Oh, B.H. (1983) " Crack band theoty for fracture of concrete", Material and Structures, RILEM, Paris, Vol.16, pp. 155-177.

Bazant, Z.P. (1984a) "Size effect in blunt fracture: Concrete, Rock, Metal", ASCE J. Engrg Mech. Vol.110, No.4, pp.518-535.

Bazant, Z.P. and Cedolin, L. (1984b) "Approximate linear analysis of concrete fracture by R-curves", ASCE J. Struct. Engrg, Vol.110, No.6, pp.1336-1355.

Bazant, Z.P. (1984c) "Continuum theory for strain-softening" ASCE J. Engrg Mech. Vol.110, No.12, pp.1666-1691.

Bazant, Z.P. (1986a) "Mechanics of distributed cracking", Appl. Mech. Review, Vol.39, pp.675-705.

Bazant, Z.P., Kim, J-K. and Pfeiffer, P.A. (1986b) "Nonlinear fracture properties from size effect tests" ASCE J. Struct. Engrg Vol.112, No.2, pp.289-307.

Bazant, Z.P. and Pfeiffer, P.A. (1987) "Determination of fracture energy from size effect and brittleness number", ACI Material J. Nov-Dec, pp.463-480.

Bazant, Z.P. and Mazars J. (1990a) "France - U.S. workshop on strain localization and size effect due to cracking and damage", ASCE J. Engrg. Mech. Vol.116, No.6, pp.1412-1424.

Bazant, Z.P. (1990b) "Recent advances in failure localization and nonlocal models", in Micromechanics of Failure of Quasi-brittle materials, S.P. Shah, S.E. Swartz and M.L. Wang eds. Elsevier Applied Science, pp.12-32.

Bazant, Z. P. and Cedolin, L. (1991) "Stability of structures: Elastic, Inelastic, Fracture and Damage Theories", Oxford University Press, New York.

Broek, D. (1968) "Some considerations on slow crack growth", Int. J. Fracture Mech., Vol.4, pp.19-34.

Carpinteri, A. (1989) "Size effects on Strength, Toughness, and Ductility", ASCE J. Engrg Mech. Vol.115, No.7, pp.1375-1393.

Cotterell, B. (1968) "Fracture propagation in organic glasses", Int. J. Fracture Mech., Vol.4, pp.209-217.

Delale, F. and Erdogan, F. (1977) "The problem of internal and edge cracks in and orthotropic strip", J. Applied Mechanics, June 1977, pp.237-242.

Dugdale, D.S. (1960) "Yielding of steel sheets containing slits", J. Mech. Phys. Solids, Vol.8, pp.100-104.

Erdogan, F., Gupra, G.D. and Cook, T.S. (1972) "Numerical solutions of singular integral equations", In "Methods of analysis and solutions of crack problems" (edited by G. C. Sih), Noordhoff, Holland. pp.368-425.

FHWA (1986) 'Improved Rigid Pavement Joints" U.S. Department of Transportation, Federal Highway Administration, Publication No. FHWA-RD-86-040.

FHWA (1989) 'Rigid Pavement Analysis and Design", U.S. Department of Transportation, Federal Highway Administration, Publication No. FHWA-RD-88-068.

FHWA (1990) "Asphalt behavior at low service temperatures", Publication No. FHWA-RD-88-078.

FHWA (1993) "Pavement Structural Design Practices", Transportation Research Board, National Cooperative Highway Research Program: NCHRP Synthesis 189.

Foote, R.M.L., Mai, Y-W. and Cotterell, B. (1986) "Crack growth resistance curves in strain-softening materials", J. Mech. Phys. Solids, Vol.34, No.6, pp.593-607.

Frankenstein, E.G. (1963). "Load test data for lake ice sheet", Technical Report 89, US Army Cold Region Research and Engineering Laboratory, Hanover, New Hampshire.

Friberg, B.F. (1954) 'Frictional resistance under concrete pavements and restraint stresses in long reinforced slabs", Highway Research Board Proc., Vol. 33, pp.167-184.

Geyer, J.F. and Nemat-Nasser, S. (1982) 'Experimental investigation of thermally induced interacting cracks in brittle solids", Int. J. Solids Structure, Vol.18, pp.349-356.

Gilbert, R.I. (1992) 'Shrinkage cracking in fully restrained concrete members", ACI Structural Journal, Vol. 89, No.2, pp.141-149.

Gradshteyn, I.S. and Rhyzhik, I.M. (1965) "Tables of integrals, series and products", Academic Press, New York.

Harr, M. E. And Leonards, G.A. (1959) 'Warping stresses and deflections in concrete pavements", Highway Research Board Proc., Vol. 38, pp.286-320.

Hillerborg, Modeer, M. and Petersson, P.E. (1976) " Analysis of crack formation and crack growth in concrete by means of fracture mechanics and finite elements", Cement and Concrete Research, **6**, pp.773-782.

Hillerborg, A. (1984) "Discussion on 'Prediction of nonlinear fracture process zone in concrete'", ASCE J. Engrg Mech. Vol.110, pp.113-117.

Hillerborg, A. (1985) "Numerical methods to simulate softening and fracture of concrete", In Fracture Mechanics of Concrete: Structural Application and Numerical Calculation, G.C. Sih and A. Di'Tommaso, eds., Martinus Nijhoff Publisher, Dordrecht, Netherlands, pp.141-170.

Irwin, G.R. (1957) "Analysis of stresses and strains near the end of a crack traversing a plate", J. Appl. Mech. Vol.24, pp.361-364.

Irwin, G.R. (1958) "Fracture", In Handbuch der Physik, B. VI (S. FlÜgge, ed.) Springer, Berlin, pp.551-590.

Jeng, Y.S. and Shah, S.P. (1985a) "Two parameter fracture model for concrete", J. Engrg Mech., ASCE, Vol.111, No.10, pp. 1227-1241.

Jeng, Y.S. and Shah, S.P. (1985b) "A fracture toughness criterion for concrete", Engrg Fracture Mech., Vol.21, No.5, pp.1055-1069.

Jeng, Y.S. Liaw, C.J. and Kim, S.C. (1993) 'Effects of temperature on early crack formation in Portland cement concrete pavements", Transportation Research Record 1388, pp.35-41.

Kaplan, M.F. (1961) "Crack propagation and the fracture of concrete", J. ACI, Vol.58, pp.591-609.

Karihaloo, B.L., Nallathambi P. (1989) "Effective crack model and tension softening laws", In SEM/RILEM Int. conf. on Fracture of Concrete and Rock, Recent Development, eds. S.P. Shah, S.E. Swartz, B. Barr, Elsevier Applied Science, pp. 701-710.

Keer, L.M. and Chantaramungkorn, K. (1975) "An elastic half plane weakened by a rectangular trench", J. Appl. Mech., Vol.42, pp.683-691.

Keer, L.M. Nemat-Nasser, S. and Oranratnachai, A. (1978) "Unstable growth of thermally induced interacting cracks in brittle Solids: Further results", Int. J. Solids Structure, Vol. 15, pp.111-126.

Lachenbruch, A. H., (1961) "Depth and Spacing of Tension Cracks," J. of Geophysical Research, Vol. 66, pp.4273.

Lang, F.C. (1941) "Temperature and moisture variations in concrete pavements", Highway Research Board Proc., Vol. 21, pp.260-272.

Li, Y.N. and Hong A.P. (1992) "Prediction of failure in notched infinite strips by the cohesive crack model", Int. J. Solids Struct. Vol.29, No.23, pp.2815-2828.

Li, Y.N. and Liang, R.Y. (1993) "The theory of boundary eigenvalue problem in the cohesive crack model and its application", J. Mech. Phys. Solids, **41**, No.2, pp.331-350.

Li, Y.N. and Bazant, Z.P. (1994) "Penetration fracture of floating ice-plate: 2D analysis and size effect", J. Engng. Mech., ASCE 120, No.7, pp 1481-1498.

Li, V.C. and Liang, E. (1986) "Fracture processes in concrete and fiber reinforced cementitious composites", ASCE J. Engrg Mech. Vol.112, No.6, pp.566-586.

Liang, R.Y. and Li, Y.N. (1991a) "Simulation of nonlinear fracture process zone in cementitious material -- A boundary element approach", Computational Mechanics, Vol.7, pp.413-427.

Liang, R.Y. and Li, Y.N. (1991b) "A study of size effect in concrete using fictitious crack model", J. Engng Mech. ASCE. Vol.117, pp.1631-1651.

Lister, C.R.B. (1974) "On the penetration of water into hot rock," Geophysics J. of the Royal Astronomical Society, London, England, Vol. 39, pp. 465-509.

Mai, Y.M. (1984) "Fracture measurements of cementitious composites", in Application of Fracture Mechanics to Cementitious Composites, NATO-ARW, Sep. 4-7, 1984, Northwestern Univ. U.S.A. S.P. Shah, ed., pp.399-429.

van Mier, J., Rots, J.G. and Bakker, A. edit (1991) "Fracture processed in concrete". Published by E. & F. N. Spon. ISBN 0419 158707. pp.581.

Mindess, S. (1983) "The application of fracture mechanics to cement and concrete: a historic review", Fracture Mechanics of Concrete, F.H. Wittmann ed. Amsterdam, Elsevier, pp.1-30.

Mindess, S. (1984) "Fracture toughness testing of cement and concrete", in Fracture Mechanics of Concrete: Material Characterization and Testing, A. Carpinteri and A.R. Ingraffea, eds. Martinus Nijhoff, The Hague, pp.67-110.

Mindess, S. And Young, J.F. (1981) 'Concrete", by Prentice-Hall, Inc., Englewood Cliffs, N.J. 07632.

Mobasher, B. Ouyang C. and Shah, S.P. (1989) "An R-curve approach to predict toughening of cement-based matrices due to fiber reinforcement", Int. J. Fracture.

Murakami, Y. (1987) "Stress intensity factors handbook", Pergamon Press, Vol. I.

Muskhelishvili, N.I. (1992). "Singular integral equations", Dover Publications, Inc., New York.

Nemat-Nasser, S. Keer, L.M. and Parihar, K.S. (1978) "Unstable growth of thermally induced interacting cracks in brittle solids", Int. J. Solids Structure, Vol.14, pp.409-430.

Nemat-Nasser, S. and Oranratnachai, A. (1979) "Minimum spacing of thermally induced cracks in brittle solids", J. Energy Resources Technology, Vol.101, pp.34-40.

Nemat-Nasser, S., Sumi, Y. and Keer, L.M. (1980) "Unstable growth of tension cracks in brittle solids: stable and unstable bifurcations, snap-through, and imperfection sensitivity ", Int. J. Solids Structure, Vol.16, pp.1017-1035.

Nied, H.F. (1987) "Periodic array of cracks in a half-plane subjected to arbitrary loading", J. Appl. Mech. Vol.54, pp.642-648.

Okamura, H., Watanabe, K. and Takano, T. (1973) "Applications of the compliance concept in fracture mechanics", Progress in flaw growth and fracture toughness testing, ASTM STP 536, pp.423-438.

Okamura, H., Watanabe, K. and Takano, T. (1975) 'Deformation and strength of cracked member under bending moment and axial force", Engrg. Fracture Mech. Vol.7, pp.531-537.

Ottosen, N. (1986) "Thermodynamic Consequences of strain softening in tension", ASCE J. Engrg Mech. Vol.112, No.11, pp.1152-1165.

Planas, J. and Elices, M. (1990) "Anomalous structural size effect in cohesive materials like concrete", in Proc. 1st Materials Engrg Congr., "Serviceability and Durability of Construction Materials, Denver, Colorado, Aug. 1990, B.A. Superenant ed., Publ. ASCE, Vol.2, pp.1345-1356.

Rashid, Y.R. (1968) "Analysis of prestressed concrete pressure vessels", Nucl. Engrg Des. Vol.7 No.4, pp.334-355.

Rice, J. And Levi, (1972) "The part-through surface crack in an elastic plate", J. Appl. Mech., ASME.,Vol.39, pp.185-194.

Richardson, J.M. and Armaghani, J.M. (1987) "Stress caused by temperature gradient in Portland cement concrete pavements" Transportation Research Record 1121, pp.7-13.

Ruth, B.E., Bloy, L.A.K. and Avital, A.A. (1982) "Prediction of pavement cracking at low temperature." Asphalt Paving Technology, Proc. Association of Asphalt Paving Technologists, Technical sessions, Vol.51, pp.53-103.

Selvadurai, A.P.S. (1979) "Elastic analysis of soil-foundation interaction", Elsevier Scientific Publishing Company, Developments in geotechnical engineering Series Vol.17.

Shah, S.P. (1989), "Whither fracture mechanics -- Keynote Lecture", In SEM/RILEM Int. conf. on Fracture of Concrete and Rock, Recent Development, S.P. Shah, S.E. Swartz, B. Barr, eds. Elsevier Applied Science, pp.1-4.

Shah, S.P. (1990) "Toughening of quasi-brittle materials due to fiber reinforcing", in Micromechanics of Failure of Quasi-brittle materials, S.P. Shah, S.E. Swartz and M.L. Wang eds. Elsevier Applied Science, pp.1-11.

Shah, S.P. edit (1991) "Toughening Mechanisms in Quasi-Brittle Materials". Kluwer Academic Publishers, NATO ASI Series E: Applied Sciences - Vol.195.

Smith, E. (1974) "The structure in the vicinity of a crack tip: A general theory based on the cohesive zone model", Engrg Fracture Mech. Vol.6, pp.213-222.

Sumi, Y., Nemat-Nasser, S. and Keer, L.M. (1980) "A new combined analytical and finite-element solution method for stability analysis of the growth of interacting tension cracks in brittle solids " Int. J. Engrg Sci. 18, pp.211-224.

Tada, H., Paris, P. and Irwin, G. (1985) "The stress analysis of cracks handbook", Del Research Corporation.

Walsh, P.F. (1972) "Fracture of plain concrete", Indian Concrete J. Vol.46, No.11, pp.469-476.

Wecharatana, M. and Shah, S.P. (1983a) "Predictions of nonlinear fracture process zone in concrete", ASCE J. Engrg Mech. Vol.109, No.5, pp.1231-1246.

Wecharatana, M. and Shah, S.P. (1983b) "A model for predicting fracture resistance of fiber reinforced concrete", Cement and Concrete Research, Vol.13, pp.819-829.

Wesevich, J.W., McCullough, B.F. and Burns, N.H. (1987) 'Stabilized subbase friction study for concrete pavements" Research report 459-1, Center for Transportation Research, The University of Texas at Austin.

Westergaard, H.M. (1925) "Computation of stresses in concrete Roads". Highway Research Board Proc., Vol. 5, pp.90-112.

Westergaard, H.M. (1926) "Analysis of stresses in concrete pavements due to variations of temperature". Highway Research Board Proc., Vol. 6, pp.201-217.

Weibull, W. (1951) "A statistical distribution function of wide applicability". J. Appl. Mech., 18, pp.293-297.

Willis, J.R. (1967) "A comparison of the fracture criteria of Griffith and Barenblatt", J. Mech. ``Phys. Solids, Vol.15, pp.151-162.

Wimsatt, A. J. And McCullough, B.F. (1989) 'Subbase friction effects on concrete pavements". In 4th international conference on "Concrete pavements design and rehabilitation", pp.3-15.

Wu, C.L., Tia, Mang and Larsen, T.J. (1993) "Analysis of structural response of concrete pavements under critical thermal-loading conditions", Proceedings of Fifth International Conference on Concrete Pavement Design and Rehabilitation. pp.317-336.

APPENDICES

APPENDIX 1

THE STRESS INTENSITY FACTOR

We note that, except for the first term in g_1 (given by equation (3-14)) function g_1 is bounded. (The last term in g_1 is bounded that can be proved by expansion of hyperbolic functions in power series.) Also the unknown function C is a bounded function. Once the unknown function is solved, the stress intensity factor can be calculated as

$$
\begin{aligned}
K &= \lim_{y\to a^+}\sqrt{2\pi(y-a)}\,\sigma_x(0,y) = \lim_{y\to a^+}\frac{\mathrm{E}}{4\pi}\sqrt{2\pi(y-a)}\int_0^a C(t)\left(\frac{a^2}{a^2-t^2}\right)^{1/2}\frac{dt}{t-y} \\
&= \lim_{y\to a^+}\frac{\mathrm{E}}{4\pi}\sqrt{2\pi(y-a)}\,a\left\{\int_0^a\frac{C(y)}{(t-y)\sqrt{a^2-t^2}}dt+\int_0^a\frac{C(t)-C(y)}{(t-y)\sqrt{a^2-t^2}}dt\right\}
\end{aligned}
\tag{1-1}
$$

If we prove any term in the brace is bounded the corresponding product in K will be equal to zero because $\lim_{y\to a^+}\sqrt{(y-a)}=0$.

Now we prove the last term in brace is bounded function.

C(t) is a smooth function that will satisfy the Hölder condition (Muskhelishvili, 1992, page.11) :

$$|C(t)-C(y)|\le M|t-y|^{\mu} \tag{1-2}$$

where M and μ are positive constants.

By using this condition the absolute value of the last term in the brace can be found as

$$\int_0^a \left| \frac{C(t)-C(y)}{(t-y)\sqrt{a^2-t^2}} \right| dt \leq \mathrm{M} \int_0^a \frac{dt}{|t-y|^{1-\mu}\sqrt{a^2-t^2}} \tag{1-3}$$

Because the exponents $(1-\mu) < 1$, this generalized integral is finite (bounded). As a result, the corresponding term in K is equal to zero and only the first term in the brace need further consideration.

The first term in the brace can be expressed as

$$\int_0^a \frac{C(y)}{(t-y)\sqrt{a^2-t^2}} dt = C(y)\int_{-a}^a \frac{dt}{(t-y)\sqrt{a^2-t^2}} + C(y)\int_0^a \frac{dt}{(t+y)\sqrt{a^2-t^2}} \tag{1-4}$$

The last term in equation (1-4) obviously is a bounded function. For the first term in equation (1-4), we first normalize the integral interval as (r = t/a):

$$\frac{C(y)}{a}\int_{-1}^1 \frac{dr}{(r-y/a)\sqrt{1-r^2}} \tag{1-5}$$

When $y \to a^+$ according to Delale and Erdogan (1977), the integral above is equal to

$$C(y)\left\{ \frac{-\pi i}{\sqrt{a^2-y^2}} + R(y) \right\} \tag{1-6}$$

where function R is bounded at a^+. So the final result of K is

$$K = \lim_{y \to a^+} \frac{\mathrm{E}}{4\pi}\sqrt{2\pi(y-a)}\,aC(y)\left\{ \frac{-i\pi}{\sqrt{a^2-y^2}} \right\} = -\frac{\mathrm{E}}{4}\sqrt{a\pi}\,C(a) \tag{1-7}$$

APPENDIX 2

ADDITIONAL COMPLIANCE FUNCTIONS

The additional compliance functions can be calculated according the formulas given by (4-42) to (4-44) using numerical integration method. Where the stress intensity factors are defined by (4-25) and (4-26). Specifically, we use Simpson's rule to perform the quadrature with the integral domain [0,1] subdivided into 200 intervals. The obtained numerical results are used as a basis to construct approximate expressions for the compliance functions.

The nondimensional compliance function for tension, given by the handbook, is

$$\lambda_{NN}^{*}(x) = \frac{4x^2}{(1-x)^2}[0.99 - x(1-x)(1.3 - 1.2x + 0.7x^2)] \tag{2-1}$$

which is very close to our numerical integration result. Using the following form of the expression, we obtain the optimum fit as

$$\lambda_{NN}^{*}(x) = \frac{4x^2}{(1-x)^2}[0.988 - x(1-x)(1.504 - 1.654x + 0.920x^2)] \tag{2-2}$$

Although visually indistinguishable, (2-2) is more accurate than (2-1).

For bending, the compliance function given by the handbook is

$$\lambda_{MM}^{*}(x) = \frac{4x^2}{(1-x)^2}(5.93 - x(19.69 - 37.14x + 35.84x^2 + 13.12x^3)) \tag{2-3}$$

which correlates reasonably well with the result of numerical integration. However, the following expression yields a far better approximation to the numerical results:

$$\lambda^{*}_{MM}(x) = \frac{24x^2}{(1-x)^2(1+2x)^2}[0.988+x(1-x)(0.413+0.282x)] \tag{2-4}$$

especially in the range where x is close to 1.

For the mixed compliance function, there is no expression listed in the handbook. Based on the result of numerical integration of the stress intensity factors, we obtain the following expression:

$$\lambda^{*}_{MN}(x) = \frac{24x^2}{(1-x)^2(1+2x)}[0.988-x(1-x)(0.578-0.689x+0.196x^2)] \tag{2-5}$$

In the actual calculation, we use our own expressions (2-2), (2-4) and (2-5). The forms of these expressions ensure the correct asymptotic limits for at both $x \to 0^+$ and $x \to 1^-$.